journal of the international meteor organization

WGN

44:5
october 2016

New IMO website
Book review: Catalogue de météorites
IMC 2016 Proceedings abstracts
Research on IAU meteor shower database
April–May video meteors

ISSN 1016-3115

WGN Vol. 44, No. 5, October 2016, pp. 127 – 178

Administrative

Conferences

Meteor Science

Preliminary results

Front cover photo

Magnitude −10 Perseid fireball, photographed from Olędy, Poland on 2016 August 11 at $23^{\mathrm{h}}58^{\mathrm{m}}$ UT using a Nikon D7200 camera equipped with 10-mm $f/3.5$ lens and 15 s exposure at ISO 16000. Photo courtesy: Mariusz Wiśniewski.

Writing for WGN

This Journal welcomes papers submitted for publication. All papers are reviewed for scientific content, and edited for English and style. Instructions for authors can be found in WGN **31:4**, 124–128, and at `http://www.imo.net/docs/writingforwgn.pdf` .

Copyright

Legal address

International Meteor Organization, Jozef Mattheessensstraat 60, 2540 Hove, Belgium.

Meet the new IMO website!

Cis Verbeeck[1]

We are proud to announce the launch of the new website of the International Meteor Organization. You can check it out at `http://www.imo.net`. The website has been totally redesigned and developed by Mike Hankey and Vincent Perlerin using Wordpress and other enhancement programs.

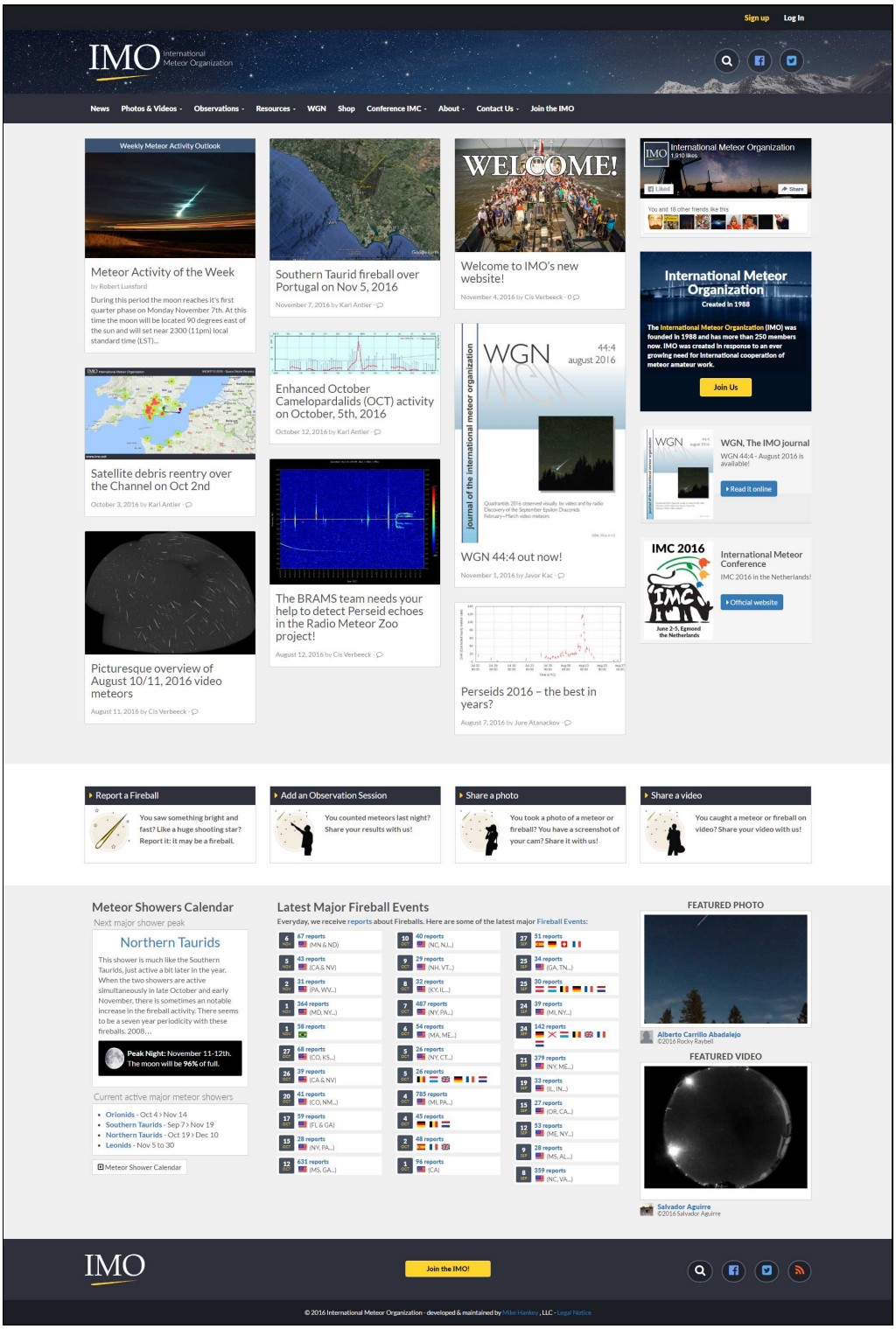

Figure 1 – Home page of the new IMO website.

[1] Bogaertsheide 5, 2560 Kessel, Belgium.
Email: `cis.verbeeck@scarlet.be`

IMO bibcode WGN-445-verbeeck-website NASA-ADS bibcode 2016JIMO...44..127V

We have created a brand new team of experts behind the website. Karl Antier is our new webmaster (`webmaster@imo.net`) and oversees the website management. Vincent Perlerin is in charge of website development. His experience ensures that the new website will be on the cutting edge of informational technology. Long-time IMO members found the old website static with important updates only occurring during major events. In order to make certain the new IMO website is a vibrant place with recent news about meteors and upcoming meteor showers, a new team of news editors was set up (Karl Antier, Jure Atanackov, Antonio Martínez Picar, and Nassia Smeets). You can help these people by suggesting news items for the IMO website via e-mail to `newsitems@imo.net`.

We also recruited meteor experts Karl Antier, Chris Peterson and Jingyuan Zhao to answer meteor questions from beginners using the e-mail address `info@imo.net`. Of course, our new site offers everything that was already on the old website: information about meteors and meteor showers, how to observe meteors, IMO's Meteor Shower Calendar, meteor software and databases, information about meteors and meteor showers, how to observe meteors, the IMO's Meteor Shower Calendar, meteor software and databases, the IMO's International Meteor Conference, the IMO's journal WGN, the IMO itself, and much more.

So what's new?

1. Any visitor of the IMO website can now create a user account. If you are IMO member, a user account has already been set up for you! You just need to generate a password at `http://www.imo.net/newsite`. Your user account enables a much more involved interaction with other meteor workers: you can access all your visual observations, upload pictures and videos, comment on posts, edit your profile, etc. Do not forget to check this out, and upload your pictures and videos!

2. A brand new online visual form and Visual Meteor Data Base, containing visual data from 1982 till now. A dynamic and user-friendly interface shows general observing statistics and allows you to access, e.g., all your visual observation sessions, all visual observations in a particular year, or all observations of a particular meteor stream in a particular year. Any data you consult will be plotted and shown in tabular form. All data is freely available for download, too.

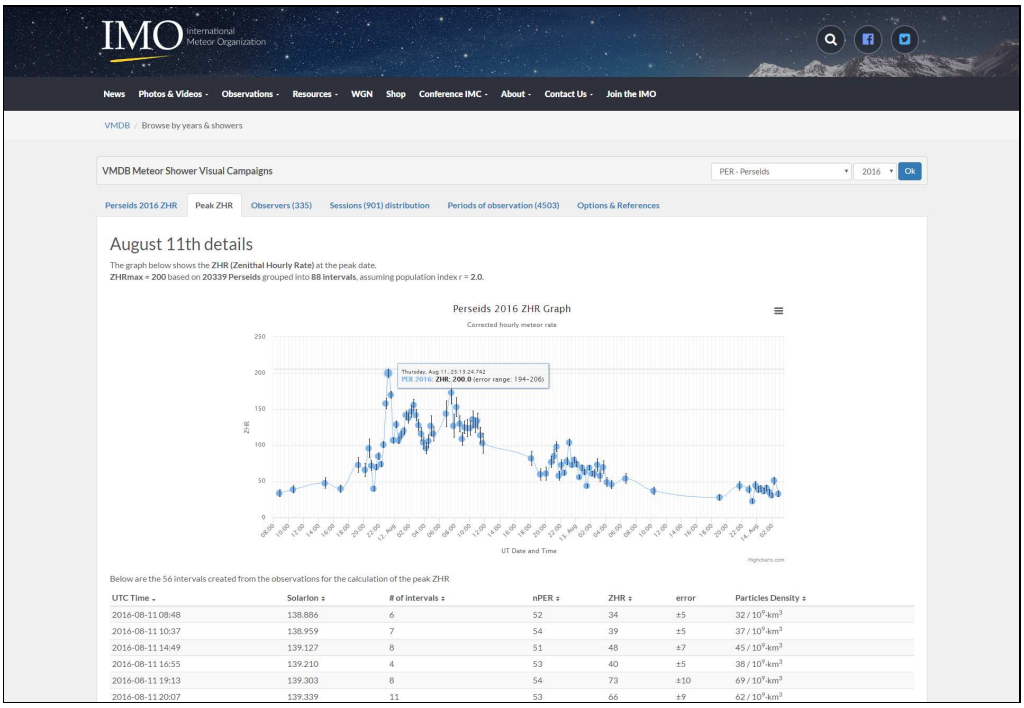

Figure 2 – Example of automatically generated activity profile based on VMDB data.

3. A link to the online fireball form, with the latest events displayed on the main page.

4. Bob Lunsford's weekly update on meteor showers: Meteor Activity of the Week.

5. WGN: everyone can download old issues (1987–2014); IMO members can download the two most recent volumes.

6. Renewed IMO shop: easy ordering of IMO publications.

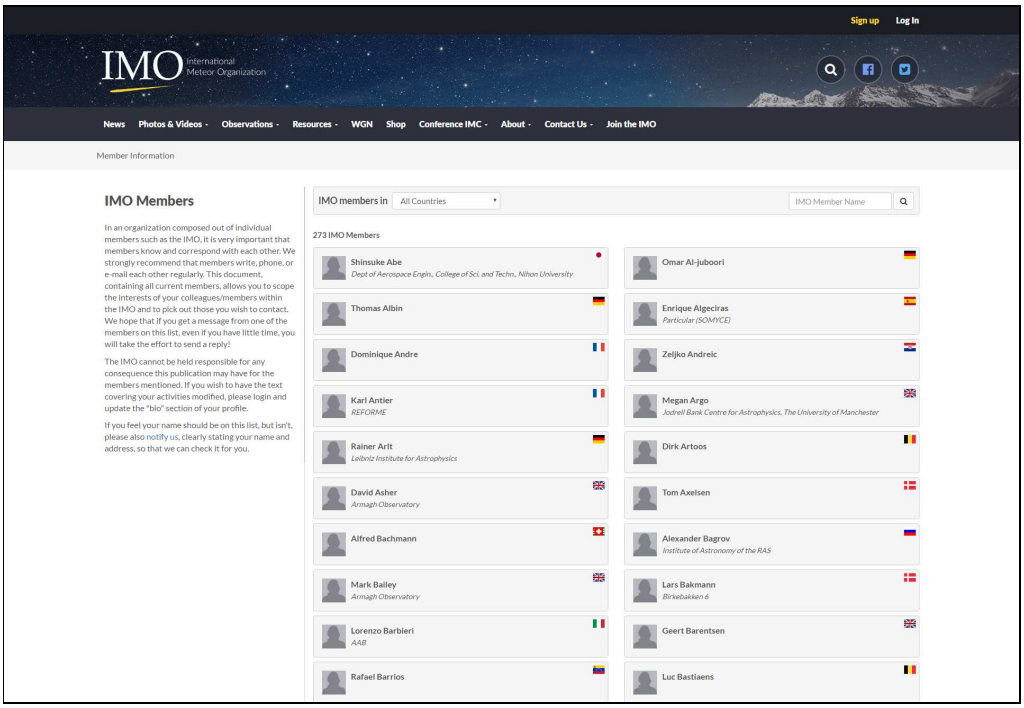

Figure 3 – The IMO members list page.

7. Easy renewal of your IMO membership. IMO members receive 6 issues of WGN per year (you can choose between electronic only or electronic + paper version).

8. Easy online voting for IMO's voting bulletins and elections, of course exclusively for IMO Voting Members.

This achievement was only possible thanks to the extraordinary efforts of Mike Hankey and Vincent Perlerin. The IMO Council is very grateful for their exceptional contribution to the IMO. A lot of testing, proofreading and updates were done in the process by Marc Gyssens (extensively), Cis Verbeeck, Karl Antier, Sirko Molau, Jürgen Rendtel, Rainer Arlt, Bob Lunsford, Bill Ward, Geert Barentsen, and Luc Bastiaens. Many thanks to all these people, to the news editors and info team, and to all people we may have forgotten!

We wish you a lot of fun visiting the new IMO website, and are interested in any feedback you may have!

In addition to the IMO website, the International Meteor Organization also has a Facebook page (`https://www.facebook.com/InternationalMeteorOrganization/`) with over 800 fans and a Twitter account (`@IMOmeteors`) with over 1300 followers. We warmly recommend you to check them out!

Do you want to be an editor for the IMO website too? Just send a mail to `webmaster@imo.net` or `cis.verbeeck@scarlet.be`.

From the Treasurer — IMO Membership/WGN Subscription Renewal for 2017

Marc Gyssens

Renewal rates

We invite all our members/subscribers to renew for 2017. The fees are as tabulated below. For those of you paying in Euros, we are happy that we can offer WGN at the same cost as last year. We also continue to offer an electronic-only subscription at a reduced rate. For those of you paying in US Dollars, notice that we have lowered the rates to better reflect the current exchange rates.

IMO Membership/WGN Subscription 2017				
Electronic + paper with surface mail delivery:		€26		US$ 35
Electronic + paper with airmail delivery (outside Europe only):		€49		US$ 65
Electronic only:		€21		US$ 25
Supporting membership:	add	€26	add	US$ 35

It is possible to renew for two years by paying double the amount.

When you renew, give a few minutes of thought to becoming a **supporting member** by paying at least double the amount due. As you may know, there is an IMO Support Fund. With this Support Fund, we offer support to meteor-related projects. Our ability to provide this service to the meteor community depends primarily on the gifts we receive from supporting members!

Another way to help meteor workers with limited funds is to offer them a gift subscription.

We already thank all our members that will renew for their continued trust in our Organization!

Payment instructions

In essence, you can still pay in the way you are used to, but in view of the changes that are brought about by the new IMO website, some explanation is due this time.

1. The main difference with the past is that every member has now a personal account. The first thing you have to do, is to log in to your account. Thereto, go to IMO website `http://www.imo.net` and click "Log In" in the upper right-hand corner (see Figure 1). You will then see the login screen (Figure 2).

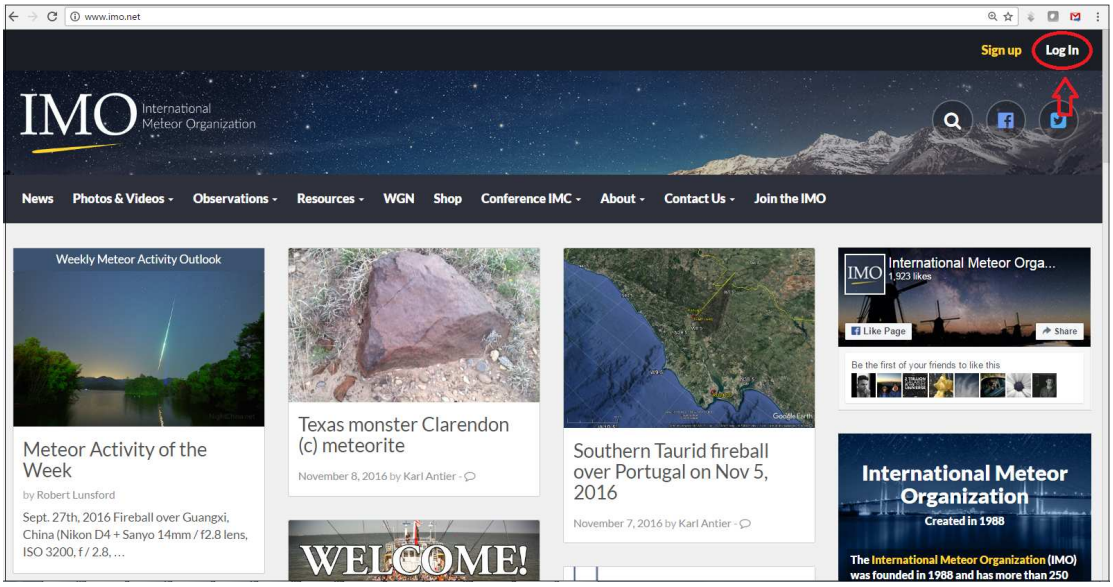

Figure 1 – First, log in to your personal account on the IMO website.

There are now two possibilities:

(a) You have already used your account. Then just login.

(b) You have never used your account before. Then click "Generate a password" (see Figure 2). You will be directed to a screen where you can fill out the email address under which you have registered as IMO Member/WGN Subscriber. Submit this information, and almost instantaneously you will receive an email containing a link to (re)set your password.

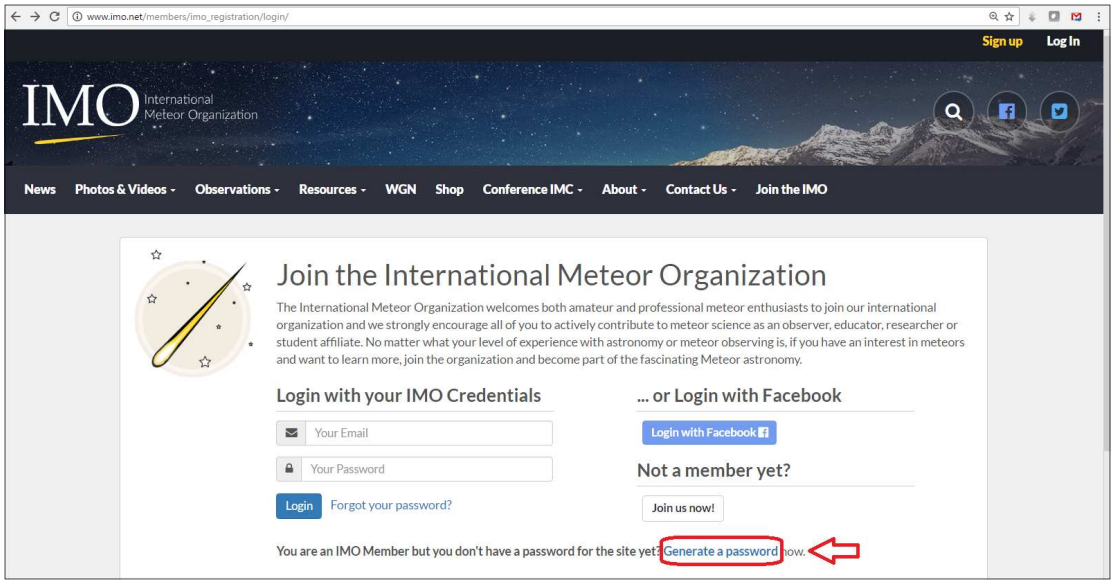

Figure 2 – Login screen. From here you can log in, or generate a password for your account by clicking "Generate a password".

Whether you log in straight away or (re)set your password (as a consequence of which you will be logged in), you will next see your profile page (see Figure 3 for an example). Notice that, when you are logged in, you can always navigate to your profile page using the pull-down menu under name in the upper right-hand corner. It is the first item in this menu.

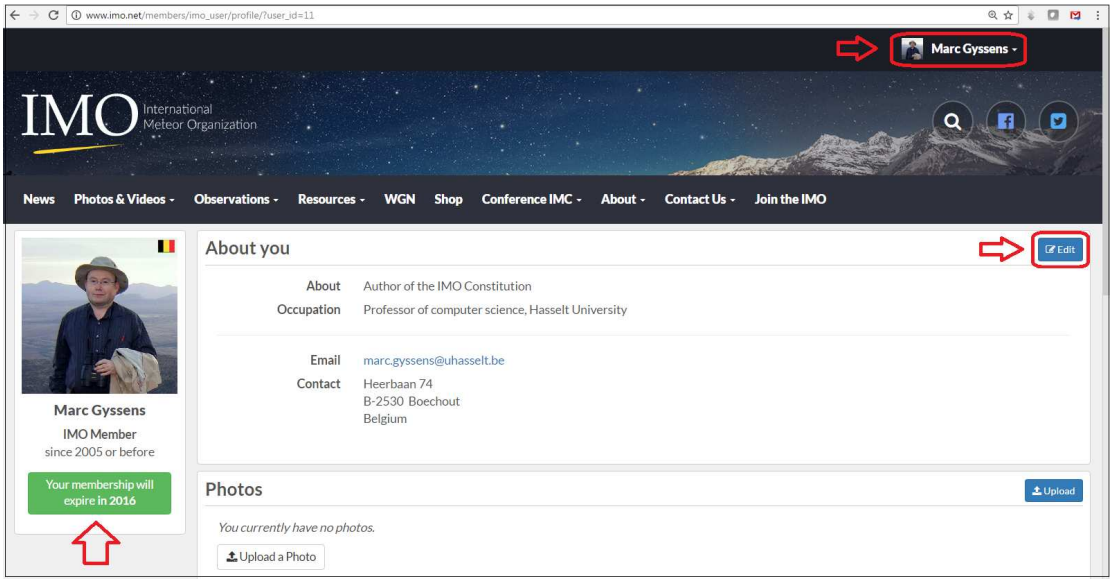

Figure 3 – Profile page. When logged in, you can always navigate to this page using the pull-down menu under your name in the upper right-hand corner. Once on your profile page, you can update your data. With the green button under your profile picture or its placeholder, you can navigate to the payment page.

2. On your profile page, you can edit your personal data by clicking "Edit" in the upper-right hand corner of the "About you" section. Please do so, and check if the data under "IMO info" are still up to date. If you change anything, do not forget to click "Save". Then return to your profile page.

3. On your profile page, you see a green button just below your profile picture or its placeholder. It gives you information on when your membership/subscription expires. For instance, in my case, it reads "Your membership will expire in 2016", signalling me that I have to renew shortly. Clicking this button will get you the renewal page (Figure 4).

4. On the renewal page you can select whether you like a standard subscription, an airmail subscription (outside Europe only), or an electronic-only subscription, and for how many years you want to renew. When you submit this information, you are directed to the payment page (Figure 5). Initially you only see the calculation of your dues, and you are asked whether you want to pay in Euros or in US Dollars.

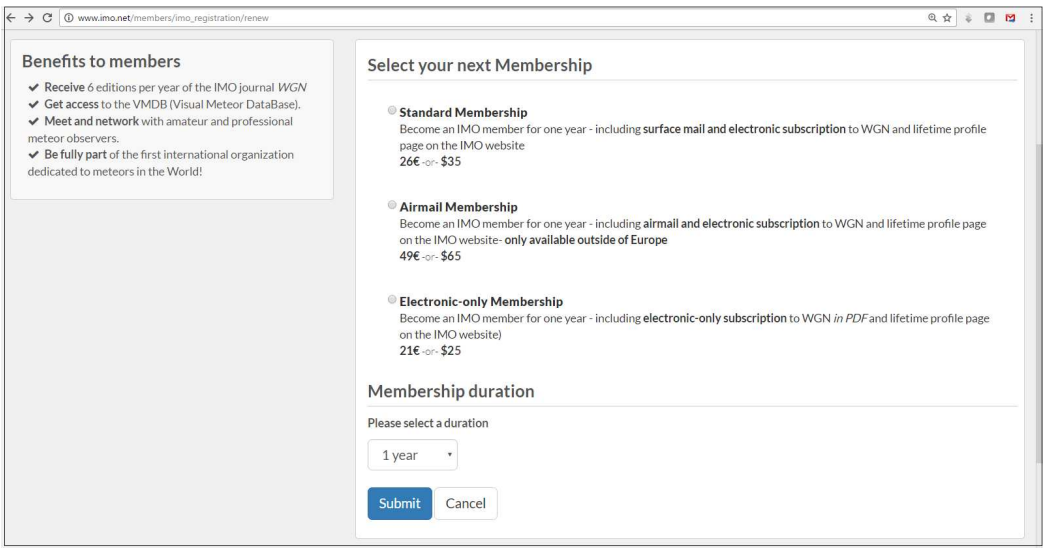

Figure 4 – Renewal page.

Submitting this information will reveal the bottom part of the page, where you are offered several payment options, taking into account your country of residence.

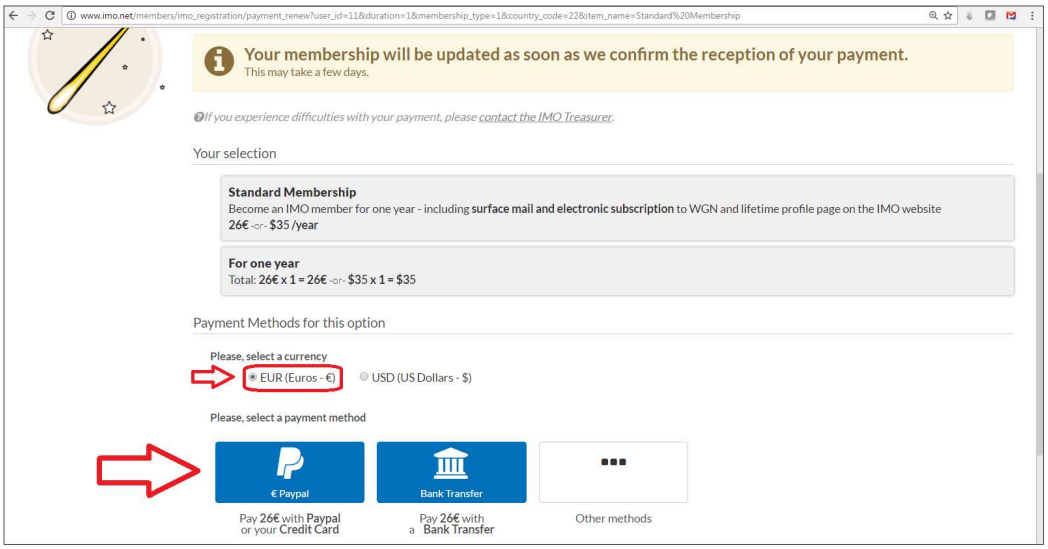

Figure 5 – Payment page. At first, you only see the calculation of your dues and the option to pay in Euros and US Dollars. Upon selecting your currency of choice, the bottom part of the page is shown with the payment options.

If you choose for a PayPal payment (or a credit card payment via PayPal), click the corresponding blue button, and you can complete the whole process in a few self-explanatory steps.

If you choose for a bank transfer of other payment options, clicking on the corresponding button will reveal information on how to pay. (In particular, if you opt for a bank transfer, you will see all the details of the IMO account you need to make the transfer.) Notice you can access this information as often as you will by repeating the steps described above. As your payment is registered manually, you can rest assured that repeatedly accessing the payment page cannot and will not give rise to duplicate registrations!

The bottom-line is that the renewal instruction are more or less the same as they used to be, except that through your personal account, you have more control. You can always consult when your membership expires, and you can update your data yourself.

If you experience any difficulties, do not hesitate to contact me at `treasurer@imo.net`.

One final request: every year, a lot of members renew late. As a consequence, back issues that already appeared have to be sent out to these members. Please support our volunteers in their bimonthly effort to have WGN shipped to you by renewing promptly! Thank you for your understanding and cooperation!

IMO bibcode WGN-445-gyssens-renewals NASA-ADS bibcode 2016JIMO...44..130G

Book review — "Catalogue de Météorites", written by Abderrahmane Ibhi

Paul Roggemans

"Catalogue de Météorites" written by Abderrahmane Ibhi, published by Musée universitaire de météorites. ISBN 978-9954-36-970-8. In French. Contact: Dr. Abderrahmane Ibhi (a.ibhi@uiz.ac.ma).

"Catalogue de Météorites" written by Dr. Abderrahmane Ibhi describes the efforts made in the past few years in Morocco to search for meteorites, to analyze the many Moroccan meteorites and to promote the general interest in meteorites and meteor astronomy. The publication of this work is part of an ambitious project with a permanent exposition of a meteorite museum at the University of Agadir. This is not only the first such initiative in Morocco but the first for the African continent as well as the Arab world.

The book introduces basic knowledge about meteorites, their origin and characteristics, described in a clear language for the general public. The second chapter describes the recent history of meteorite finds and research done in Morocco. The major efforts in this domain by the Astronomy Club Ibn Zohr are highlighted and the motivation to invest in the topic is explained.

A detailed description is given for the most important Moroccan meteorites. Most remarkable is the recent nature of all the investigations, starting with a meteorite fall on 2004 November 22. Since then several falls and finds have been scientifically studied and documented in this book. The final part is a catalogue of all meteorites of the collection of the Astronomy club Ibn Zohr, exhibited at the museum at the University Ibn Zohr, Agadir. Each meteorite is presented with a photograph and all physical characteristics. This part is most interesting for meteorite collectors.

IMO bibcode WGN-445-roggemans-book NASA-ADS bibcode 2016JIMO...44..133R

From the Treasurer—Supporting Members 2015

Marc Gyssens [1]

The following IMO Members and WGN Subscribers have paid at least double the normal membership fee for 2015 (but not necessarily *in* 2015):

Karl Antier	Lars Bakmann	Luc Bastiaens	Orlando Benitez Sanchez
Mihail Bidnichenko	David Entwistle	Karl-Heinz Gansel	Marc Gyssens
James Kinsman	Michael Kohl	Paul Lindsey	Robert Lunsford
Sirko Molau	Hiroshi Ogawa	Walter Soto	Jan Verbert
Yao Xiang			

We are very grateful to the people above for their support. In addition, some members also contributed by providing a gift membership to a friend, or by paying a friend's or colleague's registration fee for the International Meteor Conference. It must also be emphasized that several other people gave gifts smaller than the regular membership fee; of course, these gifts are equally appreciated.

All the gifts we receive go into the IMO Support Fund, which is primarily directed towards supporting meteor astronomy projects. There are no deadlines—applications can be made at any time and will be evaluated by the IMO Council on their merits as we receive them. Unfortunately, only few meteor workers or groups of meteor workers make use of this interesting facility to bring their project to a higher level. Therefore, we strongly encourage applications!

Meanwhile, we thank once again all those of you who provided support to the IMO, in whichever way you chose!

[1] Heerbaan 74, B-2530 Boechout, Belgium. E-mail: marc.gyssens@uhasselt.be

IMO bibcode WGN-445-gyssens-support NASA-ADS bibcode 2016JIMO...44..133G

Conferences

Details of the Proceedings of the International Meteor Conference, Egmond, the Netherlands, 2–5 June, 2016,

edited by Adriana Roggemans and Paul Roggemans

Compiled by Marc Gyssens

The 35th International Meteor Conference (IMC) was organized in Egmond, the Netherlands, from June 2 to 5, 2016, in conjunction with Meteoroids, which took place the week after the IMC in Noordwijk. This combination resulted in a record number of 157 participants from 30 countries. As a consequence, the proceedings of this conference, edited by Adriana and Paul Roggemans, are with 374 numbered pages the most voluminous ones ever produced. They are available digitally from the IMO website; a limited number of printed copies is also available, and they can be ordered as usual. For your convenience, the contributions and their abstracts are summarized below.

Artificial meteor test towards on-demand meteor shower

Shinsuke Abe, Lena Okajima, Hironori Sahara, Takeo Watanabe, Yuta Nojiri, and Tomohiko Nishizono

An arc-heated wind tunnel is widely used for ground-based experiments to simulate environments of the planetary atmospheric entry under hypersonic and high-temperature conditions. In order to understand details of a meteor ablation such as temperature, composition ratio, and fragmentation processes, the artificial meteor test was carried out using a JAXA/ISAS arc-heated wind tunnel. High-heating rate around 30 MW/m^2 and high-enthalpy conditions, 10 000 K arc-heated flow at velocity around 6 km/s were provided. Newly developed artificial metallic meteoroids and real meteorites such as Chelyabinsk were used for the ablation test. The data obtained by near-ultraviolet and visible spectrograph (200 and 1100 nm) and high-speed camera (50 μs) have been examined to develop more efficient artificial meteor materials. We will test artificial meteors from a small satellite in 2018.

Asteroidal meteors detected by MU radar head-echo observations

Shinsuke Abe, Johan Kero, Takuji Nakamura, Yasunori Fujiwara, Daniel Kastinen, Jun-ichi Watanabe, and Hiroyuki Hashiguchi

The recent development of the technique carried out using the middle and upper atmosphere radar (MU radar) of Kyoto University at Shigaraki (34 °.9 N, 136 °.1 E), which is large atmospheric VHF radar with 46.5 MHz frequency, 1 MW output transmission power and 8330 m^2 aperture array antenna, has established very precise orbital determination from meteor head echoes. A tremendous number, more than 150 000, of observed precise orbits of meteoroids by the MU radar meteor head-echo observation will shed light on new discoveries of meteoroids. Here we report some interesting features related with asteroids or distinct comets.

On the age and parent body of the Daytime Arietids meteor shower

Abedin Abedin, Paul Wiegert, Petr Pokorny, and Peter Brown

The Daytime Arietid meteor shower is active from mid-May to late June and is among the strongest of the annual meteor showers, comparable in activity and duration to the Perseids and the Geminids. Due to the daytime nature of the shower, the Arietids have mostly been constrained by radar studies. The Arietids exhibit a long-debated discrepancy in the semi-major axis and the eccentricity of meteoroid orbits as measured by radar and optical surveys. Radar studies yield systematically lower values for the semi-major axis and eccentricity, where the origin of these discrepancies remain unclear. The proposed parent bodies of the stream include Comet 96P/Machholz and more recently the Marsden's group of Sun-skirting comets. In this work, we present detailed numerical modelling of the Daytime Arietid meteoroid stream, with the goal to identifying the parent body and constraining the age of the stream. We use observational data from an extensive survey of the Arietids by the Canadian Meteor Orbit Radar (CMOR), in the period of 2002–2013, and several optical observations by the SonotaCo Meteor Network and the Cameras for All-sky Meteor Surveillance (CAMS).

Our simulations suggest that the age and observed characteristics of the Daytime Arietids are consistent with cometary activity from 96P, over the past 12 000 years. The sunskirting comets that presumably formed in a major comet breakup between 100 and 950 AD (Chodas and Sekanina, 2005), alone, cannot explain the observed shower characteristics of the Arietids. Thus, the Marsden Sun-skirters cannot be the dominant parent, though our simulations suggest that they contribute to the core of the stream.

IMO bibcode WGN-445-gyssens-proceedings2016 NASA-ADS bibcode 2016JIMO...44..134G

A Monte-Carlo based extension of the Meteor Orbit and Trajectory Software (MOTS) for computations of orbital elements

Thomas Albin, Detlef Koschny, Rachel Soja, Ralf Srama, and Bjoern Poppe

The Canary Islands Long-Baseline Observatory (CILBO) is a double-station meteor camera system (Koschny et al., 2013; 2014) that consists of 5 cameras. The two cameras considered in this report are ICC7 and ICC9, and are installed on Tenerife and La Palma. They point to the same atmospheric volume between both islands allowing stereoscopic observation of meteors. Since its installation in 2011 and the start of operation in 2012, CILBO has detected over 15 000 simultaneously observed meteors. Koschny and Diaz (2002) developed the Meteor Orbit and Trajectory Software (MOTS) to compute the trajectory of such meteors. The software uses the astrometric data from the detection software MetRec (Molau, 1998) and determines the trajectory in geodetic coordinates. This work presents a Monte-Carlo based extension of the MOTS code to compute the orbital elements of simultaneously detected meteors by CILBO.

An antenna, a radio and a microprocessor: which kinds of observation are possible in meteor radio astronomy?

Lorenzo Barbieri

Radio meteors are usually investigated by professional radars. Amateur astronomers cannot have transmitters, so usually they can only listen to sounds generated by a radio tuned to a TV or military transmitter. Until recently, this kind of observation has not produced good data. The experience of "RAMBo" (Radar Astrofilo Meteorico Bolognese) shows which data can be extracted from an amateur meteor scatter observatory and the results which can be achieved.

Accurate Geminid velocities with CHIPOlAtA

Felix Bettonvil

For several years, the high-resolution photographic camera CHIPOlAtA has been used to acquire precise orbits for Geminid and Perseid meteor shower members. In this paper I analyze the first set of data obtained during the Geminids 2014.

Photographic spectra of fireballs

Jiří Borovička

Two methods of spectroscopy of meteors using image intensified video cameras and classical photographic film cameras are compared. Video cameras provide large number of low resolution spectra of meteors of normal brightness, which can be used for statistical studies. Large format film cameras have been used through the history and provide high resolution spectra, which can be used to derive temperature, density, and absolute abundances of various elements in the radiating plasma. The sensitivity of films is, however, low and only spectra of bright meteors (fireballs) can be studied. Examples of photographic fireball spectra are provided.

The 2016 Quadrantids

Brando Gaetano

A report is presented on the observation of the Quadrantid shower recorded by RAMBO early January 2016. The data analysis—done by calculating the RZHR (Radar ZHR)—shows the complexity of the shower, in which the presence of multiple filaments is verified. A meteoroids mass profile is also made. Finally a comparison is made between the RAMBO radar data and the IMO visual data.

Recent shower outbursts detected by the Canadian Meteor Orbit Radar (CMOR)

Peter Brown

We present recent detections of short-duration shower outbursts as measured by the Canadian Meteor Orbit Radar (CMOR) between 2013–2016. In this interval, CMOR detected two strong shower outbursts unlinked to known showers. These included an outburst of the Kappa Cancrids (KCA, IAU 793) on January 5, 2015, and from the Gamma Lyrids (GLY, IAU 794) on February 7, 2015. Both have an orbit consistent with a Halley-type comet (HTC) or nearly isotropic-comet. Analysis of GLY activity also revealed a previously unreported annual shower, the September Ursae Majorids, (SUR, IAU 795).

The Radio Meteor Zoo: a citizen science project

Stijn Calders, Cis Verbeeck, Hervé Lamy, and Antonio Martínez Picar

Scientists from the BRAMS radio meteor network have started a citizen science project called Radio Meteor Zoo in collaboration with Zooniverse in order to identify meteor reflections in BRAMS spectrograms. First, a smallscale version of the Radio Meteor Zoo was carried out with a sample of meteor identifications in 12 spectrograms by 35 volunteers. Results are presented here and allowed us to define a method that reliably detects meteor reflections based on the identifications by the volunteers. It turns out that, if each spectrogram is inspected by 10 volunteers, hit and false detection percentages of 95%, respectively 6%, are expected. The Radio Meteor Zoo is online at `https://www.zooniverse.org/projects/zooniverse/radio-meteor-zoo`. Citizen scientists are kindly invited to inspect spectrograms.

Results from the Canadian Automated Meteor Observatory

Margaret Campbell-Brown

Some recent results from the Canadian Automated Meteor Observatory (CAMO) are presented. Comparing the begin heights and speeds of meteors between the two CAMO systems shows that the two populations, which differ by approximately an order of magnitude in mass, are quite different, with the more sensitive system recording many more slow meteors than the less sensitive system. At slow speeds for the more sensitive camera system, light curve shapes do not behave as expected, with stronger meteors having early-peaked light curves. Most meteoroids captured by the CAMO tracking system fragment in one way or another, and current ablation models are poor at predicting the nature of the fragmentation. The narrow field system is proving useful in many areas of meteor physics.

Ablation of small Fe meteoroids—first results

David Čapek and Jiří Borovička

A numerical model describing atmospheric flight of small iron meteoroids is presented. Several ablation scenarios are considered and it is discussed if these can explain a population of faint, short duration meteors with low beginning height and quick increase of brightness.

FRIPON Network status

François Colas, Brigitte Zanda, Sylvain Bouley, Jérémie Vaubaillon, Chiara Marmo, Yoan Audureau, Min Kyung Kwon, Jean-Louis Rault, Pierre Vernazza, Jérôme Gattacceca, Stéphane Caminade, Mirel Birlan, Lucie Maquet, Auriane Egal, Monica Rotaru, Laurent Jorda, Cyril Birnbaum, Cyril Blanpain, Adrien Malgoyre, Julien Lecubin, Alberto Cellino, Daniele Gardiol, Mario Di Martino, Christian Nitschelm, Jorje Camargo, M. Valenzuela, Ludovic Ferrière, Marcel Popescu, and Damien Loizeau

The FRIPON Network (Fireball Recovery and Interplanetary Observation Network) will be fully operational in 2016 (`http://www.fripon.org`). This "open source" project includes several new features that will be described in detail. We also discuss the opportunities for expansion outside France.

The main innovation is the connectivity of cameras enabling better efficiency for meteors detection, and the possibility of computing orbits in real time to organize an observation campaign within 24 hours. Another innovation is the ability to daytime detections. Statistics show that there are more meteorites in late afternoon than during the rest of the day because of their low speed.

As the project has been designed from the start to handle a large number of cameras it is easy to extend it to increase its effectiveness. I will show the next extension of the network and its operation.

The dimension added by 3D scanning and 3D printing of meteorites

Sebastiaan J. de Vet

An overview for the 3D photodocumentation of meteorites is presented, focussing on two 3D scanning methods in relation to 3D printing. The 3D photodocumention of meteorites provides new ways for the digital preservation of culturally, historically, or scientifically unique meteorites. It has the potential for becoming a new documentation standard of meteorites that can exist complementary to traditional photographic documentation. Notable applications include (i) use of physical properties in dark flight-, strewn field-, or aerodynamic modelling; (ii) collection research of meteorites curated by different museum collections, and (iii) public dissemination of meteorite models as a resource for educational users. The possible applications provided by the additional dimension of 3D illustrate the benefits for the meteoritics community.

Status of the Desert Fireball Network

Hadrien A. R. Devillepoix, Philip A. Bland, Martin C. Towner, Martin Cupák, Eleanor K. Sansom, Trent Jansen-Sturgeon, Robert M. Howie, Jonathan Paxman, and Benjamin A. D. Hartig

A meteorite fall precisely observed from multiple locations allows us to track the object back to the region of the Solar System it came from, and sometimes link it with a parent body, providing context information that helps trace the history of the Solar System. The Desert Fireball Network (DFN) is built in arid areas of Australia: its observatories get favorable observing conditions, and meteorite recovery is eased thanks to the mostly featureless terrain. After the successful recovery of two meteorites with 4 film cameras, the DFN has now switched to a digital network, operating 51 cameras, covering 2.5 million km^2 of double station triangulable area. Mostly made of off-the-shelf components, the new observatories are cost effective while maintaining high imaging performance. To process the data (ca. 70 TB/month), a significant effort has been put to writing an automated reduction pipeline so that all events are reduced with little human intervention. Innovative techniques have been implemented for this purpose: machine learning algorithms for event detection, blind astrometric calibration, and particle filter simulations to estimate both physical properties and state vector of the meteoroid. On 31 December 2015, the first meteorite from the digital systems was recovered: Murrili (the 1.68 kg H5 ordinary chondrite was observed to fall on 27 November 2015). Another 11 events have been flagged as potential meteorites droppers, and are to be searched in the coming months.

Data processing of records of meteoric echoes

Peter Dolinský

The data obtained in the period from 4 November 2014 to 31 July 2014 by our receiving and recording system was statistically processed. The system records meteoric echoes from the TV transmitter Lviv 49.739583 MHz ((49 ̊8480 N, 24 ̊0369 E, Ukraine) using a 4-element Yagi antenna with horizontal polarization (elevation of 0° and azimuth of 60°), receiver ICOM R-75 in the CW mode, and a computer with a recording using HROFFT v1.0.0f. The main goal was to identify weak showers in these data. Mayor or strong showers are visible without processing (referred at IMC 2015, Mistelbach). To find or to identify weaker showers is more difficult. Not all echoes are meteoric echoes, but also ionospheric echoes or lightning disturbances are present.

Calibration of meteor spectra

Martin Dubs and Koji Maeda

Meteor spectra give valuable information about the composition of meteors. The nonlinear dispersion of spectra together with the motion of the meteors complicates the analysis. In this presentation a simple method to calibrate spectra in wavelength and flux is presented. By an image transformation to an orthographic projection the dispersion becomes linear and the curved spectra become straight and parallel. The resulting spectra, after suitable pre-processing, can be analyzed with standard spectroscopy software.

Investigation of meteor shower parent bodies using various metrics

Bogdan Alexandru Dumitru, Mirel Birlan, Alin Nedelcu, and Marcel Popescu

The present knowledge of meteor showers identifies the small bodies of our Solar System as supply sources for meteor streams. Both comets and asteroids are considered as the origin of meteor showers. The new paradigm of "active asteroids" opens up a large field of investigation regarding the relationships between asteroids and meteors. Processes like ejection and disaggregation at impacts, rotational instabilities, electrostatic repulsion, radiation pressure, dehydration stress followed by thermal fractures, sublimation of ices are sources of matter loss from asteroids.

Our objective is to find genetic relationships between asteroids and meteor showers using metrics based on orbital elements. For this objective we selected three metrics (Southworth and Hawkins, 1963; Asher et al. 1993; and Jopek, 1993, respectively), the recent MPC database and the more recent IAU meteor shower database. From our analysis, 41 of the meteor showers have probabilities of being produced (or to be fueled) by asteroids. Our sample of asteroids contains more than 1000 objects, all of them belonging to the Near-Earth Asteroid population. The systematic approach performed, based on the physical properties of our sample, reinforced the link between asteroids and their associated meteor shower.

The challenge of meteor daylight observations

Auriane Egal, Min-Kyung Kwon, François Colas, Jérémie Vaubaillon, and Chiara Marmo

One of the goals of the FRIPON network is to perform the daylight detection of fireballs. If the cameras used are adapted to these observations, the reduction method still needs to be improved in order to reduce the high number of false detections. To deeply check the daylight reduction software, the FRIPON team is looking for observations of fireballs and atmospheric reentries during the day. For this purpose, the team has organized in emergency (in less than 10 days) an observation campaign of the reentry of the WT1190F space debris in November 2015. Although the bad weather conditions have hampered the success of the mission, it remains a great example of the value of the collaboration between scientists and amateurs, without whom this challenge would not have been overcome.

PRISMA: Italian network for meteors and atmospheric studies

Daniele Gardiol, Alberto Cellino, and Mario Di Martino

The aim of the PRISMA project is to develop the Italian participation in a network of European observing facilities whose primary targets are bright meteors (the so-called bolides and fireballs) and the recovery of meteorites. Several all-sky cameras have been recently installed in France (FRIPON project), and we propose to do the same in Italy, interconnecting the Italian network with the French one. Such a network is of great interest for the studies of interplanetary bodies and the dynamical and physical evolution of the population of small bodies of the Solar System and for the studies of collected meteorites. Those eventually recovered will be classified and investigated from the petrologic, genetic, and evolutionary points of view, analyzed for their spectral characteristics and compared with known asteroids. The possibility to measure the radioactivity of samples shortly after the fall using gamma-ray spectrometers available in the Osservatorio Astrofisico di Torino laboratories, will allow us to reveal the presence of short-lived cosmogenic radioisotopes. PRISMA is also very suitable for the purposes of atmospheric studies. This includes the statistics of cloud coverage and lightning frequencies, as well as the comparison of the optical depth measured using satellites and PRISMA cameras.

The evolution of ROAN 2016—Radio surveillance of meteors and determination of reflection points through calculation of the radio path, based on times

Tudor Georgescu, Ana Georgescu, and Cezar Lesanu

The article presents the activity calendar describing the steps until the finalization of the Allsky project in December 2016. It presents also the new developed technology for detection and localization of meteors' ionic traces, which is based on information time-stamped on the radio carrier.

The year 2016 is the final one for our project, during which our target is the creation of 25 integrated stations (radio and video, all-sky MK3 type) and to install the ROAN radio beacon. Its location will be the operation base initially, before being moved to an eastern spot, near the Ukrainian border.

The novelty of it all is brought by the newly patented technology of time-stamping.

Video meteor light curve analysis of Orionids and Geminids and developing a method for obtaining the absolute light curves of shower meteors from the single station data

Ljubica Grašić, Nikolina Milanović, and Dušan Pavlović

We developed a method for obtaining the absolute light curves of the shower meteors from single station video data. We found that even though the height of a meteor atmospheric trajectory obtained by using this method may have a large error, the absolute light curve shape is preserved. We used our method to calculate the F parameters of the Orionid and Geminid light curves. The light curves were obtained from the single station video data by the instrument with a limiting sensitivity of magnitude 3.5. We found that for our sample of the light curves the zenith distance of meteor radiant does not affect the F parameter for either of the two showers. The value of the F parameter of the Orionids obtained in this paper matches the values obtained by other authors, whilst for the Geminids it is significantly different.

Consequences of meteoroid impacts based on atmospheric trajectory analysis

Maria Gritsevich

Using dimensionless expressions, which involve the pre-atmospheric meteoroid parameters, we have built physically based parametrization to describe the changes in mass, height, velocity, and luminosity of the object along its atmospheric path. The developed model is suitable to estimate a number of crucial unknown values including the shape change coefficient, ablation rate, and surviving meteorite mass. Besides the model description, we demonstrate its application using the wide range of observational data from meteorite-producing fireballs appearing annually to larger scale impacts. In particular, this approach enabled us to recently recover the Annama meteorite which was observed from 3 stations of the Finnish Fireball Network on 19 April 2014.

Synthetic spectra of meteors

Meryem Guennoun, Michel-Andres Breton, Nicolas Rambaux, Jérémie Vaubaillon, and Zouhair Benkhaldoun

Synthetic meteor spectra provide information which help to identify the different types of meteorites resulting from a meteor. They also help anticipate what an instrument might observe in a given range of wavelengths. We developed a program that computes synthetic spectra of meteorites for which we know the chemical formula, in the case of plasma in local equilibrium. Three different examples are presented here.

Meteoroid streams and comet disintegration

Ayyub Guliyev

The results of the statistical analysis of the dynamic parameters of 114 comets that have undergone nuclear splitting are presented in the article. The list of the objects contains: comets that have split in the period of the observation; data of twin-comets; lost comets with designation D; comets with large-scale structure in the coma. We will describe these comets as "splitted". Some aspects of the following hypothesis are studied: disintegration of comet nuclei happens as the result of their collision with meteoroid streams. For the verification of this hypothesis, the position of splitted comet orbits relatively to 125 meteor streams from Kronk's list is analyzed. It was found that the total number of comet orbit nodes located close to the meteor stream planes (for distances up to 0.1 AU) is $N = 1041$. It is shown that if these comets are replaced by randomly selected different comets, N will be reduced by a factor of approximately 3.

A fast meteor detection algorithm

Pete Gural

A low latency meteor detection algorithm for use with fast steering mirrors had been previously developed to track and telescopically follow meteors in real-time (Gural, 2007). It has been rewritten as a generic clustering and tracking software module for meteor detection that meets both the demanding throughput requirements of a Raspberry Pi while also maintaining a high probability of detection. The software interface is generalized to work with various forms of front-end video pre-processing approaches and provides a rich product set of parameterized line detection metrics. Discussion will include the Maximum Temporal Pixel (MTP) compression technique as a fast thresholding option for feeding the detection module, the detection algorithm trade for maximum processing throughput, details on the clustering and tracking methodology, processing products, performance metrics, and a general interface description.

The occurrence of interstellar particles in the vicinity of the Sun: an overview—25 years of research

Mária Hajduková Jr.

Using different observational techniques, research into interstellar particles produced controversial results concerning their occurrence in the vicinity of the Sun. The proportion of possible interstellar particles to interplanetary ones was found to be much higher for small particles obtained from cosmic dust detectors in comparison with results of photographic, video, and radar meteors. This might be partly caused by different mass distributions of interstellar and interplanetary particles, and by different physical processes leading to each population. However, in the range of larger meteoroid particles, the vast majority of hyperbolic orbits were found to be as a consequence of measurement errors. We present here an overview of studies related to interstellar particles showing their flux as a function of their mass and distance from the Sun.

A tale of two fireballs

Mike Hankey and Vincent Perlerin

In this article, we briefly present two daytime fireball events that occurred in late winter of 2016. One event occurred in the United States and one in France. Both events generated hundreds of eyewitness reports via the IMO/AMS online fireball report and had the signs of meteorite dropping fireballs. The prospects for meteorite hunting were positive enough that expeditions to recover fragments from both events took place. The US effort resulted in the recovery of 6 meteorite fragments. The French event has yet to produce any meteorite finds. Here in we discuss some details of each event, the efforts undertaken to estimate the respective strewn fields and the fieldwork that followed.

Results from the CAMS Video Network

Peter Jenniskens

A status report is given on results from the CAMS meteoroid orbit and meteoroid spectroscopy survey. The survey detected some 230 meteor showers and shower components throughout the year. 70 of these are already in the IAU list of Established Meteor Showers, after 26 were verified by CAMS. An additional 55 previously known showers in need of confirmation were also validated. 19 new shower components were identified that are still in need of validation. Eighty six new showers were discovered, 54 of which were also found present in the SonotaCo meteoroid orbit database. There are ongoing efforts to expand the CAMS survey to sites spread in latitude and longitude.

Hemispherical radiating pattern antenna design for radio meteor observation

Jakub Kákona

A highly directional pattern antenna is usually used for radio meteor observations, but these types of antennas became impractical in cases where we have multiple transmitters spread around a reception station. In that situation the hemispherical sensitivity of the antenna is more important than directional antenna gain. We present a hemispherical radiation pattern antenna design which could be modified for almost any observational frequency reflective by a meteor trail. The symmetry of the radiation pattern of such antenna allows an easy construction of antenna arrays which could be used for the angular measurement of received signals.

Meteor trajectory estimation from radio meteor observations

Jakub Kákona

Radio meteor observation techniques are generally accepted as meteor counting methods useful mainly for meteor flux detection. Due to the technical progress in radio engineering and electronics a construction of a radio meteor detection network with software defined receivers has become possible. These receivers could be precisely time synchronized and could obtain data which provide us with more information than just the meteor count. We present a technique which is able to compute a meteor trajectory from the data recorded by multiple radio stations.

The multi-technique meteor observations in 2014

Anna Kartashova, Galina Bolgova, Yurij Rybnov, Olga Popova, and Dmitry Glazachev

Test multi-technique (optical and acoustical) meteor observations were organized by the Institute of Astronomy of the RAS (INASAN) and the Institute for Dynamics of Geospheres pf the RAS (IDG RAS) in 2014. The goal of our multi-technique meteor monitoring is to collect basic meteor observations and to study the formation and propagation of pressure pulses which are formed due to the interaction of meteoroids with the atmosphere.

A statistical approach to the temporal development of orbital associations

Daniel Kastinen and Johan Kero

We have performed preliminary studies on the use of a Monte-Carlo based statistical toolbox for small body solar system dynamics to find trends in the temporal development of orbital associations. As a part of this preliminary study four different similarity functions where implemented and applied to the 21P/Giacobini-Zinner meteoroid stream, and resulting simulated meteor showers. The simulations indicate that the temporal behavior of orbital element distributions in the meteoroid stream and the meteor shower differ on century size time scales. The configuration of the meteor shower remains compact for a long time and dissipates an order of magnitude slower than the stream. The main effect driving the shower dissipation is shown to be the addition of new trails to the stream.

The role of population in tracking meteorite falls in Africa

Fouad Khiri, Abderrahmane Ibhi, Thierry Saint-Gerand, Mohand Medjkane, and Lahcen Ouknine

The 158 African meteorite falls recorded during the period 1801 to 2014, account for more than 12.3% of all meteorite falls known from the world. Their rate is variable in time and in space. The number of falls continues to grow since 1860. They are concentrated in countries which exhibit large population (mainly rural population) with an uniform distribution. Generally, the number of falls follows the increase of the population density (coefficient of correlation $r = 0.98$). The colonial phenomenon, the education of population in this field, the population lifestyle and the rural exodus, are also factors among others which could explain the variability of the recovery of meteorite falls in Africa. In this note, we try by a statistical study, to examine the role of the African population in tracking meteorite falls on this continent.

Height computation of a fireball

Detlef Koschny

This article describes the first height computation of a bright fireball which the author performed in 1977.

Simultaneous analogue and digital observations and comparison of results

Pavel Koten, Rostislav Štork, Petr Páta, Karel Fliegel, and Stanislav Vítek

Double-station observations using analogue video cameras are carried out at the Ondřejov observatory since 1998. Recently new digital cameras MAIA were developed and introduced. Both systems are based on the same type of image intensifier. To evaluate the enhanced properties of the new cameras several simultaneous campaigns with both systems were accomplished.

Meteors and meteorites spectra

Jakub Koukal, Jiří Srba, Sylvie Gorková, Libor Lenža, Martin Ferus, Svatopluk Civiš, Antonín Knížek, Petr Kubelík, Tereza Kaiserová, and Pavel Váňa

The main goal of our meteor spectroscopy project is to better understand the physical and chemical properties of meteoroids. Astrometric and spectral observations of real meteors are obtained via spectroscopic CCD video systems. Processed meteor data are inserted to the EDMOND database (European viDeo MeteOr Network Database) together with spectral information. The fully analyzed atmospheric trajectory, orbit, and also spectra of a Leonid meteor/meteoroid captured in November 2015 are presented as an example. At the same time, our target is the systematization of spectroscopic emission lines for the comparative analysis of meteor spectra. Meteoroid plasma was simulated in a laboratory by laser ablation of meteorites samples using an (ArF) excimer laser and the LIDB (Laser Induced Dielectric Breakdown) in a low pressure atmosphere and various gases. The induced plasma emissions were simultaneously observed with the Echelle Spectrograph and the same CCD video spectral camera as used for real meteor registration. Measurements and analysis results for few selected meteorite samples are presented and discussed.

Retrieving meteoroids trajectories using BRAMS data: preliminary simulations

Hervé Lamy and Cédric Tétard

One of the main goals of the BRAMS project is to retrieve meteoroids trajectories from multi-station observations. In this paper a large number of meteoroid trajectories are simulated and several criteria are discussed to select trajectories compatible with multi-station observations. The criteria are the altitude of the specular reflection points, the minimum power detectable at a given station, and the time delays observed between appearances of meteor echoes at each receiving station. Finally, future improvements of these simulations are considered.

Easy way to estimate meteor brightness on TV frames

Vladislav A. Leonov and Alexander V. Bagrov

The traditional method of the meteor brightness measurements claims that the meteor brightness is equal to the stellar magnitude of a star that looks like a meteor in the brightest point of its track. This rule was convenient for the comparison of meteor observations by different observers and for the analysis of the brightness distributions of meteors from observed showers. This traditional method suffers from systematic errors, particularly those that arise from using stellar brightness measured in specific spectral wave bands different from the observer's ones, but mainly due to neglecting the influence of the meteor angular velocity on the real meteor brightness. To get a proper estimate of the meteor brightness that is a measure of the ground meteor illumination in the non-systematic units, an observer must take into account that the effective exposition of a meteor image in any resolution element of its track is a few times shorter than the corresponding exposition of a star image in the same frame. We propose a very simple method for improved estimations of meteor brightness by applying a correction to the meteor stellar magnitude obtained within the traditional framework.

Photometric stellar catalogue for TV meteor astronomy

Vladislav A. Leonov and Alexander V. Bagrov

Photometry for ordinary astrophysics was carefully developed for its own purposes. As stars radiation is very similar to the blackbody radiation, astronomers measure star illumination in wide or narrow calibrated spectral bands. This is enough for star photometry with precise accuracy and for measuring their light flux in these bands in energetic units. Meteors are moving objects and do not allow collection of more photons then they emit. So meteor observers use the whole spectral band that can be covered by sensitivity of their light sensors. This is why measurements of stellar magnitudes of background stars by these sensors are not the same as catalogued star brightness in standard photometric spectral bands. Here we present a special photometric catalogue of 93 bright non-variable stars of the northern hemisphere, that can be used by meteor observers of standard background whose brightness are calculated in energetic units as well as in non-systematic stellar magnitudes in spectral wavelength of the WATEC 902 sensitivity.

ROAN remote radio meteor detection sensor

Cezar Eduard Lesanu

Only few meteor enthusiasts across the world today, approaches systematically the radio meteor detection technique, one of the reasons being the difficulty to build and install proper permanent antennas, especially when low-VHF frequency opportunity transmitters are used as illuminators. Other reasons were in the past the relatively high cost of the entire system, receivers and computers, and not ultimately the high power consumption of the system in a 24/7 operation, when using regular personal computers. The situation changed in the recent years with the advent of the low cost software defined radio SDR receivers and low consumption/cost single board computers SBC. A commercial off-the-shelf hardware based remote radio meteor detection sensor is presented.

Calibration of occasionally taken images using principles of perspective

Esko Lyytinen and Maria Gritsevich

Recent years brought a large number of observational data of fireballs accidentally captured by dash-type cameras. In addition to directly measured azimuth-directions from satellite images, direct lines and their perspective properties can be used for the calibration of the camera. We have updated our calibration program taking this into account and we discuss the methods in this paper and we apply them to a recent case of a fireball seen in Thailand (September 7, 2015).

The KUT meteor radar: An educational low cost meteor observation system by radio forward scattering

Waleed Madkour and Masa-yuki Yamamoto

The Kochi University of Technology (KUT) meteor radar is an educational low cost observation system built at Kochi, Japan, by successive graduate students since 2004. The system takes advantage of the continuous VHFband beacon signal emitted from Fukui National College of Technology (FNCT) for scientific usage all over Japan by receiving the forward scattered signals. The system uses the classical forward scattering setup similar to the setup described by the International Meteor Organization (IMO), gradually developed from the most basic single antenna setup to the multi-site meteor path determination setup. The primary objective is to automate the observation of the meteor parameters continuously to provide amounts of data sufficient for statistical analysis. The developed software system automates the observation of the astronomical meteor parameters such as meteor direction, velocity and trajectory. Also, automated counting of meteor echoes and their durations are used to observe mesospheric ozone concentration by analyzing the duration distribution of different meteor showers. The meteor parameters observed and the methodology used for each are briefly summarized.

Meteor spectra using high definition video camera

Koji Maeda and Yasunori Fujiwara

We have carried out observations of meteor spectra using high-definition video camera systems in Japan and we present the first results using this system. The camera, α7s (Sony) had a 35-mm full-frame high sensitive CMOS sensor and could capture high-definition video. It was equipped with a 24-mm–50-mm lens and 300–600 grooves/mm grating. The detection of spectra was done by the UFOCaptureHD2 software (SonotaCo). The limiting magnitude for a meteor spectrum was around magnitude 0. We obtained more than three hundred meteor spectra within partial spectra during one year. The classification according to the main element (Mg, Na, Fe) abundances of meteors resulted in 91% of classifiable meteor belonging to the main stream type.

Effects of meteor head plasma distribution on radar cross sections and derived meteoroid masses

Robert A. Marshall, Sigrid Close, Peter Brown, and Yakov Dimant

We present calculations that relate meteor head echo radar cross sections to the meteor head plasma distribution. We use a forward model of radar scattering from meteor plasma using a finite-difference time-domain (FDTD) model of the electromagnetic wave interaction with the plasma. This model computes the meteor head RCS for a given meteor plasma distribution, specified with a peak plasma density and a characteristic size. We then relate measured RCS values to the input size and density parameters to better characterize the meteor plasma. We present simulation results that show that the RCS is directly related to the overdense meteor area; that is, the cross-section area of the meteor inside which the plasma frequency exceeds the radar frequency. This provides a direct estimate of the meteor plasma size from a given RCS measurement. Next we investigate the effect of the assumed plasma distribution. We study the RCS resulting from Gaussian, parabolic exponential, and $1/r^2$ distributions. Comparing the different calculated RCS from these different distributions to three-frequency head echo data from the CMOR radar, we show that the $1/r^2$ distribution provides the best fit to the data. However, given uncertainties in the data, we cannot conclude that any distribution is the most valid. In addition, we show that the choice of distribution assumed can alter the resulting line density q by an order of magnitude for the same data.

Numerical simulation of the BRAMS interferometer in Humain

Antonio Martínez Picar, Christophe Marqué, Cis Verbeeck, Stijn Calders, Sylvain Ranvier, Emmanuel Gamby, Michel Anciaux, Cédric Tétard, and Hervé Lamy

The Royal Belgian Institute for Space Aeronomy (BISA) operates a network for radio meteor studies based in Belgium. One of the receiving stations is located in the Humain Radio-Astronomy Station (HuRAS) and consists of an array of five 3-element Yagi antennas. In this paper the results of detailed numerical simulations are presented in order to obtain a first approach for the direction finding capability of this interferometer.

Construction of a meteor orbit calculation system for comprehensive meteor observation

Satoshi Mizumoto, Waleed Madkour and Masa-yuki Yamamoto Kochi University

At Kochi University of Technology (KUT), the development of an HRO (Ham-band Radio meteor Observation) - Interferometer (IF) was started in 2003, and we realized the meteor orbit calculation system by multiple-site radio observation with GPS time-keeping combining with the 5 channel (5ch) HRO-IF in 2012. Here, we introduce a future plan of comprehensive meteor observation by radio, optical, and infrasound observation.

Flux density, population index, perception coefficient, and the Moon

Sirko Molau

While analyzing sporadic meteors recorded by the IMO Video Meteor Network in the first half of 2015 we found systematic variations of the flux density and population index correlating with the lunar phase. At times of Full Moon, the measured flux density is 15% smaller than average, and at New Moon 15% higher. Likewise, the measured population index is 10% larger than the average at New Moon, and 10% smaller at Full Moon. While searching for the root cause of this systematic bias we analyzed two parameters in detail. If a perception coefficient is calculated and applied to each camera, the scatter in flux density can be reduced by 40% and the population index shows fewer outliers. However, the correlation with the lunar phase remains unaltered. Another parameter in question is the NoiseLevel segmentation threshold, which is applied when segmenting a background image for stellar limiting magnitude calculation. It could be shown that this threshold did not converge to a stable solution in the previous implementation of MetRec. An improved procedure is proposed, analyzed and implemented. Whether this solves the lunar phase correlation can only be answered when sufficient observations with the new software version are collected.

Current progress in the understanding of the physics of large bodies recorded by photographic and digital fireball networks

Manuel Moreno-Ibáñez, Maria Gritsevich, Josep Ma. Trigo-Rodríguez, and Esko Lyytinen

The basic equations of motion of a meteor in the atmosphere require a concise knowledge about the body physical properties, such as the bulk density, shape, mass, etc. These properties do change during the flight and they also depend on the observations' reliability and camera resolution. The usual way of tackling this problem relies on using average values which are retrieved either from previous experience or from the observations available from the astrometric reduction of each specific event. Alternatively, a different approach is suggested. Instead of using the average values as input data, all unknowns can be gathered into dimensionless parameters, retrievable from the observations with the help of inverse techniques. This methodology has already been implemented in several scientific studies. In order to demonstrate the applicability of the model, we have already used archived data from the Meteorite Observation and Recovery Project (MORP) operated in Canada between 1970 and 1985 as well as selected recent fireball records from the Spanish Fireball and Meteorite Recovery (SPMN) Network. Recently, a correction which accounts for real atmosphere conditions has also been successfully included in the model. Our next steps foresee fireball data processing obtained by the Finnish Fireball Network (FFN) and the SPMN.

Large meteoroid's impact damage: review of available impact hazard simulators

Manuel Moreno-Ibáñez, Maria Gritsevich, and Josep Ma. Trigo-Rodríguez

The damage caused by meter-sized meteoroids encountering the Earth is expected to be severe. Meteor-sized objects in heliocentric orbits can release energies higher than 10^8 J either in the upper atmosphere through an energetic airblast or, if reaching the surface, their impact may create a crater, provoke an earthquake or start up a tsunami. A limited variety of cases has been observed in the recent past (e.g., Tunguska, Carancas or Chelyabinsk). Hence, our knowledge has to be constrained with the help of theoretical studies and numerical simulations. There are several simulation programs which aim to forecast the impact consequences of such events. We have tested them using the recent case of the Chelyabinsk superbolide. Particularly, Chelyabinsk belongs to the ten to hundred meter-sized objects which constitute the main source of risk to Earth given the current difficulty in detecting them in advance. Furthermore, it was a detailed documented case, thus allowing us to properly check the accuracy of the studied simulators. As we present, these open simulators provide a first approximation of the impact consequences. However, all of them fail to accurately determine the caused damage. We explain the observed discrepancies between the observed and simulated consequences with the following consideration. The large amount of unknown properties of the potential impacting meteoroid, the atmospheric conditions, the flight dynamics and the uncertainty in the impact point itself hinder any modelling task. This difficulty can be partially overcome by reducing the number of unknowns using dimensional analysis and scaling laws. Despite the description of physical processes associated with atmospheric entry could be still further improved, we conclude that such approach would significantly improve the efficiency of the simulators.

Measurements of CCD optical linearity for magnitude determination during meteor observations

Andrey Murtazov and Alexander Efimov

The results of investigating the dependency "light flux - magnitude" are presented. This dependency is used to determine the meteor brightness on CCD frames. This dependency is shown to be linear with the signal-to-noise ratio exceeding 10 dB. However, with low signal-to-noise ratio it is non-linear. This should be taken into account while measuring the faint meteors on single frames.

Astronomy through the microscope: a workshop during the opening night of the 2016 IMC

Gert Jan Netjes and Sebastiaan de Vet

During the IMC, workshop meteoritical thins sections were shown live with a microscope connected to the beamer. This article will provide a background to thin sections, what we can learn from them and the tour through the Solar System we can take with them.

PaDe—The particle detection program

Theresa Ott, Esther Drolshagen, Detlef Koschny, and Bjoern Poppe

This paper introduces the Particle Detection program PaDe. Its aim is to analyze dust particles in the coma of the Jupiter-family comet 67P/Churyumov-Gerasimenko which were recorded by the two OSIRIS (Optical, Spectroscopic, and Infrared Remote Imaging System) cameras onboard the ESA spacecraft Rosetta, see, e.g., Keller et al. (2007). In addition to working with the Rosetta data, the code was modified to work with images from meteors. It was tested with data recorded by the ICCs (Intensified CCD Cameras) of the CILBO-System (Canary Island Long-Baseline Observatory) on the Canary Islands; compare Koschny et al. (2013). This paper presents a new method for the position determination of the observed meteors.

The PaDe program was written in Python 3.4. Its original intent is to find the trails of dust particles in space from the OSIRIS images. For that it determines the positions where the trail starts and ends. They were found using a fit following the so-called error function (Andrews, 1998) for the two edges of the profiles. The positions where the intensities fall to the half maximum were found to be the beginning and end of the particle. In the case of meteors, this method can be applied to find the leading edge of the meteor. The proposed method has the potential to increase the accuracy of the position determination of meteors dramatically. Other than the standard method of finding the photometric center, our method is not influenced by any trails or wakes behind the meteor. This paper presents first results of this ongoing work.

Evaluating video digitizer errors

Chris Peterson

Analog output video cameras remain popular for recording meteor data. Although these cameras uniformly employ electronic detectors with fixed pixel arrays, the digitization process requires resampling the horizontal lines as they are output in order to reconstruct the pixel data, usually resulting in a new data array of different horizontal dimensions than the native sensor. Pixel timing is not provided by the camera, and must be reconstructed based on line sync information embedded in the analog video signal. Using a technique based on hot pixels, I present evidence that jitter, sync detection, and other timing errors introduce both position and intensity errors which are not present in cameras which internally digitize their sensors and output the digital data directly.

Sungrazing comets and meteoroids

Eduard Pittich and Nina Solovaya

We studied the dynamical behavior of meteoroids ejected from sungrazing comets upon their arrival to the central part of the solar system. In order to get a clear insight into the geometry and detectability of such meteoroids, some model computations have been performed. It assumed that dust particles emitted from the comets with low velocity are affected by the gravitational forces of the Sun and planets, the Poynting-Robertson effect, and the pressure of the solar wind. Some of these particles come to the vicinity of the Earth, crossing its orbit, and can be candidates for collisions. Mean value of the orbital elements of the Kreutz sungrazers were applied for model computations.

Werkgroep Meteoren—70 years and counting

Urijan Poerink and Sebastiaan J. de Vet

In 2016, the Meteor Section of the Royal Dutch Association for Meteorology and Astronomy celebrated its 70 years' jubilee. In this paper we provide a brief historical narrative that incorporates the main developments and events of the Meteor Section, spanning seven decades of meteor observations in the Netherlands.

Novel methods for 3D numerical simulation of meteor radar reflections

Jukka Räbinä, Sanna Mönkölä, Tuomo Rossi, Johannes Markkanen, Maria Gritsevich, and Karri Muinonen

We use two novel methods for numerical simulation of meteor radar reflections. The one is based on the discrete exterior calculus, time-dependent simulations, and a control-based approach for accelerating the time evolution. The other is implemented as a time-harmonic solver based on the volume integral equation method for electric current. Despite the different framework, both methods give the solution in frequency domain. We model the radar reflections in a three-dimensional space as time-harmonic electromagnetic scattering from plasmatic obstacles. This makes our study different from the more conventional numerical simulations concerning scattering by a solid obstacle without a plasma model.

Meteor detections at the Metsähovi Fundamental Geodetic Research Station (Finland)

Arttu Raja-Halli, Maria Gritsevich, Jyri Näränen, Manuel Moreno-Ibáñez, Esko Lyytinen, Jenni Virtanen, Nataliya Zubko, Jouni Peltoniemi, and Markku Poutanen

We provide an overview and present some spectacular examples of the recent meteor observations at the Metsähovi Geodetic Research Station. In conjunction with the Finnish Fireball Network, the all-sky images are used to reconstruct atmospheric trajectories and to calculate the pre-impact meteor orbits in the Solar System. In addition, intensive collaborative work is pursued with the meteor research groups worldwide. We foresee great potential of this activity also for educational and outreach purposes.

An attempt to explain VLF propagation perturbations associated with single meteors

Jean-Louis Rault and Jean-Jacques Delcourt

A first evidence of sudden changes in the amplitude of distant VLF radio transmissions related to single meteors was found during Geminid 2010 meteor shower radio observations. Based on many similar observations gathered during different meteor showers, this paper is dedicated to the corresponding physical phenomena involved at the level of the D layer of the Earth ionosphere.

Sixty-five years of meteor radar research at Adelaide

Iain M. Reid and Joel Younger

Over 65 years of radar research using meteor radar at Adelaide University in Australia is very briefly reviewed.

Minor meteor shower activity

Jürgen Rendtel

Video meteor observations provide us with data to analyze structures in minor meteor showers or weak features in flux profiles. Samples obtained independently by other techniques allow to calibrate the data sets and to improve the confidence of results as demonstrated with a few results. Both, the confirmation of events predicted by model calculation and the input of observational data to improve the modelling results may help to better understand meteoroid stream evolution processes. Furthermore, calibrated data series can be used for studies of the long-term evolution of meteor shower activity.

The radio meteor signal path from transmitter to spectrogram: an overview

Tom Roelandts

In this paper, we present an overview of the radio meteor signal path, from the sinusoidal carrier wave that is initially transmitted, to the spectrogram that is typically used as the final result in the receiving chain. We describe the amplitude modulation and Doppler shift that is caused by the meteor, the combination of the reflected with the directly received signal at the antenna, the down conversion in the receiver, the sampling, and the down sampling in software. A simulation of the complete process results in detailed plots at each of these steps.

Status of the CAMS-BeNeLux Network

Paul Roggemans, Carl Johannink, and Martin Breukers

An overview is being given of the further expansion of the CAMS@BeNeLux network since the previous IMC, July 2015 until May 2016. The weather proved less favorable than in the year before, but thanks to a number of new cameras and extra observing stations, the overall performance of the network remained at the same level in spite of the often poor weather circumstances.

This paper compares the Kappa-Cygnids performance of 2015 with the analyses made for the 2014 data, following the same methodology. In 2015 the Kappa Cygnids were remarkable absent which confirms the periodic nature of the abundant Kappa-Cygnids display in 2014.

The CAMS@BeNeLux network was the first to draw attention to enhanced activity of the newly discovered Chi Cygnids meteor shower with 5 accurate orbits in the night of 14–15 September 2015. A search through a selection of all orbits of September 2015 yield 71 possible Chi Cygnid orbits of which 18 were selected to calculate the average orbital elements.

eMeteorNews: website and PDF journal

Paul Roggemans, Richard Kacerek, Jakub Koukal, Koen Miskotte, and Roman Piffl

Amateur meteor workers have always been interested to exchange information and experience. In the past this was only possible via personal contacts by letter or by specialized journals. With internet a much faster medium became available and plenty of websites, mailing lists, Facebook groups, etc., have been created in order to communicate about meteors. Today there is a wealth of meteor data circulating on internet, but the information is very scattered and not directly available to everyone. The authors have been considering how to organize an easy access to the many different meteor related publications. The best solution for the current needs of amateur meteor observers proved to be a dedicated website combined with a PDF journal, both being free available without any subscription fee or registration requirement. The authors decided to start with this project and in March 2016 the website meteornews.org has been created. A first issue of eMeteorNews was prepared in April 2016. The year 2016 will be a test period for this project. The mission statement of this project is: "Minimizing overhead and editorial constraints to assure a swift exchange of information dedicated to all fields of active amateur meteor work."

An overview of the CILBO spectral observation program

Regina Rudawska, Joe Zender, and Detlef Koschny

The video equipment can be easily adopted with a spectral grating to obtain spectral information from meteors. Therefore, in recent years, spectroscopic observations of meteors have become quite popular. The Meteor Research Group (MRG) of the European Space Agency has been working on upgrating the analysis of meteor spectra as well, operating image-intensified camera with objective grating (ICC8). ICC8 is located on Tenerife station of the double-station camera setup CILBO (Canary Island Long-Baseline Observatory). The pipeline software processes data with the standard calibration procedure (dark current, flat field, lens distortion corrections). While using the position of a meteor recorded by ICC7 camera (zero order), the position of the first order spectrum as a function of wavelength is computed. Moreover, thanks to the double meteor observations carried out by ICC7 (Tenerife) and ICC9 (La Palma), the trajectory of a meteor and its orbit is determined. This, merged with simultaneously measurement of meteor spectrum from ICC8, allow us to identify the source of the meteoroid. Here, we report on preliminary results from a sample of meteor spectra collected by CILBO-ICC8 camera since 2012.

ESA/ESTEC Meteor Research Group—behind the scenes

Regina Rudawska

The ESA/ESTEC Meteor Research Group consists of a team people with one goal: understand the effects of meteoric phenomena on planetary atmospheres and surfaces, as well as on spacecraft. The team carries out observational and theoretical studies in order to increase our knowledge of the small particle complex in the Solar System. This talk addresses a number of tasks within the group seen from a perspective of a research fellow.

Meteor reporting made easy—the Fireballs in the Sky smartphone app

Eleanor Sansom, Jay Ridgewell, Phil Bland, and Jonathan Paxman

Using smartphone technology, the award-winning "Fireballs in the Sky" app provides a new approach to public meteor reporting. Using the internal GPS and sensors of a smartphone, a user can record the start and end position of a meteor sighting with a background star field as reference. Animations are used to visualize the duration and characteristics of the meteor. The intuitive application can be used in situ, providing a more accurate eye witness account than after-the-fact reports (although reports may also be made through a website interface). Since its launch in 2013, the app has received over 2000 submissions, including 73 events which were reported by multiple users. The app database is linked to the Desert Fireball Network in Australia (DFN), meaning app reports can be confirmed by DFN observatories. Supporting features include an integrated meteor shower tool that provides updates on active showers, their visibility based on moon phase, as well as a tool to point the user toward the radiant. The locations of reports are also now shown on a live map on the Fireballs in the Sky webpage.

Croatian Meteor Network: ongoing work 2015–2016

Damir Šegon, Denis Vida, Korado Korlević, and Željko Andreić

Ongoing work of the Croatian Meteor Network (CMN) between the 2015 and 2016 International Meteor Conferences is presented. The current sky coverage is considered, software updates and updates of orbit catalogues are described. Furthermore, the work done on meteor shower searches, international collaborations as well as new fields of research are discussed. Finally, the educational efforts made by the CMN are described.

Fireballs from Australian Desert Fireball Network—search for similar orbits

Lukáš Shrbený, Pavel Spurný, and Phil A. Bland

We studied the fireball activity from the Desert Fireball Network records from 2006 to 2014 and identified a couple of time periods with increased number of fireballs. We searched for orbital similarities among the fireballs in these time periods and have found members of 10 individual meteor showers and two groups of similar orbits that do not correspond to any known meteor shower.

On the accuracy of orbits from video meteor observations

Ivica Skokić, Damir Šegon, and Goran Kurtović

The velocity limits of the meteor shower's geocentric velocity distribution from the CAMS meteoroid database were determined and used to calculate perturbed orbits. These were compared with the mean stream orbit using the DSH dissimilarity criterion. It was found that for the slow meteor showers (Alpha Capricornids and Geminids), the resulting orbits are within the generally accepted cutoff values for stream associations, while for the faster showers (Perseids, Orionids, and Quadrantids) the resulting orbits differ significantly from their mean stream orbit.

Collisional lifetimes of meteoroids

Rachel Halina Soja, G. J. Schwarzkopf, Maximilian Sommer, Jérémie Vaubaillon, Thomas Albin, Jens Rodmann, Eberhard Grün, and Ralf Srama

Collisions of meteoroids with interplanetary dust grain fragments particles, dispersing larger particles amongst lower mass intervals. Here we use the method of Grün et al. (1985) and the IMEM interplanetary dust model to calculate the collisional lifetimes for different orbits, and for particles in different meteor showers. The timescales are usually long—of order 10^4 years for 1 mm grains on Jupiter-family and Hally-type comet orbits. However, near-Sun orbits particles suffer more frequent collisions and therefore have much shorter lifetimes. We discuss factors that affect the accuracy of these calculations.

EN091214 Žd'ár—one of the most precisely documented meteorite fall

Pavel Spurný, Jiří Borovička, Jakub Haloda, Lukáš Shrbený, and Tomáš Zikmund

This contribution will provide an overview of the current status of fireball observations conducted by the Astronomical Institute of the Czech Academy of Sciences in Ondřejov and will bring a detailed analysis of the Žd'ár nad Sázavou meteorite fall in the Czech Republic on 9 December 2014, which is one of the most precisely determined and predicted meteorite fall in history.

The Swedish Allsky Meteor Network: first results

Eric Stempels and Johan Kero

The Swedish Allsky Meteor Network started operations with two cameras in early 2014 and has since grown steadily. Currently, seven stations are active and several more will come online in the near future. The network to a large degree relies on low-cost stations run by private individuals or small societies of amateur astronomers. Originally based on the Danish meteor network Stjerneskud, the central node of Uppsala University provides the network with the necessary infrastructure, such as a continually updated software distribution and automatic processing of data from all stations. Although covering a very large land mass with relatively low resources is challenging, there have up to now been several well-observed events, often in collaboration with observations from neighboring countries. We give a short overview of the network's current status, chosen technical solutions, and some results.

No sign of the 2015 Daytime Sextantids through combined radio observations

Giancarlo Tomezzoli and Lorenzo Barbieri

To investigate the presence or absence of the daytime Sextantids in the year 2015, the EurAstro Radio Station (EARS) in Munich (DE) performed a combined radio observation campaign together with the Radio Astronomy and Meteor Bologna (RAMBO) radio station located in Bologna (IT). The combined radio observations of EARS and RAMBO are in mutual agreement and confirm that, as in the year 2014, also in the year 2015 no evidence has existed of a meteor activity due the 2015 daytime Sextantids.

AMOS—trajectory and orbital data from SVMN and Canary Islands

Juraj Tóth, Leonard Kornoš, František Ďuriš, Pavol Zigo, Štefan Gajdoš, Dušan Kalmančok, Jozef Vilǵi, Jaroslav Šimon, Marek Buček, Miquel Serra-Ricart, Juan Carlos Perez, Javier Licandro, Ovidiu Vaduvescu, and Jürgen Rendtel

The Slovak Video Meteor Network based on four stations from October 2013 (double station from 2009) and two cameras on the Canary Islands from March 2015 have recorded several tens of thousands meteors by the end of 2015. Naturally, only a part (about 20%) was observed simultaneously. Using precise all-sky astrometry (Borovička, 1995) and our own trajectory and orbit program based on Ceplecha (1987), we gained the reliable video meteors database for further meteor studies.

Expedition Atacama—project AMOS in Chile

Juraj Tóth and Stanislav Kaniansky

The Slovak Video Meteor Network operates since 2009 (Tóth et al., 2011). It currently consists of four semiautomated all-sky video cameras, developed at the Astronomical Observatory in Modra, Comenius University in Bratislava, Slovakia. Two new generations of AMOS (All-sky Meteor Orbit System) cameras operate fully automatically at the Canary Islands, Tenerife and La Palma, since March 2015 (Tóth et al., 2015). As a logical step, we plan to cover the southern hemisphere from Chile. We present observational experiences in meteor astronomy from the Atacama Desert and other astronomical sites in Chile. This summary of the observations lists meteor spectra records (26) between November 5–13, 2015, mostly Taurid meteors, single- and double-station meteors as well as the first light from the permanent AMOS stations in Chile.

AMOS-Spec—meteor spectra from Modra Observatory

Juraj Tóth, Pavol Matlovič, Regina Rudawska, Pavol Zigo, and Dušan Kalmančok

We present results from the meteor spectra program at Modra observatory, Slovakia (Comenius University in Bratislava) in the period November 2013–April 2016. The advantage of the program is the presence of the Slovak Video Meteor Network and close collaboration with the European Fireball Network and CEMENt and EDMONd networks which provide trajectory and orbital data for almost all observed meteor spectra.

Rediscovery of Polish meteorites

Zbigniew Tymiński, Marcin Stolarz, Przemysław Żołądek, Mariusz Wiśniewski, and Arkadiusz Olech

The total number of Polish registered meteorites (by July 2016) including the meteoritical artifacts as Czestochowa Raków I and II is 22. Most of them are described by the pioneer of Polish Meteoritics Jerzy Pokrzywnicki who also identified the meteorite fall locations. In recent years prospectors found impressive specimens of known Polish meteorites such as Morasko: 34 kg, 50 kg, 164 kg, 174 kg and 261 kg or Pultusk: 1578 g, 1576 g, 1510 g, 610 g and 580 g expanding and determining precisely the known meteorite strewn fields.

A (revised) confidence index for the forecasting of meteor showers

Jérémie Vaubaillon

A confidence index for the forecasting of meteor showers is presented. The goal is to provide users with information regarding the way the forecasting is performed, so several degrees of confidence is achieved. This paper presents the meaning of the index coding system.

Software for Analysis of Visual Meteor Data: R package MetFns—workshop report

Kristina Veljković

New version of the package MetFns for analysis of visual meteor data, written in statistical software R, was presented on the workshop.

Summary of the Open Session at the IMC 2016

Cis Verbeeck, Megan Argo, Peter Brown, Sirko Molau, Jürgen Rendtel, and Antonio Martínez Picar

The Open Session at the IMC 2016 took place on Friday, June 3rd, 2016, evening (21:30-22:30), and was intended to accommodate beginners' questions about meteor astronomy. Megan Argo moderated a panel of experts, consisting of Peter Brown, Sirko Molau, Jürgen Rendtel, and Antonio Martínez Picar.

Open-source meteor detection software for low-cost single-board computers

Denis Vida, Dario Zubović, Damir Šegon, Peter Gural, and Robert Cupec

This work aims to overcome the current price threshold of meteor stations which can sometimes deter meteor enthusiasts from owning one. In recent years small card-sized computers became widely available and are used for numerous applications. To utilize such computers for meteor work, software which can run on them is needed. In this paper we present a detailed description of newly-developed open-source software for fireball and meteor detection optimized for running on low-cost single board computers. Furthermore, an update on the development of automated open-source software which will handle video capture, fireball, and meteor detection, astrometry and photometry is given.

Big data era in meteor science

Dejan Vinković, Maria Gritsevich, Vladimir Srećković, Bojan Pečnik, Gyula Szabó, Victor Debattista, Petr Škoda, Ashish Mahabal, Jouni Peltoniemi, Sanna Mönkölä, Areg Mickaelian, Esa Turunen, Jakub Kákona, Jarkko Koskinen, and Victor Grokhovsky

Over the last couple of decades technological advancements in observational techniques in meteor science have yielded drastic improvements in the quality, quantity, and diversity of meteor data, while even more ambitious instruments are about to become operational. This empowers meteor science to boost its experimental and theoretical horizons and seek more advanced science goals. We review some of the developments that push meteor science into the big data era that requires more complex methodological approaches through interdisciplinary collaborations with other branches of physics and computer science. We argue that meteor science should become an integral part of large surveys in astronomy, aeronomy and space physics, and tackle the complexity of micro-physics of meteor plasma and its interaction with the atmosphere.

Statistical approach to meteoroid shape estimation

Vladimir Vinnikov, Maria Gritsevich, Daria Kuznetsova, Olga Krivonosova, Dmitry Zhilenko, and Leonid Turchak

This paper describes a statistically-based technique for meteoroid shape estimation. The idea to obtain the preentry shape from a distribution of fragment masses is derived from the experiments on brittle fracturing, that produce multiple fragments of sizes less than or equal to the least dimension of the body. The fragment masses determine the number of fragments as a power law with exponential cutoff. The initial form of the fragmented body is essentially indicated by the value of this scaling exponent.

Catalogue of representative meteor spectra

Vlastimil Vojáček, Jiří Borovička, Pavel Koten, Pavel Spurný, and Rostislav Štork

We present a library of low-resolution meteor spectra that includes sporadic meteors, members of minor meteor showers, and major meteor showers. These meteors are in the magnitude range from +2 to −3, corresponding to meteoroid sizes from 1 mm to 10 mm. This catalogue is available online at the CDS for those interested in video meteor spectra.

2014 Southern δ-Aquariid observing campaign—carried out from Crete

Thomas Weiland

With a peak ZHR of 15–20 at the end of July, the Southern δ-Aquariids rank as a major annual shower, but observation is often neglected in favor of the much more active Perseids of August, mainly as a consequence of their southerly radiant, which makes the stream a prominent target from low latitudes and the southern hemisphere. The extended activity period of more than a month, lacking a distinctive peak, and the paucity of bright meteors does not enhance interest of most observers, either. Nevertheless, one has not to go too far south in order to monitor the stream properly to gain scientific results. The Greek island of Crete, at the southernmost tip of Europe, is such a place, offering sufficiently dark skies and a 90% probability of clear weather in July and August. Encouraged by a New Moon on July 26th an eight-night-long visual observing campaign was carried out in 2014. As a consequence, I managed to record nearly 250 Southern δ-Aquariids within 40 hours of effective observing time. An impression of the campaign together with a summary of the results is presented.

Current status of Polish Fireball Network

Mariusz Wiśniewski, Przemysław Żołądek, Arkadiusz Olech, Zbigniew Tymiński, Maciej Maciejewski, Karol Fietkiewicz, Mariusz Gozdalski, Marcin Przemysław Gawroński, Tomasz Suchodolski, Maciej Myszkiewicz, Marcin Stolarz, and Krzysztof Polakowski

The PFN started in March 2004. Most of its observers are amateurs, members of the Comets and Meteors Workshop. The network consists of 40 continuously working stations, where nearly 80 sensitive CCTV video and digital cameras operate. During the years 2011–2015, PFN cameras recorded 215049 single events. Using these data. 34 608 trajectories and orbits have been calculated.

Space fireworks for upper atmospheric wind measurements by sounding rocket experiments

Masa-yuki Yamamoto

Artificial meteor trains generated by chemical releases by using sounding rockets flown in upper atmosphere were successfully observed by multiple sites on ground and from an aircraft. We have started the rocket experiment campaign since 2007 and call it "Space fireworks" as it illuminates resonance scattering light from the released gas under sunlit/moonlit condition. By using this method, we have acquired a new technique to derive upper-atmospheric wind profiles in twilight condition as well as in moonlit night and even in daytime. Magnificent artificial meteor train images with the surrounding physics and dynamics in the upper atmosphere where the meteors usually appear will be introduced by using fruitful results by the "Space firework" sounding rocket experiments in this decade.

Exploring the relationship between meteor parameters based on photographic data

Yulia Yancheva, Simona Hristova, and Eva Bojurova

The paper presents an attempt to investigate the relationship between the luminosity and the linear length of the meteors, based on photographic observations of the Geminid meteor shower during the night of maximum in December 2015.

Radar observations of the Volantids meteor shower

Joel Younger, Iain Reid, and Damian Murphy

A new meteor shower occurring for the first time on 31 December 2015 in the constellation Volans was identified by the CAMS meteor video network in New Zealand. Data from two VHF meteor radars located in Australia and Antarctica have been analyzed using the great circle method to search for Volantids activity. The new shower was found to be active for at least three days over the period 31 December 2015–2 January 2016, peaking at an apparent radiant of $\alpha = 119\overset{\circ}{.}3 \pm 3\overset{\circ}{.}7$ and $\delta = -74\overset{\circ}{.}5 \pm 1\overset{\circ}{.}9$ on January 1st. Measurements of meteoroid velocity were made using the Fresnel transform technique, yielding a geocentric shower velocity of 28.1 ± 1.8 km s^{-1}. The orbital parameters for the parent stream are estimated to be $a = 2.11$ AU, $e = 0.568$, $i = 47\overset{\circ}{.}2$, with a perihelion distance of $q = 0.970$ AU.

Taurids 2015

Przemysław Żołądek, Arkadiusz Olech, Mariusz Wiśniewski, Regina Rudawska, Marcin Bęben, Tomasz Krzyżanowski, Maciej Myszkiewicz, Marcin Stolarz, Marcin Gawroński, Mariusz Gozdalski, Tomasz Suchodolski, Walburga Węgrzyk, and Zbigniew Tymiński

Enhanced activity of the Southern Taurids has been detected in the evening of 31 October 2015. Polish Fireball Network cameras detected several bright meteors and fireballs including extremely bright events at $18^{\rm h}05^{\rm m}$ UT and $23^{\rm h}13^{\rm m}$ UT. Trajectories and orbital elements have been calculated, the orbits of both fireballs have been compared with the NEO orbital database. Three asteroids on very similar orbits have been found—2015TX24, 2005UR, and 2015TF50. All these bodies have orbital periods close to a 7:2 resonance with Jupiter.

International Meteor Conference 2017, Petnica, Serbia, September 21–24, 2017

Dušan Pavlović, Snežana Todorović, and Miroslav Živanović

The International Meteor Conference 2017 will be hosted by Petnica Science Center in Petnica, a village near the city of Valjevo, Serbia, from September 21 to September 24, 2017. Here we present some basic information about this conference, as presented at the International Meteor Conference 2016 in Egmond, the Netherlands.

Meteor Science

Research on the IAU meteor shower database

Masahiro Koseki[1]

We are apt to consider the IAU Shower Database (2016 March 17, abbreviated SD hereafter) as the most reliable reference for meteor observations especially for the 'established showers', but it includes many problematic data. We found many input errors, misprints, and confusion in the identification of meteor showers. First, we see a lack of a consistent use of expressions. Second, we find many data errors which we tried to detect and remove by recalculating the orbits based on the radiant data and vice versa the radiants from the orbits. Third, there is a mixture of the definition of showers. In order to check the consistency of shower identifications, we compute the distance of all combinations of the SD entries except for the insufficient data entries by using the Southworth-Hawkins D-criterion. There are many showers which have nearer neighbours than entries of the shower itself. This work shows the results of the investigations for the 'established showers'. It is recommended to use the SD to search the collected data and not to use it as a confirmed and solid list. The author intends to stimulate discussion of the term 'established shower'.

Received 2016 August 30

1 Introduction

I am a member of the 'Working Group on Meteor Shower Nomenclature (2015–2018)' as an IMO representative because I published several papers on meteor showers in WGN. The following explanation for the group is published at the site of the nomenclature working group (`http://www.ta3.sk/IAUC22DB/MDC2007/Dokumenty/task_group.php`): The commission has established a Working Group on Meteor Shower Nomenclature with the objective to formulate a descriptive list of established meteor showers that can receive official names during the next IAU General Assembly. This task aims to uniquely identify all existing meteor showers and establish unique names: as an example of the value of such a definitive catalogue would be to facilitate the establishment of associations between meteor showers and parent bodies among the many Near-Earth Objects that are being discovered.

Although a definitive catalogue should be the goal, I found obvious errors in the SD while I investigated data of meteor showers, the results of which were published somewhere in WGN. It is necessary to find and clarify the problematic information and to publish them e.g. in WGN. Here, we investigate the problems found in the version of 2016 March 17 and compare them with the 2015 September 19 version. In this paper, we use the designation IAUNo+Code+AdNo, where AdNo refers to the line in the respective SD entry (starting with AdNo=0).

2 Problematic data entries in the SD

2.1 Insufficient entries

There are 25 entries lacking orbital data, as well as radiant point and/or geocentric velocity. We cannot calculate their orbital elements and use them for further researches because they are insufficient or incomplete. This concerns the following entries (IAUNo+Code+AdNo):

014XOR0, 029DLE0, 030PSC0, 050VIR0, 095DCA0, 110AAN0, 118GNO0, 160OSC0, 163SAG0, 247TAU0, 290ALL0, 291GVR0, 292OPH0, 293.DCE0, 294DMA0, 295JAQ0, 296SIS0, 297DAQ0, 298IAQ0, 299OAR0, 306COL0, 310APY0, 313ECR, 316BHD0, 503NNA0.

Hence, we can examine 1159 entries in sections 2.6 and 3, although the 2016 March 17 version has 1184 entries.

2.2 Discrepancy between the peak activity and the node

The ecliptic longitude of the Sun at the peak shower activity ($\lambda_\odot$) disagrees with the longitude of the ascending node (Ω) in many entries. Table 1 shows the difference between the listed $\lambda_\odot$ and the supposed peak activity ($\lambda'_\odot$) by Ω except for 18 entries lacking the peak or the node.

When we calculate the orbit based on the radiant point and the geocentric velocity with the listed $\lambda_\odot$, this discrepancy leads to somewhat different orbits compared to the listed data. Table 2 shows the recalculated result with the listed elements of 011EVI1 as an example. It is obvious that the radiant data $(\alpha, \delta, V_g, \lambda_\odot)$ disagree with the elements. If we estimate the radiant from the orbit, we will get a wrong radiant. The SD might use adopted $\lambda_\odot$ using a different source or observations from the listed orbits.

We had better been careful to observe the shower at the supposed maximum, because the listed $\lambda_\odot$ in the SD may be adopted values not coinciding in time between the radiant and the orbit. We show that the entries need careful attention in Table 3. There are ten entries with $|\lambda_\odot - \lambda'_\odot| > 50$. The misprints or the erroneous $\lambda_\odot$ or Ω (the node should be reversed because of the radiant point location) cause these large deviations (see 2.6).

[1]The Nippon Meteor Society (NMS), 4-3-5Annaka, Annaka-shi, Gunma-ken, 379-0116 Japan. Email: `geh04301@nifty.ne.jp`

IMO bibcode WGN-445-koseki-iau
NASA-ADS bibcode 2016JIMO...44..151K

Table 1 – The difference between the peak shower activity and the node shown in degrees.

Difference	0	< 0.1	< 0.2	< 0.3	< 0.4	< 0.5	< 1	< 2	< 3	< 4	< 5	< 10	< 20	< 30	< 40	< 50	$50 <$
N	583	43	71	84	61	49	111	49	20	14	11	35	16	8	1	0	10

Table 2 – The first line shows the listed values (except for the eccentricity: the eccentricity given here is calculated from the perihelion distance and the semi-major axis. The SD does not give the eccentricity in several cases and we discuss this problem later). The second line gives the recalculated results from radiant data based on the listed $\lambda_\odot$ and the third line based on the suggested $\lambda'_\odot$ by the ascending node.

Code	α	δ	V_g	$\lambda_\odot$	e	q	i	ω	Ω	a
011EVI1	174.3	4.7	34.2	354	0.911	0.234	3.5	308.0	334.5	2.637
				354	1.160	0.485	2.3	267.4	354.0	−3.038
				334.5	0.904	0.217	3.6	310.1	334.5	2.271

Table 3 – The entries with $|\lambda_\odot - \lambda'_\odot| > 5$ (listed peak of shower activity ($\lambda_\odot$) deviates from the node by more than 5 degrees).

	$\lambda_\odot$	$\lambda'_\odot$	$\lvert\lambda_\odot - \lambda'_\odot\rvert$
002STA0	224	217.3	6.7
005SDA0	125.6	132.2	6.6
011EVI0	354	280.5	73.5
011EVI1	354	334.5	19.5
012KCG1	145.2	139.4	5.8
017NTA1	224	212.7	11.3
020COM0	274	283.3	9.3
039NAL0	349	173.9	175.1
055ASC1	55.2	42.7	12.5
065GDE0	80.4	87.0	6.6
067NSA0	78	91.7	13.7
069SSG0	78	99.4	21.4
076KAQ1	179	186.6	7.6
083OCG0	206	195.9	10.1
091JZA0	292	299.1	7.1
093VEL1	296	325.7	29.7
093VEL2	296	323.7	27.7
097SCC0	296.3	306.9	10.6
098ECO0	307.1	294.1	13.0
100XSA0	304.9	296.0	8.9
103TCE1	321	330.7	9.7
103TCE2	321	326.7	5.7
105OCN0	323.4	311	12.4
105OCN3	323.4	302.7	20.7
105OCN4	323.4	299.7	23.7
113SDL0	326.4	146.4	180.0
125SAL0	358.8	178.8	180.0
126SGE0	1	332.9	28.1
135SGV0	22.7	32.7	10.0
137PPU0	33.6	213.64	180.0
138ABO0	36.7	29.2	7.5
139GLI0	39	15.9	23.1
140XLI0	39	28.6	10.4
142MDR0	29.2	19.9	9.3
147PAQ0	60	239.7	179.7
150SOP0	56.7	236.7	180.0
157ICA0	62	56.7	5.3
173BTA0	96.7	102.7	6.0
195BIN0	157.3	165.7	8.4
203GLE0	148.7	141.8	6.9
214BCP0	167.7	327.7	160.0
215NPI3	184	174.4	9.6
217OPC0	174	183	9.0
220NDR0	170.3	162.6	7.7
223GVI0	184	165.8	18.2
232BCN0	213	204.7	8.3
234EPC0	195	188.2	6.8
235LCY0	199	189.6	9.4
236GPS0	200	229.8	29.8
239GPU0	202.7	238	35.3
243ZCN0	225	235.4	10.4
244PAR0	227	219.3	7.7
248IAR0	233.6	222.3	11.3
250NOO1	245	240	5.0
258DAR0	262.2	270.0	7.8
267JNO0	307.9	292.5	15.4
270FAO0	318	138	180.0
273PBO0	42.1	53.6	11.5
274NUM0	54.4	44.3	10.1
289DNA0	256.5	251.1	5.4
325DLT0	85.5	181.7	96.2
347BPG0	36.0	30.0	6.0
484IOA0	234.7	200.4	34.3
507UAN1	96	101.0	5.0
533JXA2	119	112.7	6.3
549FAN1	112	118.0	6.0
624OAR0	295.0	204.4	90.6
644JLL0	288	277.7	10.3
645PHC0	13	195.0	178.0
715ACL0	183	189.6	6.6

2.3 Lack of the eccentricity

241 entries lack the eccentricity data, though showing other orbital elements, but they are given in the original paper for almost all entries. It seems that Jenniskens omitted the eccentricity in his 'working list' (Jenniskens, 2006) and the IAUMDC followed his work. The eccentricity used in section 3.1 is calculated from the perihelion distance and the semi-major axis, because these supplementary eccentricities are sufficiently accurate for such a survey.

Table 4 – The first line shows the IAU SD entry and the second line gives the data published in the original paper.

LP	Code	α	δ	V_g	$\lambda_\odot$	e	q	i	ω	Ω	a	Reference
00014	003SIA0	334.7	−14.2	33.8	131.7		0.208	6.9	131.8	311.7	2.364	Cook, 1973 (IAU)
		333.3	−14.7	33.8	131.0	0.912	0.208	6.9	131.8	311.0	2.36	Cook, 1973 (orig.)

Table 5 – The differences between listed orbital elements and recalculated ones. The third columns exclude the numbers already counted in the second columns and so on; for $|\Delta e|$, 73 is the number of entries with the difference between 0.01 and 0.02, etc.

	No data	< 0.01	< 0.02	< 0.03	< 0.04	< 0.05	< 0.1	< 0.2	< 0.3	< 0.4	< 0.5	$0.5 <$
$\|\Delta e\|$	438	565	73	42	25	13	20	5	1	0	0	2
$\|\Delta q\|$	196	824	76	35	16	6	18	8	3	0	0	2
	No data	< 1	< 2	< 3	< 4	< 5	< 10	< 20	< 30	< 40	< 50	$50 <$
$\|\Delta i\|$	184	896	46	22	10	6	8	4	3	1	2	2
$\|\Delta\omega\|$	186	698	145	44	40	18	25	13	4	3	0	8
$\|\Delta\Omega\|$	180	979	1	1	0	1	4	4	1	1	0	12

2.4 B1950.0 or J2000.0

In the SD we find data referring to different equinoxes. The radiant coordinates and the nodes are converted to J2000.0 but the inclination and the argument of the perihelion remain at B1950.0 in many cases. Table 4 shows this disorder for an example. Cook used B1950.0 and the second line gives his original value. The SD changes the radiant point and the node into J2000.0 but other elements remain in the B1950.0 system. There are other types of equinox discrepancies in the SD. However, we use the listed values as they are in section 3.1, because these small changes do not cause important differences for this survey.

2.5 Parentheses: velocity in the geocentric velocity column with parentheses gives pre-atmospheric ones

The SD lists several values in parentheses. If we download the list in `.csv` format and convert it to an EXCEL file, EXCEL would change values with parentheses to negative ones automatically. We need to treat the downloaded file as text and check what the parentheses mean. Some of them might indeed mean the supposed value but giving the pre-atmospheric velocity instead of the geocentric velocity.

2.6 Mistypes in the SD, misprints in the original paper(s) and unknown discrepancies

We find odd entries in the SD: the original paper did not include the listed value, some values are set into a different column, a listed data set does not exist in the original paper and so on. Therefore, we need to check the consistency of radiant data with the orbit: we recalculate its orbit based on radiant data $(\alpha, \delta, V_g, \lambda_\odot)$ and, moreover, recalculate the radiant from the listed orbit.

2.6.1 Recalculation of orbits

The SD lists the adopted solar longitudes $\lambda_\odot$ in some cases as discussed in 2.2 (see Table 2). For calculating the orbit, we use the solar longitude of the peak activity estimated from the node and not the listed $\lambda_\odot$. The first column 'No data' in Table 5 shows the number of entries which lack the orbital element or data needed for the orbit recalculation. Again, we notice many entries which lack the eccentricity, that is more than two times larger than the number with missing other elements. There are more than 180 entries which lack the radiant and/or the geocentric velocity data needed for the recalculation. The second column (< 0.01 to < 1) shows the number of entries for which the recalculated element almost coincides with the listed values; for the eccentricity $|\Delta e|$ and the perihelion distance $|\Delta q|$ the entries of the difference between the recalculated ones and the listed values less than 0.01 are 565 and 196, respectively, and the inclination $|\Delta i|$, the argument of the perihelion $|\Delta\omega|$ and the ascending node $|\Delta\Omega|$ the entries of the differences less than 5 degrees are 184, 186 and 180 respectively. The third columns are the number between the second and fourth columns and so on; for $|\Delta e|$ the entries with a difference between 0.01 and 0.02 are 73.

We can see the most part of the SD radiant data are consistent with the elements, but it is necessary to note the number of entries in discordance is not so little.

2.6.2 Recalculation of radiant positions

Though there are many radiant position (RP) calculation methods, the most simple and effective way is the altering of the argument of perihelion in order to intersect the meteoroid orbit with the orbit of the Earth. Table 6 shows the comparison between the listed values and recalculated ones. It is clear that the major part of the SD is in accordance within the data set. Although we know that the radiant near the antiapex might be diffuse with small changes in the orbital elements (e.g. Kresak, 1970), several entries are beyond our sense – cannot be understood.

2.6.3 Discrepancies in the SD

Here we examine the questionable entries discussed in the preceding two sections in detail. The results are shown in Table 7 and the note to the Table 7. Problematic data are shown in italics and the underlined

Table 6 – Differences between the listed RPs and geocentric velocities and the recalculated values. The units of ΔV_g are km/s and ΔRP means the distance in degrees between the listed RP and the recalculated one.

	No data	< 0.1	< 0.2	< 0.3	< 0.4	< 0.5	< 1	< 2	< 3	< 4	< 5	$5 <$
ΔV_g	30	796	125	74	37	25	60	25	4	7	0	1
	No data	< 1	< 2	< 3	< 4	< 5	< 10	< 20	< 30	< 40	< 50	$50 <$
ΔRP	26	917	128	46	22	11	19	9	1	1	1	3

lines indicate the data which disagree for the radiant and the orbit. References are shortened and websites shown in the SD are listed in the note. We use the suggested values of the note to calculate D_{SH} in the next section 3.

3 Confusion of the classification of established meteor showers

The differences in the perception of a 'meteor shower' cause the confusion on the one hand. Differences in the detection methods, depending on the conception, play a more important role in the problems on the other hand (Koseki, 2014a). Some use the distribution of radiants while others use the similarity in orbits to detect the showers. We apply the Southworth-Hawkins criterion $D_{\rm SH}$ (Southworth and Hawkins, 1963) to check the consistency of streams in the SD and found many problematic combinations of meteor shower entries. The author would like to focus on the so-called 'established meteor showers', because showers in the 'working list' are less clear naturally.

3.1 $D_{\rm SH}$ distribution within individual showers

We saw the problematic data entries in the SD and, therefore, the following studies use the correction by the author (see 2.6.3: Table 7 and the notes). There remains a small number of entries having discrepancies between the radiant data and the orbital elements. Nothing has been done in these cases because it is unknown why such discrepancies are caused and where the errors are. There are several entries with no given orbital data although radiant data are listed. Then the orbits calculated from radiant data by the author (see 2.6.1) are used for such entries to compute $D_{\rm SH}$.

The SD includes 112 established meteor showers. Among these, there are 10 showers with only one member (i.e. with only one listed orbit) and 36 showers with only two members. Hence the term 'established showers' does not mean confirmed showers by multiple observations, that is, by other techniques or at different opportunities. Table 8 gives the summary of the minimum, the maximum and the neighbours $D_{\rm SH}$ distributions for the established showers. We can see the minimum $D_{\rm SH}$ of 12 showers out of 102 and the maximum of 31 showers out of 66 are over 0.2 and, in contrast to this, 55 showers out of 112 have $D_{\rm SH} < 0.2$ to neighbouring showers. The discrimination level might be set at $D_{\rm SH} < 0.2$, though $D_{\rm SH} < 0.2$ is the condition for the classification of individual meteors to a meteor shower (Southworth and Hawkins, 1963) and not for the discrimination between the mean orbits, though $D_{\rm SH}$ is only a suggestive measure discriminating meteors between meteor showers. Table 8 indicates there is no objective standard for meteor shower classification. We investigate several interesting cases including 19 meteoroid streams having nearer neighbour(s) than their self kin below and consider what is necessary to do for the SD.

3.2 Typical examples of problematic classification

3.2.1 Alpha-Capricornids as an example for a representative stream

It is said that the α-Capricornids are a complex ecliptic stream (Lindblad, 1971b). The SD includes 9 entries as shown in Table 9 and they are in good agreement with each other. But there are 5 entries with $D(A, B) < 0.2$ for 001CAP0, namely 0692EQA0 (0.095), 623XTC0 (0.099), 467ANA0 (0.136), 467ANA1 (0.156), 472ATA1 (0.158). Especially, 623XTC0 enters the 001CAP region; 623XTC0 (0.050) for 1CAP1. It is necessary to study whether these streams are independent and not just occasional coincidences.

3.2.2 Southern and Northern ι-Aquariids

The original 'Southern ι-Aquarids' noticed by Wright et al. (1957) are close to 003SIA and this former 033NIA seems to be more active than the recently observed 033NIA. The Southern ι-Aquariids were once called an 'established shower' and degraded to 'working list' though $D_{\rm SH}$ distances within 003SIA are small enough. The reason for the degradation and the elimination is not clear. 003SIA2 (Brown et al., 2008: CMOR1) was stated as 'removed' and another SIA of CMOR2 (Brown et al., 2010) are not referred to in 003SIA. There are several sources called 'Southern ι-Aquarids' (Table 10) and they are not referred to in the SD though some of them might be included to 003SIA.

The Northern ι-Aquariids describe late July to early August activities in Aquarius naturally (Wright et al., 1957) but are now used for late August activities. They have a difference in age by more than 50 years and these old and new activities may be different. Meteor activities in the antihelion region (ANT) area are very complex and the ι-Aquariid activity is just above the background. The old term 'Northern ι-Aquarids' suggests there might be two different activities: one occurs at $\lambda_\odot < 130$ and another at $\lambda_\odot > 150$ (Table 11).

The similarities between listed 033NIA members are not good (Table 12) and there are nearby activities earlier and later: $D_{\rm SH}$(33NIA0, 473LAQ1) = 0.118, $D_{\rm SH}$(33NIA2, 215NPI0) = 0.088. Members of 033NIA listed in the SD might be divided into two or three

Table 7 – The problematic data in the SD.

Code	α	δ	V_g	$\lambda_\odot$	e	q	i	ω	Ω	a	Reference
001CAP2	*303.4*	*–10.6*	*22.2*	*123.8*	*0.766*	*0.594*	*7.2*	*267.6*	*123.8*	*2.540*	Hasegawa, 2001
001CAP6	305.7	−9.4	22.4	126.1	*0.770*	*0.586*	*7.4*	*268.4*	*127.9*		SonotaCo, 2009
003SIA1	339.0	–15.6	34.8	126.9	0.929	0.190	8.6	137.5	306.9	2.676	Dutch Meteor Society 2001
005SDA3	*333.7*	−16.1	41.4	125.6	0.976	0.069	27.2	152.8	305.6	2.875	Cook, 1973
007PER6	48.2	58.1	*59. 1*	140.0	0.950	0.949	113.1	150.4	139.3	9.57	Jenniskens et al., 2016
011EVI0	182.1	2.6	29.2	280.5	0.851	0.382	3.5	*349.1*	*280.5*	2.562	Jenniskens, 2006
020COM1	159.7	31.6	63.0	265.7		*0.541*	*139.4*	*265.0*	*283.3*	*14.4*	SonotaCo, 2009
020COM6	163.7	*39.7*	64	261.7		*0.81*	138	249	261.7	*3.76*	Kashcheyev and Lebedinets, 1967
026NDA2	*339.6*	*–4.7*	*42.3*	139.6	0.973	0.070	20.4	332.6	139.6	2.62	Jacchia, 1963
031ETA4	338.3	−0.8	65.4	46.3	*0.968*	*0.662*	*166.1*	*107.9*	*58.1*	*20.881*	SonotaCo, 2009
032DLM1	163.7	*39.7*	64	261.7		*0.81*	138	249	261.7	*3.76*	Kashcheyev and Lebedinets, 1967
033NIA0	328.4	−5.6	31.2	*147.7*	0.84	0.260	5.0	308.0	147.7	*1.625*	Cook, 1973
033NIA1	*328*	−4.7	27.6	145.1	0.852	0.358	7.4	297.4	145.1	2.419	Dutch Meteor Society 2001
039NAL0	158.7	31	11.1	173.9	0.550	0.907	6.9	*43.3*	*173.9*	2.016	Jenniskens, 2006
045PDF0	267.1	69.4	22.9	8.3		0.995	36.3	*1793*	8.3	3.020	Jenniskens, 2006
052OUM0	174.7	66.7	*27.1*	66.3	0.653	1.017	16.7	170.5	66.3	2.93	Lindblad, 1971b
083OCG0	*317.8*	*52.6*	*17.2*	*195.9*	*0.647*	*0.976*	*25.0*	*198.6*	*195.9*	*2.764*	Sekanina, 1973
091JZA0	70.3	60.1	12.1	299.1	*0.758*	*0.643*	11.6	209.3	299.1	2.653	Jenniskens, 2006
096NCC1	134.2	14.1	26.7	300.2	0.77	*(0.371)*	*0.3*	116.7	*297.1*	*(1.61)*	Nilson, 1964
096NCC4	130.7	19.7	26.4	297.1	0.783	0.397	*4.9*	291.3	*120.2*	1.829	Sekanina, 1976
097SCC0	134.1	10.1	*(26.8)*	306.9	*0761*	0.475	6.3	100.7	126.9	2.114	Terentjeva, 1989
107DCH0	254.4	−86.1	42.6	324.7	0.93	0.95	*42.6*	330	144.7	13.571	Gartrell and Elford, 1975
107DCH1	179.6	−83.3	34.2	325.7	0.44	0.93	*34.2*	340	145.7	1.661	Gartrell and Elford, 1975
107DCH2	208.3	−78.2	42	325.7	0.60	0.94	*42.0*	338	145.7	2.35	Jopek et al., 1999
110AAN4	157.2	−9.5	45.0	*312. 0*	0.965	0.143	58.6	138.3	133.4	3.57	Jenniskens et al., 2016
113SDL0	137.7	*17.8*	17.4	146.4	0.666	0.729	4.3	69.0	146.4	2.182	Terentjeva, 1989
113SDL2	148.6	18.6	17.3	334.7	0.588	0.804	9.8	237.2	334.7	1.950	Jenniskens, 2006
117DCQ0	346.7	*–23.7*	14.1	324.7	0.62	0.82	2.1	299	144.7	2.16	Gartrell and Elford, 1975
121NHY1	*158.6*	−11.3	19.3	4.6	0.714	0.718	9.6	70.8	184.6	2.521	Terentjeva, 1989
123NVI1	*174.3*	*8.7*	23.0	353.5	0.628	0.728	3.7	252.7	353.5	1.955	Kronk, 1988
125SAL0	141.8	−7	11.9	178.8	0.550	0.907	6.9	*221.8*	*358.8*	2.016	Jenniskens, 2006
137PPU0	110.4	−45.1	15	213.64	0.663	1.00	21	359	*33.640*	2.97	Jenniskens, 1994
138ABO0	218.8	14.5	20.9	29.2	0.719	0.759	19.1	258.8	29.2	2.704	Porubcan and Gavajdova, 1994
147PAQ0	350.9	−3.5	64	239.7	0.80	0.56	174.1	*270.4*	*239.7*	2.78	Nilsson, 1964
172ZPE2	*67.4*	23.4	26.4	75.0	0.7841	0.335	3.8	58.4	75.0	1.55	Brown et al., 2008
173BTA2	87.3	19.3	*31.4*	98.1	*0.845*	0.34	6	*224*	278.1	2.2	Lovell, 1954

Notes to the Table 7:

001CAP2 `http://adsabs.harvard.edu/abs/2001ESASP.495...55H`, Hasegawa (2001)
Hasegawa did not give such data though gave 6 components with their individual orbits of member meteors.

001CAP6 `http://adsabs.harvard.edu/abs/2009JIMO...37...55S`
SonotaCo did not give the orbital elements and the listed values are the same as 001CAP4 (Jopek et al., 2003).

003SIA1 Dutch Meteor Society 2001
The radiant data discords with its orbit. This orbit gives $Ra = 1.16$ (the radius at the ascending node of the shower is 1.16 au) at $\Omega = 306.9$ ($\lambda_\odot = 126.9$). If we use $\lambda_\odot = 131.7$ as listed or $\Omega = 126.9$, the calculated orbit and the estimated radiant both do not give satisfying values.

Table 7 – (continued)

Code	α	δ	V_g	$\lambda_\odot$	e	q	i	ω	Ω	a	Reference
176PHE0	31.6	−47.7	*47*	*110.3*	*0.62*	*0.96*	*82*	*31*	*290.3*	2.5	Weiss, 1960
176PHE1	31.6	−47.7	*47*	*110.3*	*1.0*	*0.97*	*87*	*24*	*290.3*	*Inf.*	Cook, 1973
183PAU0	340.7	−25.7	40.5	123.7		0.17	45	*114*	*303.7*	*4.31*	Kashcheev et al., 1967
202ZCA0	119.7	19	43.8	146.9	0.99	0.05	*21.1*	*206.5*	326.9	5.00	Nilsson, 1964
207SCS0	*33*	*68.9*	*69.1*	*172.8*	*0.939*	*0.968*	*162.4*	*176.1*	*172.8*	*15.8*	Jenniskens, 2006
213BRC0	337	−47	*21*	160.3	0.730	0.852	16.9	50.8	340.3	3.16	Jenniskens, 2006
214BCP0	305.7	−12.8	37	*167.7*		0.170	13.0	43.0	327.7	2.429	Jopek .... ???
223GVI0	168.4	3.6	*23.3*	165.8		0.616	0.9	273.2	345.8	2.037	Sekanina, 1976
230ICS0	*36.7*	*66*	*66.3*	*208.7*	*0.989*	*0.644*	*128.5*	*109.8*	*208.7*	*59.0*	Jenniskens, 2006
239GPU0	110.1	−44	*39.2*	238	0.945	0.980	71.6	16.1	58.0	17.8	Jenniskens, 2006
250NOO5	90.5	15.3	43.1	246	0.991	0.1066	*67.1*	142.37	66.0	12.01	Brown et al., 2010
251IVI0	210.4	−3.8	29	224.3	*0.191*	*0.985*	10.1	60.7	224.3	*1.217*	Sekanina, 1976
270FAO0	88.8	9.4	9.4	138	0.558	0.954	3.5	22.4	*318.0*	2.16	Jenniskens, 2006
286FTA0	*58*	16.8	21.7	240.2	0.704	0.529	3.2	97.4	60.2	1.79	Jenniskens, 2006
320OSE0	242.7	0.5	38.9	275.5	0.88	0.164	56.5	38.8	*275.9*	1.37	Brown et al., 2008
325DLT0	56.7	11.5	36.4	181.7	0.9337	0.104	23.2	210.8	*1.7*	1.57	Brown et al., 2008
337NUE2	61.5	4.3	67.1	163.0	0.916	0.867	150.7	43.7	*53.2*	7.04	Jenniskens et al.,2016
345FHE1	*270.9*	*41.5*	*42.8*	*344*	*0.932*	*0.971*	*71.3*	*163.6*	*343.9*	*5.66*	Jenniskens et al.,2016
345FHE2	*270.9*	*41.5*	*42.8*	*344.0*	*0.932*	*0.971*	*71.3*	*163.6*	*343.9*	*5.66*	Jenniskens et al.,2016
347BPG0	350.5	27.8	41	36.0	0.890	0.3036	62.7	61.11	*30.0*	2.76	Brown et al., 2010
347BPG1	*354.3*	*30.8*	*44.2*	*42*	*0.944*	*0.347*	*69.1*	*68.0*	*42.3*	*6.13*	Jenniskens et al., 2015
347BPG2	*354.3*	*30.8*	*44.2*	*42.0*	*0.944*	*0.347*	*69.1*	*68.0*	*42.3*	*5.16*	Jenniskens et al., 2016
351DTR0	35.9	34.1	26.2	46.0	*0868*	0.5613	16.2	92.58	46.0	4.24	Brown et al., 2010
452TVI0	196.9	−1.0	14.9	039.6	0.683	0.856	*2.4 4*	230.5	039.6		Rudawska and Jenniskens, 2014
476ICE0	4.8	−1.4	26.9	177.2	0.832	0.421	3.4	*134.0*	357.2		Rudawska and Jenniskens, 2014
479SOO0	79.2	*12. 1*	67.6	185.6	0.928	0.774	159.3	058.1	5.6		Rudawska and Jenniskens, 2014
484IOA0	27.6	17.3	13.8	200.4	0.652	0.836	3.4	*193.7*	*200.4*	2.40	Rudawska and Jenniskens, 2014
507UAN1	7.1	40.3	59.3	101	0.910	0.849	117.8	*130.0*	101.0	8.85	Jenniskens et al., 2016
514OMC0	315	−30	64.6	66	0.982	0.535	*142.4*	87	246	27	Segon et al., 2013
530ECV2	192.0	−18.1	68.1	302.2	0.847	0.820	*50.1*	50.1	122.2	5.29	Jenniskens et al., 2016
533JXA2	41.5	10.7	68.9	112.7	0.969	0.860	170.4	312.4	*292.7*	18.0	Jenniskens et al., 2016
548FAQ*1*	318.2	−2.1	37.7	112.7	0.929	0.140	34.8	322.2	112.7		Andreic et al., 2014
549FAN1	20.5	46.6	60.2	112	0.922	0.898	117.9	139.8	*118.0*	7.71	Jenniskens et al., 2016
624OAR0	131.2	+13.4	28.6	204.4	0.830	0.311	005.8	120.9	024.4	1.84	Jenniskens et al., 2015
644JLL0	140.6	+23.4	39.1	277.7	0.951	0.098	022.4	327.3	*277.7*	2.04	Jenniskens et al., 2016
645PHC0	300.1	−11.6	67.8	195	0.880	0.761	163.3	120.3	195.0	4.63	Jenniskens et al., 2014
715ACL0	77.1	+64.8	59.8	189.6	1.061	0.964	109.8	201.3	*189.6*	−15.80	Jenniskens et al., 2016

Notes to the Table 7:

005SDA3 `http://adsabs.harvard.edu/abs/1973WASSP.319..183C`, Cook (1973)
The right ascension and the node are in error and should be read 333.7 and 305.6 respectively based on the original paper. But, probably $\alpha = 338.7$ instead of $\alpha = 333.7$, because the recalculated inclination and the argument of perihelion become close to listed values by this change.

007PER6 Jenniskens et al. (2016; Icarus, 266, 331)
Two extra spaces are included in the geocentric velocity column; $V_g = 59.1$.

011EVI0 `http://adsabs.harvard.edu/abs/2006mspc.book.....J`, Jenniskens (2006)
The argument of the perihelion and the ascending node may be misprinted in the referenced book reciprocally, i.e. $\omega = 280.5$ and $\Omega = 349.1$, but the discrepancy remains. Still $Rd = 0.84$ (the radius of the descending node of the shower is 0.84 au) at $\Omega = \lambda_\odot = 349.1$ after this change.

Table 7 – (continued)

Notes to the Table 7:

020COM1 http://adsabs.harvard.edu/abs/2009JIMO...37...55S
SonotaCo did not give the orbital elements and the listed values are the same as 020COM0 (Jenniskens, 2006).

020COM6 http://adsabs.harvard.edu/abs/1967SCoA...11..183K
Four columns are in error and should be read $\delta = 29.7, e = 0.81, q = 0.71$ and $a = 3.74$ based on the referenced paper.

026NDA2 http://adsabs.harvard.edu/abs/1963mmc..book..774J, Jacchia (1963)
It is proper to cite http://adsabs.harvard.edu/full/1957AJ.....62..225W. Jacchia used two meteors listed in this paper to give the data but listed the pre-atmospheric velocity (=42.28) not the geocentric velocity and the mean geocentric velocity is calculated as 40.63. Why Jacchia listed different RP is unknown, though his Northern ι-Aquariids is predicted at this point at that time.

031ETA4 http://adsabs.harvard.edu/abs/2009JIMO...37...55S
SonotaCo did not give the orbital elements and the listed values are the same as 031ETA5 (Jopek et al., 2010).

032DLM1 http://adsabs.harvard.edu/abs/1967SCoA...11..183K
Same as 020COM6. Four columns are in error (see 020COM6).

033NIA0 http://adsabs.harvard.edu/abs/1973NASSP.319..183C, Cook, 1973
It is proper to cite http://adsabs.harvard.edu/full/1957AJ.....62..225W. Cook quoted Jacchia's paper (http://adsabs.harvard.edu/abs/1963mmc..book..774J) but gave somewhat different data from Jacchia's. Jacchia probably used meteors of the paper mentioned in 026NDA2 to calculate mean values but listed not the mean radiant point but estimated one corresponding to $\lambda_\odot = 132.5$ not 147. Originally $a = 1.75$ not 1.625 which is derived from $e = 0.84$ and $q = 0.26$.

033NIA1 Dutch Meteor Society 2001
The right ascension of the radiant might be 338 instead of 328.

039NAL0 http://adsabs.harvard.edu/abs/2006mspc.book.....J, Jenniskens (2006)
This radiant locates north above the ecliptic and, therefore, the node should be 353.9 and the argument of perihelion 223.3.

045PDF0 http://adsabs.harvard.edu/abs/2006mspc.book.....J
A dot is lacking in the argument of the perihelion; $\omega = 179.3$.

052OUM0 http://adsabs.harvard.edu/abs/1971SCoA...12....1L, Lindblad, 1971b
The geocentric velocity is not given in the listed article and the mean value of the member meteors equals 13.49.

083OCG0 http://adsabs.harvard.edu/abs/1973Icar...18..253S, Sekanina (1973)
083OCG0 is a mixture of S2-59 and S2-61 (abbreviations used hereafter are the same ones (Table 5 of Koseki, 2009)).

	α	δ	V_g	$\lambda_\odot$	e	q	i	ω	Ω	
083OCG06	317.8	52.6	17.2	195.9	0.647	0.976	25	198.6	195.9	
S2-59	316.7	52.5	17.2	191.5	0.538	0.930	25.5	216.0	191.5	Alpha-Cygnids
S2-61	300.0	50.8	17.2	195.9	0.647	0.976	25.0	198.6	195.9	Delta-Cygnids

091JZA0 http://adsabs.harvard.edu/abs/2006mspc.book.....J, Jenniskens (2006)
Rd=0.68 at $\lambda_\odot = 299.1$. The listed perihelion distance 0.643 might be misprinted in Jenniskens' book and the eccentricity is 0.643 instead and, then, the perihelion distance should be 0.947.

096NCC1 http://adsabs.harvard.edu/abs/1964AuJPh..17..205N
The inclination and the node are in error; $i = 4.9$ and $\Omega = 120.2$ (originally 119.5 in B1950.0). Nilson did not give the perihelion distance but gave the inverse of the semi major axis and the eccentricity. Parentheses mean the calculated value by the editor but parentheses mean negative value in Microsoft Excel.

096NCC4 http://adsabs.harvard.edu/abs/1976Icar...27..265S
The inclination and the node are in error; $i = 1.5$ and $\Omega = 297.1$ (originally 296.4 in B1950.0).

097SCC0 http://adsabs.harvard.edu/abs/1989JIMO...17..242T
The parenthesized value of the geocentric velocity is the pre-atmospheric velocity; $V_g = 24.4$. A dot is lacking in the argument of the eccentricity; $e = 0.761$.

107DCH0 http://adsabs.harvard.edu/abs/1975AuJPh..28..591G, Gartrell and Elford (1975)
The inclination is mistaken for the geocentric velocity and the original article shows $i = 70.2$.

107DCH1 http://adsabs.harvard.edu/abs/1975AuJPh..28..591G, Gartrell and Elford (1975)
The inclination is mistaken for the geocentric velocity and the original article shows $i = 61.9$.

107DCH2 http://adsabs.harvard.edu/abs/1999md98.conf..307J, Jopek et al. (1999)
The inclination is mistaken for the geocentric velocity and the original article shows $i = 75.0$.

110AAN4 Jenniskens et al. (2016; Icarus, 266, 331)
Two extra spaces are included in the LaSun column ($\lambda_\odot$); $\lambda_\odot = 312.0$.

Table 7 – (continued)

Notes to the Table 7:

113SDL0 http://adsabs.harvard.edu/abs/1989JIMO...17..242T, Terentjeva (1989)
The declination might be misprinted in original paper and it is suggested $\delta = 7.8$ is reasonable.

113SDL2 http://adsabs.harvard.edu/abs/2006mspc.book.....J, Jenniskens (2006)
The radiant data discords with its orbit and the reason why this discrepancy causes is unknown.

117DCQ0 http://adsabs.harvard.edu/abs/1975AuJPh..28..591G, Gartrell and Elford (1975)
The declination might be misprinted in original paper and it is suggested $\delta = -13.7$ is reasonable.

121NHY1 http://adsabs.harvard.edu/abs/1989JIMO...17..242T, Terentjeva (1989)
The right ascension might be misprinted in the original paper and it is suggested $\alpha = 168.6$ is reasonable.

123NVI1 http://adsabs.harvard.edu/abs/1988msdc.book.....K, Kronk (1988)
Kronk did not show the radiant point in his book and the radiant does not fit the orbit. He does not mention this shower in his recent book (Kronk, 2014).

125SAL0 http://adsabs.harvard.edu/abs/2006mspc.book.....J, Jenniskens (2006)
The argument of perihelion and the ascending node should be reversed ($\omega = 41.8, \Omega = 178.8$), because the radiant lies south below the ecliptic.

137PPU0 http://adsabs.harvard.edu/abs/1994A%26A...287..990J, Jenniskens (1994)
Should be referred: http://adsabs.harvard.edu/abs/2006mspc.book.....J, Jenniskens (2006). The ascending node should be reversed ($\Omega = 213.64$), because the radiant lies south below the ecliptic.

138ABO0 http://adsabs.harvard.edu/abs/1994P%26SS...42..151P, Porubcan and Gavajdova (1994)
The radiant data discords with its orbit and the reason why this discrepancy causes is unknown. $Rd = 1.14$ at $\lambda_\odot = 29.2$.

147PAQ0 http://adsabs.harvard.edu/abs/1964AuJPh..17..205N, Nilsson (1964)
The argument perihelion and the ascending node should be reversed ($\omega = 90.4, \Omega = 59.7$), because the radiant lies north above the ecliptic.

172ZPE2 http://adsabs.harvard.edu/abs/2008Icar..195..317B
The right ascension of the radiant is in error and should be read 57.4.

173BTA2 http://adsabs.harvard.edu/abs/1954meas.book.....L, Lovell (1954)
The radiant coordinate is given from Lovell's ephemeris for $\lambda_\odot = 98$ and converted to J2000.0. Lovell gave the eccentricity as 0.85 and listed here elements for B1950.0. Lovell listed V instead of V_g and, therefore, V_g should be modified into 29.3 km/s. The argument of perihelion should be read 244, because Lovell gave $\pi(= \omega + \Omega)$ as 162. If we converted Lovell's original data (Table 156 line 1) into J2000.0, we would get following result.

α	δ	V_g	$\lambda_\odot$	e	q	i	ω	Ω	a
86.4	17.9	29.3	98.9	0.85	0.34	6	244	278.9	2.2

176PHE0 http://adsabs.harvard.edu/abs/1960AuJPh..13..522W, Weiss (1960)
176PHE1 http://adsabs.harvard.edu/abs/1973NASSP.319..183C, Cook (1973)
176PHE0 and 176PHE1 are not two sources but one. Weiss did not give geocentric velocity and its orbit. 176PHE0 and 176PHE1 are given as two 'likely extremes' by Cook and, therefore, $V_g = 44$ km/s for 176PHE0 as lower limit and $V_g = 50$ km/s for 176PHE1 as upper limit.

183PAU0 Kashcheev et al. (1967)
This entry seems to use Jenniskens' book (Jenniskens, 2006). Jenniskens misquoted the reference SCA 7 (1963) instead of SCA 11 (1967) in his book. Moreover, the argument of the perihelion and the ascending node in Kashcheyev and Lebedinets' paper SCA 11 are $\omega = 114$ and $\Omega = 303$ respectively but their Russian book (Kashcheyev et al, 1967) gave them as 134 and 305, respectively. They gave the eccentricity as 0.96 and, therefore, this entry should be changed as follows.

α	δ	V_g	$\lambda_\odot$	e	q	i	ω	Ω	a
340.7	−25.7	40.5	125.7	0.96	0.17	45	134	306	4.25

202ZCA0 http://adsabs.harvard.edu/abs/1964AuJPh..17..205N, Nilsson (1964).
Recalculated orbit suggests the inclination and the argument of the perihelion might be in error and, if we use this change ($i = 8.5, \omega = 201.4$) 202ZCA0 become close to 202ZCA1, though we do not change the elements in the following section.

207SCS0 http://adsabs.harvard.edu/abs/2006mspc.book.....J, Jenniskens (2006)
The listed geocentric data gives unreliable orbit and, on the other hand, the orbital elements indicate distant RP; might be called as chi Aurigids. $Rd = 0.97$ at $\lambda_\odot = 172.8$.

213BRC0 http://adsabs.harvard.edu/abs/2006mspc.book.....J, Jenniskens (2006)
Jenniskens gives 21.0 km/s as geocentric velocity but it seems to be pre-atmospheric velocity. It should be, therefore, $V_g = 17.8$ km/s.

214BCP0 Jopek .... ??? (reference as shown in the SD)
LaSun ($\lambda_\odot$) is in error and should be read $\lambda_\odot = 327.7$.

223GVI0 http://adsabs.harvard.edu/abs/1976Icar...27..265S
The geocentric velocity is in error and should be read $V_g = 20.7$. Sekanina gave the eccentricity as 0.698 not blank.

Table 7 – (continued)

Notes to the Table 7:

230ICS0 http://adsabs.harvard.edu/abs/2006mspc.book.....J, Jenniskens (2006)
The listed geocentric data gives unreliable orbit and, on the other hand, the orbital elements indicate a distant RP; might be called as 31 Leonis Minorids. $Rd = 0.96$ at $\lambda_\odot = 208.7$.

239GPU0 http://adsabs.harvard.edu/abs/2006mspc.book.....J, Jenniskens (2006)
Jenniskens quoted IMO's $V_g = 43.0$ km/s in his book and this seems more proper than listed $V_g = 39.2$ km/s, because IMO's value fits for the orbit.

250NOO5 http://adsabs.harvard.edu/abs/2010Icar..207...66B
The inclination is in error and should be read $i = 26.0$.

251IVI0 http://adsabs.harvard.edu/abs/1976Icar...27..265S, Sekanina (1976)
The listed orbit does not approach the Earth's orbit around $\lambda_\odot = 224.3$. Jenniskens misused the perihelion distance and the semi-major axis in his book. S3-262 is the most probable candidate for this as following line.

	α	δ	V_g	$\lambda_\odot$	e	q	i	ω	Ω	a	
S3-262	210.2	−3.7	29.0	224.3	0.816	0.329	10.1	60.7	224.3	1.79	Iota-Virginids

270FAO0 http://adsabs.harvard.edu/abs/2006mspc.book.....J, Jenniskens (2006)
This radiant locates south under the ecliptic and, therefore, the node should be 138.0.

286FTA0 http://adsabs.harvard.edu/abs/2006mspc.book.....J, Jenniskens (2006)
Jenniskens gives the right ascension of the radiant as 58.2. This entry is based only 2 orbits and, therefore, the insufficient data might cause the inconsistency between the radiant and the orbit.

320OSE0 http://adsabs.harvard.edu/abs/2008Icar..195..317B, Brown et al. (2008)
The IAU 3 letter code of 320OSE was 320OMS formerly (2015 Sep 19 version).

325DLT0 http://adsabs.harvard.edu/abs/2008Icar..195..317B, Brown et al. (2008)
The node is misprinted in the original paper and should be 265.5.

337NUE2 Jenniskens et al. (2016; Icarus, 266, 331)
The node is in error and should be 343.0 in accordance with the maximum solar longitude.

345FHE1 Jenniskens et al. (2016; Icarus, 266, 355)
345FHE2 Jenniskens et al., (2016, Icarus, 266, 355)
These are duplicate entries.

347BPG0 http://adsabs.harvard.edu/abs/2010Icar..207...66B
The node is in error and should be read $\Omega = 36.0$.

347BPG1 Jenniskens et al. (2015; Icarus, accepted)
347BPG2 Jenniskens et al. (2016; Icarus, 266, 355)
These are duplicate entries except for the semi-major axis. Jenniskens himself lists $a = 5.16$ but 6.13 is better because of the eccentricity and the perihelion distance.

351DTR0 http://adsabs.harvard.edu/abs/2010Icar..207...66B
A dot is lacking in the eccentricity column; $e = 0.868$.

452TVI0 http://adsabs.harvard.edu/abs/2014me13.conf..217R
An extra space is included in the inclination column; $i = 2.44$.

476ICE0 http://adsabs.harvard.edu/abs/2014me13.conf..217R, Rudawska and Jenniskens (2014)
The argument of perihelion is probably in error and might be 104: $Ra = 1.83$ at $\lambda_\odot = 177.2$.

479SOO0 http://adsabs.harvard.edu/abs/2014me13.conf..217R
An extra space is included in the declination column; $\delta = 12.1$, though the former version list correctly; $\delta = +12.1$.

484IOA0 http://adsabs.harvard.edu/abs/2014me13.conf..217R, Rudawska and Jenniskens, 2014
The node is in error and should be 234.7 in accordance with the maximum solar longitude. The discrepancy in the argument of the perihelion is unknown and might be 233.7.

507UAN1 Jenniskens et al. (2016; Icarus, 266, 384)
The node is in error and should be 96.0 in accordance with the maximum solar longitude.

514OMC0 http://adsabs.harvard.edu/abs/2013JIMO...41...70S, Segon et al. (2013)
The inclination might be misprinted in the original paper and might be 152.4.

530ECV2 Jenniskens et al. (2016; Icarus, 266, 355)
The inclination is obviously in input error (same as the argument of perihelion) and $i = 158.4$.

533JXA2 Jenniskens et al. (2016; Icarus, 266, 355)
Node is in error and should be 299.0 in accordance with the maximum solar longitude.

548FAQ1 http://adsabs.harvard.edu/abs/2014JIMO...42...90A
There is no first number of a set of parameters for given shower and, therefore, should be read AdNo=0.

Table 7 – (continued)

Notes to the Table 7:
549FAN1 Jenniskens et al. (2016, Icarus, 266, 355)
The node is in error and should be 112.0 in accordance with the maximum solar longitude.

624OAR0 Jenniskens et al. (2015; Icarus, in press)
The listed radiant (2015 September 19 version) is not located in Aries but in Cancer. The estimated radiant from the listed orbit is located in Aries. This line may be a mixture of different data sets but the problem is corrected in the 2016 March 17 version (listed radiant data not found in Jenniskens' article). The real problem is not the change but many amateurs, including myself, could not be aware of such changes. There is no announcement from IAUMDC what and where are the changes. We cannot notice even when the changes were effected without watching IAUMDC site every day.

644JLL0 Jenniskens et al. (2016; Icarus, 266, 384)
The node is in error and should be 288.0 in accordance with the maximum solar longitude.

645PHC0 Jenniskens et al. (2014, Icarus, subm.)
This radiant (2015 September 19 version) is not located in Cancer but on the border of Capricorn and the estimated radiant from the listed orbit is located in Cancer. This line may be a mixture of different data set but the problem is corrected in 2016 March 17 version (listed radiant data not found in Jenniskens' article).

715ACL0 Jenniskens et al. (2016; Icarus, 266, 384)
The node is in error and should be 183.0 in accordance with the maximum solar longitude.

Table 8 – D_{SH} distribution. MIN: the lowest D_{SH} within the stream i.e., over all possible pairs of orbits listed in the SD for the stream). MAX: the highest D_{SH} within the stream. Neighbour: D_{SH} of the closest neighbour (i.e., among all the other streams).

D_{SH}	MIN	MAX	Neighbour
< 0.1	75	14	22
0.1–0.2	15	21	33
0.2–0.3	7	11	22
0.3–0.4	5	8	24
0.4–0.5	0	7	8
$0.5 <$	0	5	3
Total	102	66	112

sources or should be checked by their raw data to find how the discrimination between 473LAQ or 215NPI can be done. Careful research is necessary to confirm the 033NIA.

The ecliptic meteor showers do not always have two branches (northern and southern). It is not good to call some of NIA members listed in the SD as Northern ι-Aquariids, because the radiant of the 033NIA is located far from ι Aquarii and seems to be different from the original one (Wright et al., 1957). The circumstances of Northern δ-Aquariids (026NDA) are similar to 033NIA and it is proper to be called β-Piscids (=342BPI).

3.2.3 Southern and Northern Taurids

The 'Taurid complex' is really complex and we can barely divide the Northern Taurids and Southern Taurids. Sekanina (1970) wrote that the Taurids cannot be separated by radio observations. Jenniskens et al. (2016), however, identified many sub-showers: 626LCT0, 628STS0, 637FTR0, 625LTA0, 624XAR0, 630TAR0, 631DAT0. Such difference are caused by the definition of a meteor shower and the activity detection method.

The underlined values in Table 13 exceed $D > 0.2$ but there are many other entries within this limit. There are 15 entries with $D(A, B) < 0.2$ for STA0:
626LCT0 (0.020), 628STS0 (0.051), 637FTR0 (0.065), 017NTA5 (0.090), 625LTA0 (0.108), 624XAR0 (0.116), 630TAR0 (0.151), 017NTA6 (0.158), 017NTA2 (0.159), 017NTA1 (0.168), 017NTA3 (0.169), 631DAT0 (0.171), 025NOA1 (0.178), 028SOA0 (0.182), 28SOA1 (0.198) and two daytime streams; 173BTA0 (0.125), 172ZPE0 (0.187).
There is no combination with $D_{SH} > 0.2$ except for the assortment with CMOR observations (002STA2 and 002STA4: Brown et al., 2008 and 2010), though within the CMOR observations themselves D_{SH}(2STA2, 2STA4) = 0.041. The 'Taurid complex' is one of the ANT activities, and it is the most remarkable one. The start and end of the activity is not clear. Both CMOR observations include September activities of ANT and reject those of November.

Koseki (2012) insisted that the 'Taurids' consist of three components: two southern centres and a northern one. This simplicity in NTA can explain the smaller distances within 017NTA than those within 002STA (Table 14). 017NTA4 of SonotaCo shows rather large distance from others. We find D_{SH}(017NTA4, 017NTA5) = 0.180, because these observations extend to the end of the activity at $\lambda_{\odot} = 258.0$ when 256ORN is active. 017NTA5 of CMOR2 (Brown et al., 2010) is located south of the ecliptic and could be contaminated by meteors from 002STA seriously.

3.2.4 Kappa-Cygnids

Though the maximum distance is not too large D_{SH} (012KCG3, 012KCG6) = 0.225, the similarities among each other are not good (Table 15, cf. subsection 3.2.1). Moreover, there are 7 neighbour entries with $D_{SH} < 0.2$, especially 197AUD1 (0.080) for 012KCG7 and 470AMD2 (0.146) for 012KCG6. Meteor activities from

Table 9 – D_{SH} matrix of 001CAP; DSH(001CAP0, 001CAP1) = 0.054 and so on.

	001CAP0	001CAP1	001CAP2	001CAP3	001CAP4	001CAP5	001CAP6	001CAP7	001CAP8
001CAP0	—	0.054	0.058	0.023	0.020	0.050	0.024	0.049	0.031
001CAP1	0.054	—	0.072	0.046	0.040	0.058	0.037	0.038	0.035
001CAP2	0.058	0.072	—	0.071	0.067	0.023	0.052	0.064	0.043
001CAP3	0.023	0.046	0.071	—	0.010	0.060	0.024	0.047	0.036
001CAP4	0.020	0.040	0.067	0.010	—	0.055	0.019	0.042	0.029
001CAP5	0.050	0.058	0.023	0.060	0.055	—	0.037	0.062	0.035
001CAP6	0.024	0.037	0.052	0.024	0.019	0.037	—	0.046	0.021
001CAP7	0.049	0.038	0.064	0.047	0.042	0.062	0.046	—	0.030
001CAP8	0.031	0.035	0.043	0.036	0.029	0.035	0.021	0.030	—
mean	0.038	0.048	0.056	0.040	0.035	0.048	0.033	0.047	0.032

Table 10 – Meteoroid streams called 'Southern ι-Aquarids'. Abbreviations used here are the same ones (Table 5 of Koseki, 2009) and shower names in the table are given by the original authors.

No.	α	δ	V_g	$\lambda_\odot$	$\lambda - \lambda_\odot$	β	e	q	i	ω	Ω	Stream
K1-90	328.7	−17.8	33.0	127.7	197.0	−4.8	0.88	0.26	8.0	126.0	307.7	S ι-Aquariids
S2-47	336.0	−8.8	28.8	136.9	197.6	1.1	0.836	0.277	1.4	307.7	136.7	Southern ι-Aquarids
S3-137	343.6	−2.9	24.5	138.0	205.8	3.7	0.76	0.25	4.4	319.2	137.9	Southern ι-Aquarids
L1-60	320.7	−14.8	35	124.7	193.7	0.5	0.925	0.27	0.0	70.7	355.5	Southern ι-Aquarids
L1-110	348.7	−9.7	41	142.5	203.3	−4.5	0.959	0.119	12.6	143.9	322.5	Southern ι-Aquarids

Table 11 – Meteoroid streams called 'Northern ι-Aquarids'. Abbreviations and shower names are same as Table 10.

No.	α	δ	V_g	$\lambda_\odot$	$\lambda - \lambda_\odot$	β	e	q	i	ω	Ω	Stream
LE-313	326.1	−3.4	39.0	118.3	208.8	9.7	0.940	0.100	28.9	328.8	118.3	Northern ι-Aquarids?
K1-91	321.7	−7.8	35.0	120.7	200.8	6.9	0.890	0.200	12.0	313.0	120.7	N ι-Aquariids
NI-61.7.11	326.9	−12.1	30.0	126.0	199.0	1.2	0.850	0.234	6.9	312.5	126.0	N.ι-Aquarids?
S2-50	352.5	−0.8	28.2	152.2	200.6	2.2	0.823	0.242	3.2	313.5	152.2	Northern ι-Aquarids
S3-159	350.1	0.6	26.1	153.1	198.1	4.4	0.777	0.302	5.2	307.4	153.1	Northern ι-Aquarids
LI-78	354.6	1.3	31.0	162.1	193.5	3.3	0.830	0.326	4.0	299.7	162.1	Northern ι Aquarids

Table 12 – D_{SH} matrix of 033NIA.

	033NIA0	033NIA1	033NIA2	033NIA3	033NIA4	033NIA5
033NIA0	—	0.222	0.177	0.170	0.316	0.060
033NIA1	0.222	—	0.380	0.369	0.132	0.270
033NIA2	0.177	0.380	—	0.024	0.482	0.153
033NIA3	0.170	0.369	0.024	—	0.474	0.145
033NIA4	0.316	0.132	0.482	0.474	—	0.367
033NIA5	0.060	0.270	0.153	0.145	0.367	—

Table 13 – D_{SH} matrix of 002STA.

	002STA0	002STA1	002STA2	002STA3	002STA4	002STA5
002STA0	—	0.106	0.213	0.029	0.214	0.040
002STA1	0.106	—	0.117	0.110	0.110	0.083
002STA2	0.213	0.117	—	0.216	0.041	0.187
002STA3	0.029	0.110	0.216	—	0.217	0.035
002STA4	0.214	0.110	0.041	0.217	—	0.188
002STA5	0.040	0.083	0.187	0.035	0.188	—

Table 14 – D_{SH} matrix of 017NTA.

	017NTA0	017NTA1	017NTA2	017NTA3	017NTA4	017NTA5	017NTA6
017NTA0	—	0.118	0.127	0.040	0.073	0.118	0.086
017NTA1	0.118	—	0.050	0.099	0.172	0.098	0.083
017NTA2	0.127	0.050	—	0.097	0.188	0.080	0.057
017NTA3	0.040	0.099	0.097	—	0.108	0.079	0.051
017NTA4	0.073	0.172	0.188	0.108	—	0.180	0.152
017NTA5	0.118	0.098	0.080	0.079	0.180	—	0.061
017NTA6	0.086	0.083	0.057	0.051	0.152	0.061	—

Table 15 – D_{SH} matrix of 12KCG.

	012KCG0	012KCG1	012KCG2	012KCG3	012KCG4	012KCG5	012KCG6	012KCG7
012KCG0	—	0.151	0.060	0.153	0.129	0.129	0.123	0.111
012KCG1	0.151	—	0.123	0.144	0.133	0.093	0.180	0.166
012KCG2	0.060	0.123	—	0.104	0.128	0.138	0.151	0.152
012KCG3	0.153	0.144	0.104	—	0.135	0.183	0.225	0.216
012KCG4	0.129	0.133	0.128	0.135	—	0.091	0.209	0.110
012KCG5	0.129	0.093	0.138	0.183	0.091	—	0.172	0.085
012KCG6	0.123	0.180	0.151	0.225	0.209	0.172	—	0.157
012KCG7	0.111	0.166	0.152	0.216	0.110	0.085	0.157	—
mean	0.122	0.141	0.122	0.166	0.133	0.127	0.174	0.142

Table 16 – D_{SH} matrix of 13LEO.

	013LEO0	013LEO1	013LEO2	013LEO3	013LEO4	013LEO5	013LEO6	013LEO7	013LEO8
013LEO0	—	0.014	0.008	0.035	0.017	0.144	0.051	0.296	0.041
013LEO1	0.014	—	0.014	0.023	0.010	0.155	0.063	0.307	0.051
013LEO2	0.008	0.014	—	0.034	0.017	0.145	0.052	0.297	0.041
013LEO3	0.035	0.023	0.034	—	0.025	0.173	0.083	0.327	0.069
013LEO4	0.017	0.010	0.017	0.025	—	0.161	0.068	0.312	0.057
013LEO5	0.144	0.155	0.145	0.173	0.161	—	0.093	0.158	0.105
013LEO6	0.051	0.063	0.052	0.083	0.068	0.093	—	0.245	0.016
013LEO7	0.296	0.307	0.297	0.327	0.312	0.158	0.245	—	0.259
013LEO8	0.041	0.051	0.041	0.069	0.057	0.105	0.016	0.259	—

Table 17 – D_{SH} matrix of 020COM.

	020COM0	020COM1	020COM2	020COM3	020COM4	020COM5	020COM6	020COM7	020COM8
020COM0	—	0.286	0.836	0.252	0.135	0.380	0.337	0.230	0.187
020COM1	0.286	—	0.956	0.392	0.167	0.107	0.265	0.084	0.102
020COM2	0.836	0.956	—	0.863	0.915	1.035	0.704	0.936	0.922
020COM3	0.252	0.392	0.863	—	0.308	0.492	0.409	0.310	0.318
020COM4	0.135	0.167	0.915	0.308	—	0.256	0.310	0.129	0.070
020COM5	0.380	0.107	1.035	0.492	0.256	—	0.335	0.182	0.199
020COM6	0.337	0.265	0.704	0.409	0.310	0.335	—	0.268	0.275
020COM7	0.230	0.084	0.936	0.310	0.129	0.182	0.268	—	0.064
020COM8	0.187	0.102	0.922	0.318	0.070	0.199	0.275	0.064	—

the Cygnus-Draco area from July to September are very complex and the κ-Cygnids have two different components: one has recurrent nature of 7 years and another annual (Koseki, 2014b). The definition of κ-Cygnids may be different from one researcher to another and observations are contaminated by sporadics and neighbour showers.

The κ-Cygnids have eight entries in the SD and all are based on optical observations, especially by photo and video. It is obvious that this shower is rich in bright meteors and visual meteor rates are low like, for example, 020COM. The recurrent nature of the 7 years was discovered by photo and video observations, but this nature is not detectable by visual observations (Rendtel and Arlt, 2016). There are confusions with the AUD and also ZDR (Koseki, 2014b). It is necessary to study the so-called κ-Cygnids and activities from the surrounding region in the sky more carefully.

3.2.5 Leonids

The 013LEO7 represents a singular radiant (Table 16), although other observations such as 013LEO5 seem to have some similarity to it. These are from CMOR observations (Brown et al., 2008 and 2010) and detected by a 3D wavelet method. It is noteworthy to note that both CMOR observations list the end of Leonids activity too early: 013LEO5 ($\lambda_\odot$ = 238), 013LEO7 ($\lambda_\odot = 237$). It might be suggested 013LEO7 is contaminated by sporadics and other showers; D_{SH}(013LEO5, 020COM2) = 0.274.

It is necessary to note that the geocentric velocity of the 013LEO7 is about 3 km/s lower than the others. This is no large difference but causes the large difference in D_{SH}. We would meet a similar problem in case of high geocentric velocity showers and from the region near the Apex such as the Perseids, Comae Berenicids and so on.

3.2.6 Comae Berenicids

The 032DLM is now combined with 020COM in the SD, but historically, the DLM was first noticed by Whipple (1954) in photographic meteor data obtained by small cameras. Secondly, 090JCO (January Comae Berenicids) was detected in Super-Schmidt meteors by McCrosky and Posen (1959), and lastly, COM was searched by Lindblad (1971c) on the basis of the similarity between DLM and JCO. If we widened the search for their precursor and successor, we could find them already in late November and still in February. There is a confusion on the range of COM in the SD and it causes one

Table 18 – The ecliptic longitudes of the Sun at the peak shower activity ($\lambda_\odot$) of the SD's COM; the suggested $\lambda'_\odot$ of 020COM0 is 283.3 in accordance with the node.

	020COM0	020COM1	020COM2	020COM3	020COM4	020COM5	020COM6	020COM7	020COM8
$\lambda_\odot$	274	265.7	264	275.9	277.4	262.2	261.7	268	274.0

of the largest discrepancies in this D_{SH} survey in the SD (Table 17).

The ecliptic longitudes of the Sun at the peak shower activity ($\lambda_\odot$) of SD's COM differs widely (see Table 18). Koseki (2011) derived $\lambda_\odot$ for DLM, COM and JCO separately from photographic meteors; $\lambda_\odot = 262.0$ (DLM), $\lambda_\odot = 282.9$ (COM), $\lambda_\odot = 296.9$ (JCO).

Koseki (2011) stressed that the DLM is the most conspicuous of these based on SonotaCo's video observations and the numbers of photographic meteors of DLM, COM and JCO (11, 5 and 11 meteors, respectively). It is clear that the Comae Berenicids are placed in the middle part of these in time and location. However, the main activity contribution is from the DLM. If we combine them as one, we should better call them DLM but not COM. It is necessary to note the meteor scene is very different by different observational techniques and the meteor activity varies widely from year to year. Generally, the JCO might have been more active in the 1950's than now.

3.2.7 Tau-Herculids and June Bootids

The 061TAH is close to 186EUM1 ($D_{SH} = 0.133$) and 170JBO0 ($D_{SH} = 0.148$), and 170JBO is closer to 186EUM1 ($D_{SH} = 0.115$). Koseki (2015) discussed four meteor activity centres near the 061TAH and the 170JBO.

061TAH has one entry of Lindblad (1971b) only, but Koseki (2015) confirmed that activity also. Both are based on photographic observations of the middle of the 20th century and there are neither radar nor video observations by now. Koseki (2015) noted that the earlier activity ($50 < \lambda_\odot < 55$) seems to be closely related to the recent orbit of 73P/Schwassmann-Wachmann 3 and it is noticeable in recent data collected by SonotaCo. However, it does not occur in photographic meteors of the middle of the 20th century. The 061TAH0 data listed in the SD is historical data and does not represent recent observations because of changes in the comet's orbit. The photographic observations of 061TAH are the historical ones and are better put in another category (historical records).

The 170JBO has one entry of one photographic meteor record but Koseki (2015) found 8 June Bootid video meteors in SonotaCo 2010 data. The 'Winneckids' returned in 2010 in succession to the 1998 (Hashimoto and Osada, 1998) and 2004 (Sato, 2004) events. These are clear recurrent events. It seems to be fair to include historical visual records of both showers (Nakamura 1930 for 061TAH and Denning 1916 for 170JBO) in the SD as well as 063COR0.

3.3 Meteoroid streams having nearer neighbour(s) than self kin

There are 19 streams having nearer neighbour(s) than the closest distance between the listed entries within the stream (Table 19). As an example, the third line shows the nearest combination within 002STA is D_{SH} (002STA0, 002STA3) = 0.029 but there is closer neighbour exists; D_{SH}(002STA0, 626LCT0) = 0.020 (see

Table 19 – Meteoroid streams having nearer neighbour(s) than self kin. # indicates the neighbour encounters at another node; the twin streams.

The closest within the shower			The closest neighbour			Node
	D_{SH}			D_{SH}		
002STA0	0.029	002STA3	002STA0	0.020	626LCT0	
011EVI0	0.139	011EVI2	011EVI2	0.125	123NVI0	
017NTA0	0.040	017NTA3	017NTA0	0.013	632NET0	
021AVB2	0.094	021AVB3	021AVB3	0.051	452TVI0	
097SCC0	0.168	097SCC2	097SCC2	0.095	096NCC1	
100XSA0	0.187	100XSA1	100XSA0	0.092	150SOP1	#
128MKA0	0.225	128MKA1	128MKA1	0.134	639TAC0	#
152NOC0	0.167	152NOC2	152NOC0	0.165	357PHP0	
165SZC0	0.342	165SZC2	165SZC2	0.027	370MIC0	
172ZPE0	0.114	172ZPE1	172ZPE2	0.103	155NMA1	
175JPE2	0.023	175JPE6	175JPE6	0.011	522SAP0	
197AUD0	0.316	197AUD1	197AUD1	0.080	012KCG7	
202ZCA0	0.337	202ZCA1	202ZCA1	0.140	381DPL0	
257ORS0	0.096	257ORS1	257ORS3	0.053	636MTA0	
320OSE0	0.209	320OSE1	320OSE0	0.114	330SSE1	
326EPG0	0.153	326EPG1	326EPG0	0.124	327BEQ0	
327BEQ0	0.376	327BEQ1	327BEQ1	0.111	766BAD0	
335XVI0	0.085	335XVI1	335XVI0	0.082	520MBC1	#
337NUE0	0.231	337NUE2	337NUE1	0.112	552PSO0	

Table 20a – D_{SH} matrix of 011EVI.

	011EVI0	011EVI1	011EVI2
011EVI0	—	0.255	0.139
011EVI1	0.255	—	0.266
011EVI2	0.139	0.266	—

Table 20b – Possible southern branch of 011EVI.

	124SVI0	S3-32	LE-111	K1-2
124SVI0	—	0.097	0.089	0.130
S3-32	0.097	—	0.092	0.137
LE-111	0.089	0.092	—	0.165
K1-2	0.130	0.137	0.165	—

Table 20c – Possible reconstruction of 011EVI (comparing with 011EVI2).

	011EVI2	123NVI0	136SLE0	T1-32	LE-112	L1-52
011EVI2	—	0.125	0.138	0.147	0.108	0.142
123NVI0	0.125	—	0.086	0.181	0.190	0.126
136SLE0	0.138	0.086	—	0.220	0.203	0.178
T1-32	0.147	0.181	0.220	—	0.082	0.090
LE-112	0.108	0.190	0.203	0.082	—	0.139
L1-52	0.142	0.126	0.178	0.090	0.139	—

3.2.3). It is necessary to study them precisely to find out whether they are really independent streams and the classification is proper.

3.3.1 002STA

See the text in subsection 3.2.3.

3.3.2 011EVI

Recent video observations show distinct activity of the 011EVI (011EVI2 is the good example) but it is not so clear in prior radar and photographic observations. 011EVI0 and 011EVI1 listed as former observations of EVI seem to be irrelevant to the recent EVI activity 011EVI2 (Table 20a).

Former photographic and radar observations of 'EVI' might be reconstructed as shown Table 20c. L1-52 (designated Southern Virginids) is nearer to 011EVI2 than 011EVI1 (L1-62=Northern Virginids). Terent'eva had pointed to the similarity of a further shower to L1-52, called η-Virds (T1-32) previously. Table 20b suggests that 011EVI2 does not represent the central activity of the former 'EVI' and can be rather a different new activity.

It is interesting to note that there might be a southern branch of the 011EVI (Table 20b). Both, the S2-15 (=124SVI0) and the S3-32 are named 'Southern Eta-Virginids' by the original author.

3.3.3 017NTA0

See the text in subsection 3.2.3.

3.3.4 021AVB

α-Viginids are initially named by McCrosky and Posen (1959) for Virginids activity in early May. AVB1 is provided by the reference '`http://adsabs.harvard.edu/abs/1963SCoA....7..261S`', but Southworth and Hawkins (1963) included McCrosky and Posen's α-Virignid meteors in their sigma-Leonids. 021AVB2 and 021AVB3 came from similar surveys within photographic meteors by Lindblad (1971a & b) who included McCrosky and Posen's α-Viginids in σ-Leonids as well. No reference is given for the 021AVB0 and both, 021AVB0 and 021AVB1, are quite distant from the α-Virginis (Table 21a). AVB could be reconstructed with the HVI and TVI, excluding 021AVB0 and 021AVB1 (Table 21b).

Table 21a – D_{SH} matrix of 021AVB.

	021AVB0	021AVB1	021AVB2	021AVB3	021AVB4
021AVB0	—	0.247	0.333	0.284	0.378
021AVB1	0.247	—	0.202	0.175	0.213
021AVB2	0.333	0.202	—	0.094	0.117
021AVB3	0.284	0.175	0.094	—	0.127
021AVB4	0.378	0.213	0.117	0.127	—

Table 21b – D_{SH} matrix of reconstructed 021AVB with related streams.

	021AVB2	021AVB3	021AVB4	343HVI0	343HVI2	452TVI0
021AVB2	—	0.094	0.117	0.139	0.173	0.133
021AVB3	0.094	—	0.127	0.215	0.248	0.051
021AVB4	0.117	0.127	—	0.175	0.216	0.171
343HVI0	0.139	0.215	0.175	—	0.093	0.244
343HVI2	0.173	0.248	0.216	0.093	—	0.275
452TVI0	0.133	0.051	0.171	0.244	0.275	—

Table 22 – D_{SH} matrix of 097SCC

	097SCC0	097SCC1	097SCC2	097SCC3
097SCC0	—	0.330	0.168	0.197
097SCC1	0.330	—	0.461	0.218
097SCC2	0.168	0.461	—	0.293
097SCC3	0.197	0.218	0.293	—

Table 23 – D_{SH} matrix of 152NOC.

	152NOC0	152NOC1	152NOC2
152NOC0	—	0.758	0.167
152NOC1	0.758	—	0.621
152NOC2	0.167	0.621	—

Table 24 – D_{SH} matrix of 165 SZC.

	165SZC0	165SZC1	165SZC2
165SZC0	—	0.411	0.342
165SZC1	0.411	—	0.451
165SZC2	0.342	0.451	—

3.3.5 097SCC

Both the Northern and Southern δ-Cancrids are such diffuse and weak showers that the data entries do not show good agreement particularly in SCC. 097SCC1 might be neither a member of SCC nor of NCC (Table 22). 097SCC2 seems to be affected by NCC strongly: D_{SH}(096NCC1, 097SCC2) = 0.095. The δ-Cancrids were detected first by Lindblad (1971b) in photographic meteors and Sekanina (1973, 1976) confirmed it by radar observations. It is necessary to note that both of them did not separate the δ-Cancrids into northern and southern branches: L1-28=096NCC2 (δ Cancrids), S2-4=096NCC3 (Delta-Cancrids), S3-11=096NCC4 (Delta-Cancrids). Terent'eva's θ Cncds(T1-9) covers both branches and represents the center of the δ-Cancrids. Molau et al. (2013) stated they could not detect 097SCC separately from 096NCC. Jenniskens (2006) distinguishes two branches and IAUMDC followed the separation. Both, the 096NCC6 and 097SCC3 are derived from the video observations of Jenniskens et al. (2016) and D_{SH} between them is 0.131. The closest neighbour of SCC3 is not the member of 097SCC but 096NCC3=S2-4; D_{SH}(097SCC3, 096NCC3) = 0.109. Though it is possible to recognize two branches in Jenniskens' video observations, it seems not to be proper to divide former observations into two branches. It is necessary to accumulate many more data for the distinction of two branches.

3.3.6 100XSA

100XSA1(=S3-14) is named the Daytime xi Sagittariids and 100XSA0(=S3-9) is the January Sagittariids. XSA has only two entries and they are combined within the second radio meteor project (Sekanina, 1976). XSA has been confirmed neither by other observations using different techniques nor on another occasion. There are many more night time showers than the twins and also daytime activities (Helion source) surrounding XSA. It should show sufficient evidence to call XSA as an 'established shower'.

3.3.7 128MKA

D_{SH}(128MKA0, 128MKA1) = 0.225 seems to be too large to confirm this as an 'established shower'. 128MKA0 and 128MKA1 are based on small number of radar meteors, 7 and 3 respectively. MKA is located within the Helion source and it is necessary to confirm this activity by using a huge volume of data.

3.3.8 152NOC

The large values of D_{SH} suggest that 152NOC is an erroneous combination of independent entries (Table 23). 152NOC0 (S3-57=Gamma-Pegasids) might bear a relation to K1-55 (D_{SH} = 0.062) and LE-163 (D_{SH} = 0.110).

152NOC2 is from the first CMOR observations (Brown et al., 2008) but the NOC from the second CMOR observations (Brown et al., 2010) is omittted from the SD. D_{SH} between this second observation and 152NOC2 D_{SH} = 0.054 and they might be related with S3-58 (May Piscids) and K1-47. D_{SH} for the second observations are 0.116 and D_{SH} = 0.114 respectively. The peak activity of 152NOC1 ($\lambda_{\odot}$ = 64.4) is much later than others and near strong daytime showers (Daytime Arietids) though not with a clear relation to them.

3.3.9 165SZC

The D_{SH} values given in Table 24 provide no base for the assumption of the 165SZC being one shower. 165SZC0(=GE6.08) is based on only 4 meteors, though GE6.09 listed in Kronk's book as June Aquilids having 13 meteors is not quoted as NZC in the SD. Jenniskens (2006) quoted GE6.08 only as SZC and this is the first mention of the name Southern Aquilids. 165SZC1 results from the first CMOR observations (Brown et al., 2008) but SZC from the second CMOR observations (Brown et al., 2010) is omittted in the SD. Both of them are near 165SZC0 in both the radiant point and the solar longitude of the maximum activity, but the difference of several degrees in the radiant point and of about 5 km/s in the geocentric velocity give rise to the difference of more than 20 degrees in the inclination between them and 165SZC0. 165SZC2 is active later than 165SZC0 and 165SZC1 by more than 20 days and seems to be an independent activity. If we consider the possible error in the geocentric velocity among the small number of meteors of the 165SZC0, it might be possible to use the name SZC for 165SZC0, 165SZC1 and the second CMOR observations of SZC.

3.3.10 172ZPE

ZPE is the twin of STA and may contain several subshowers. 155NMA1 (D_{SH} = 0.103 for 172ZPE2) can be an additional member of ZPE.

3.3.11 175JPE

JPE become active recently because there is no JPE observation by photo and by radar in the 20th century. Early observations before 2010 175JPE0 and 175JPE1 cannot be good examples of JPE (Table 25). 522SAP0 D_{SH} = 0.011 for 175JPE6 should be included in JPE.

Table 25 – D_{SH} matrix of 175JPE.

	175JPE0	175JPE1	175JPE2	175JPE3	175JPE4	175JPE5	175JPE6
175JPE0	—	0.513	0.315	0.356	0.365	0.352	0.329
175JPE1	0.513	—	0.343	0.366	0.413	0.434	0.333
175JPE2	0.315	0.343	—	0.098	0.115	0.130	0.023
175JPE3	0.356	0.366	0.098	—	0.138	0.175	0.094
175JPE4	0.365	0.413	0.115	0.138	—	0.052	0.104
175JPE5	0.352	0.434	0.130	0.175	0.052	—	0.125
175JPE6	0.329	0.333	0.023	0.094	0.104	0.125	—

3.3.12 197AUD

The SD lists 197AUD0 (S3-149=Phi-Draconids) as AUD but not S3-147 (August Draconids) although D_{SH} (197AUD1, S3-147) = 0.110 and D_{SH}(197AUD0, 197AUD1) = 0.316. The 197AUD0 might be a number of sporadic or Toroidal meteors. 197AUD1 has many possible kins including S3-147: T1-112 (D_{SH} = 0.039), L1-207 (D_{SH} = 0.076), LE-445 (D_{SH} = 0.100), LE-441 (D_{SH} = 0.118) and T1-110 (D_{SH} = 0.171). It is necessary to note that L1-207 and T1-110 are classified as ζ-Draconids and LE-445 as κ-Cygnids by the original authors.

Could 197AUD be rebuilt with these kin? It is very difficult to answer, because 197AUD1 has very close connection with other SD meteor showers. The closest to 197AUD1 is 12KCG7 (D_{SH} = 0.080 as shown Table 19) and D_{SH} of 197AUD1 to other showers; 470AMD2 (0.108), 012KCG0 (0.121), 470AMD0 (0.123), 470AMD1 (0.125), 012KCG6 (0.131), 012KCG5 (0.149) and so on. Meteor activities near the Cygnus–Draco border are very complex and 073ZDR0 should be reviewed too (see Koseki, 2014b).

3.3.13 202ZCA

202ZCA0(NI-61.8.5) has no certain companion and D_{SH} (202ZCA0, 202ZCA1) = 0.337. 202ZCA1 results from the second observation of CMOR (Brown et al., 2010) and is close to 381DPL0 (D_{SH} = 0.140), but 202ZCA was not detected by the first CMOR observations (Brown et al., 2008).

3.3.14 257ORS

It is possible to reconstruct the 257ORS as listed in Table 26 by adding 286FTA and 636MTA, and 256ORN might be reorganized also. But, both ORS and ORN are active between the Taurids and the δ-Cancrids (NCC and SCC) and listed as entries in Table 26 themselves. They might be tainted by each other and by strong ANT activities. It is necessary to confirm the distinction identifying the member meteors in the raw data of every observation. It should be future work whether the stream suggested in Table 26 is proper.

3.3.15 320OSE

The 320OSE0 had been named as OSM originally in the first observations of CMOR (Brown et al., 2008) and was not detected in the second observations of CMOR (Brown et al., 2010). The 330SSE were detected by both CMOR observations (330SSE0 and 330SSE1), and 320OSE0 is nearer to 330SSE than 320OSE1. It is, therefore, possible to reconstruct 320OSE and 330SSE as Table 27 adding 788NHR. They are situated near the Helion source and the discrimination between OSE and SSE needs a more careful classification of raw data.

Table 26 – D_{SH} matrix of 257ORS and related entries.

	257ORS0	257ORS1	257ORS2	257ORS3	286FTA0	286FTA1	636MTA0
257ORS0	—	0.096	0.140	0.265	0.139	0.128	0.258
257ORS1	0.096	—	0.107	0.226	0.193	0.192	0.204
257ORS2	0.140	0.107	—	0.137	0.226	0.201	0.123
257ORS3	0.265	0.226	0.137	—	0.310	0.277	0.053
286FTA0	0.139	0.193	0.226	0.310	—	0.061	0.321
286FTA1	0.128	0.192	0.201	0.277	0.061	—	0.293
636MTA0	0.258	0.204	0.123	0.053	0.321	0.293	—

Table 27 – D_{SH} matrix of 320 OSE and related entries.

	320OSE0	320OSE1	330SSE0	330SSE1	330SSE2	788NHR0
320OSE0	—	0.209	0.141	0.114	0.125	0.195
320OSE1	0.209	—	0.270	0.253	0.248	0.332
330SSE0	0.141	0.270	—	0.032	0.119	0.139
330SSE1	0.114	0.253	0.032	—	0.096	0.155
330SSE2	0.125	0.248	0.119	0.096	—	0.234
788NHR0	0.195	0.332	0.139	0.155	0.234	—

Table 28 – D_{SH} matrix of 326EPG and related entries.

	326EPG0	326EPG1	327BEQ0
326EPG0	—	0.153	0.124
326EPG1	0.153	—	0.143
327BEQ0	0.124	0.143	—

3.3.16 326EPG

It is better to reconstruct this with 327BEQ0 as shown in Table 28 (see section 3.3.17. 327BEQ).

3.3.17 327BEQ

The 327BEQ seems to be an apparent combination; D_{SH}(326BEQ0, 326BEQ1) = 0.376. The 326BEQ0 should be included in the 326EPG (see section 3.3.16), and 326BEQ1 might be a loose member of 164NZC or may form a subgroup with 164NZC0, 766BAD0: D_{SH}(326BEQ1, 164NZC0) = 0.157, D_{SH}(326BEQ1, 766BAD0) = 0.111.

3.3.18 335XVI

520MBC is the twin of 335XVI.

3.3.19 337NUE

The 337NUE lies on the southern border of the Apex area and near the Southern Toroidal region. Rich sporadic activities hindered the reliable detection of this shower and the listed 337NUE entries are dispersed (Table 29a). Orbital elements of high speed and near the Apex showers can be altered by small differences in the radiant point and in the velocity (see 3.2.5. Leonids). It may be possible to reorganize 337NUE with neighbouring activities as given in the Tables 29b and 29c.

3.3.20 supplementary note: 221DSX

The SD does not list the first observation of the DSX NI-61.9.2 though it is close to the DSX naturally: 221DSX0 (D_{SH} = 0.033), 221DSX1 (D_{SH} = 0.131), 221DSX2 (D_{SH} = 0.083), 221DSX3 (D_{SH} = 0.027), 221DSX4 (D_{SH} = 0.065). This is only an example and there might be other lacks of proper references. The SD lists showers in a researcher's view. We see the incompleteness of the SD shown above; far kin are combined into one on the one hand, the closer neighbours or important sources are disregarded. The SD should more objective.

Table 29a – D_{SH} matrix of the 337NUE.

	337NUE0	337NUE1	337NUE2
337NUE0	—	0.429	0.231
337NUE1	0.429	—	0.628
337NUE2	0.231	0.628	—

Table 29b – D_{SH} matrix of 337NUE subgroup with 552PSO.

	337NUE1	552PSO0	552PSO1
337NUE1	—	0.112	0.207
552PSO0	0.112	—	0.250
552PSO1	0.207	0.250	—

Table 29c – D_{SH} matrix of 337NUE subgroup with 430POR.

	337NUE0	337NUE2	430POR0
337NUE0	—	0.231	0.227
337NUE2	0.231	—	0.223
430POR0	0.227	0.223	—

3.4 Discussions about confusions in the shower list

The problems reviewed above are caused by very composite sources. We might sort them into eight.

1. *Differences in the meteor shower definition*
   There are many differences in meteor shower/meteoroid stream detection techniques (see Koseki, 2014a). Some investigators used the differences in D_{SH} as the discrimination level in search of meteoroid streams and others used the similarity of shower radiant distribution and of the geocentric velocity. Meteoroid streams detected by D_{SH} (e.g. Lindblad 1971b) seem to be narrower in their activity period and tighter in their orbits than those found by the wavelet technique used in CMOR (e.g. Brown et al., 2008).

2. *Formerly produced frameworks limit the later combinations*
   As an example, 021AVB0 and 021AVB1 seem to hinder us from regarding 342HVI and 452TVI as members of 021AVB (see 3.3.4). Several meteor showers in the SD are not the combination of the closest within all entries because of the formerly settled frameworks and, therefore, such meteor showers should be reconstructed within other frameworks.

3. *Different activity given the same name*
   For example, the names AUD and ZDR were given to different observations in different versions of the SD (see 3.2.4 and also Koseki, 2014b). Both, the northern and southern ι-Aquariids seem to be in confusion on what activity is properly called this way (see 3.2.2 and 3.3.12). The Northern δ-Aquariids had been named for late July–early August meteor activity in the Aquarius area as well as Southern δ-Aquariids, though NDA in the SD implies middle-late August activity in Pisces.

4. *The differences by observational techniques*
   We can imagine meteor showers detected by radar are rich in fainter meteors than optical ones. If the magnitude ratios or mass index are different, we cannot see one meteor shower but it can be another one (see Koseki, 2014a). 242XDR and 325DLT are from radar observations having only one observation and have been not detected by optical observations. 061TAH is from photographic data and 73ZDR from video data, and both have not been found by radar observations. It is noticeable that observations of the 175JPE are video observations except for 175JPE0 (visual) and 12KCG has been observed by optical methods (see 3.2.4).

5. *Annual activity fluctuation*
   COR, JBO and TAH are listed as the established showers but they are historical ones or of recurrent nature. Their orbits, not their parent comets, have not been reduced precisely. Hoffmeister's orbit for COR is based on visual estimate and JBO and TAH orbits seem to be determined poorly. 137PPU, 198BHY and 254PHO are the records of outbursts and have not been noticed on other occasions. The author revealed the periodic activity of KCG (see 3.2.4 and also Koseki, 2014b) and we see KCG different in average years.

6. D_{SH} *four dimensional space distorts observational errors*
   Meteor showers of higher geocentric velocity are affected by the error in velocity stronger than slower showers (see 3.2.5), because the change in the geocentric velocity, especially for near Apex source, alters the orbit radically. The change in the eccentricity exerts on DSH directly and, more, the direction of the orbital axis is weighted by the mean of the eccentricity.

7. *Weak shower activity and abundant sporadic activity*
   Meteor activities are impressive in the area of Antihelion, Apex and Toroidal areas. Except for special cases, such as Geminids, Leonids and Quadrantids, it is very difficult to distinguish meteor shower activities from sporadics around such areas. The Taurids are one of the most active showers in the ANT area but the conclusions of researchers differ widely (see 3.2.3). The difficulties are much larger in other showers and streams (e.g. 3.3.4).

8. *Successive or neighbouring multiple shower activities*
   COM is located near the Apex and the Toroidal area and, more, the DLM leads and the JCO follows it. If we would perceive meteor activity in November and early December around the tail of the Leonids as the latest 013LEO activity, 013LEO is a neighbour to COM (see 3.2.6). If we would consent meteor activity in September around the Pisces as early TAU and those of December around the sword of Orion as late TAU, many small meteor showers listed as independent meteor showers in the SD could be included in TAU (see 3.2.3).

4 Conclusions

The current SD is a conglomerate. It started as Jenniskens' 'working list' (Jenniskens, 2006) and has been piled up and data of different nature has been added. The list is not constructed uniformly and individual entries have different history and quality; orbital elements are given by B1950.0 in some entries and by J2000.0 in others, for an example.

There is a nomenclature for the showers but no concrete definition for the showers themselves. This discrepancy has not been introduced only by the SD but by the researchers themselves. Different meteor showers (including rich sporadic activities) might be combined into one entry in some cases, and one broad shower may be divided into groups (sub showers) in the SD. We, especially amateurs, need to be careful to use the SD and need to know that the first line of the entry for each shower does not imply the most reliable data.

If we would try to construct a meteor shower database, we need the observational raw data:
1) Any published "meteor shower list" represents the author's view. The definition of a meteor shower/ meteoroid stream may be different among several researchers.
2) A published "meteor shower list" cannot give any information on the 'not detected showers/streams' though there might be weak traces of them in the analysed data.
3) The interruption of observations, the period of the activity and the use of mean elements introduce confusion to the list. It is necessary to check the elements at the peak of the activity.
4) Meteor activities change year by year and, therefore, it is useful to check the activity level above the sporadics observed by the same devices.

References

Brown P., Weryk R. J., Wong D. K., and Jones J. (2008). "A meteoroid stream survey using the Canadian Meteor Orbit Radar. I. Methodology and radiant catalogue". *Icarus*, **195**, 317–339.

Brown P., Wong D. K., Weryk R. J., and Wiegert P. (2010). "A meteoroid stream survey using the Canadian Meteor Orbit Radar. II. Identification of minor showers using a 3D wavelet transform". *Icarus*, **207**, 66–81.

Denning W. F. (1916). "Remarkable meteoric shower on June 28". *Mon. Not. Roy. Astron. Soc.*, **76**, 740–743.

Hashimoto T. and Osada K. (1998). "June Bootid outburst: Optical observations from Japan". *WGN, Journal of the IMO*, **26:6**, 263–266.

IAUMDC (2016). "IAUMDC Shower Database". `http://www.ta3.sk/IAUC22DB/MDC2007/index.php` . (Updated 2016 Mar. 17, by Z. Kanuchova and T. J. Jopek).

Jenniskens P. (2006). *Meteor Showers and their parent comets.* Cambridge University Press. Table 7, 'Working list of cometary meteor showers', pages 691–746 (`http://www.astro.sk/~ne/IAUMDC/STREAMLIST/meteoroidstreamworkinglist.pdf`).

Jenniskens P., Nénon Q., Albers J., Gural P. S., Haberman B., Holman D., Morales R., Grigsby B. J., Samuels D., and Johannink C. (2016). "The established meteor showers as observed by CAMS". *Icarus*, **266**, 331–354.

Kashcheyev B. L., Lebedinets V. N., and Lagutin M. F. (1967). *Meteor phenomena in the Earth's atmosphere*. Nauka. (in Russian).

Koseki M. (2009). "Meteor shower records: A reference table of observations from previous centuries". *WGN, Journal of the IMO*, **37:5**, 139–160.

Koseki M. (2011). "Coma Berenicids and related activities". *WGN, Journal of the IMO*, **39:6**, 159–166.

Koseki M. (2012). "Three components of 'Taurids"'. *WGN, Journal of the IMO*, **40:4**, 129–138.

Koseki M. (2014a). "Various meteor scenes I: The perception and the conception of a 'meteor shower"'. *WGN, Journal of the IMO*, **42:5**, 170–180.

Koseki M. (2014b). "Various meteor scenes II: Cygnid-Draconid Complex (κ-Cygnids)". *WGN, Journal of the IMO*, **42:5**, 181–197.

Koseki M. (2015). "Various meteor scenes III: Recurrent showers and some minor showers". *WGN, Journal of the IMO*, **43:1**, 14–27.

Kresak L. (1970). "The dispersion of meteoroids in meteor streams. I. The size of the radiant areas". *BAC*, **21**, 153–170.

Kronk G. W. (2014). *Meteor Showers: An Annotated Catalog, Second Edition*. Springer.

Lindblad B. A. (1971a). "A computerized stream search among 2401 photographic meteor orbits". *Smithsonian Contributions to Astrophysics*, **12**, 14–24.

Lindblad B. A. (1971b). "Meteor streams". *Space Research*, pages 287–297.

Lindblad B. A. (1971c). "A stream search among 865 precise photographic meteor orbits". *Smithsonian Contributions to Astrophysics*, **12**, 1–13.

McCrosky R. E. and Posen A. (1959). "New photographic meteor shower". *Astronomical Journal*, **64**, 25–27.

Molau S., Kac J., Berko E., Crivello S., Stomeo E., Igaz A., Barentsen G., and Goncalves R. (2013). "Results of the IMO Video Meteor Network – January 2013". *WGN, Journal of the IMO*, **41:2**, 61–66.

Nakamura K. (1930). "On the observation of faint meteors, as experienced in the case of those from the orbit of comet Schwassmann-Wachmann, 1930d". *Mon. Not. Roy. Astron. Soc.*, **91**, 204–209.

Rendtel J. and Arlt R. (2016). "Kappa Cygnid rate variations over 41 years". *WGN, Journal of the IMO*, **44:3**, 62–66.

Sato M. (2004). (His prediction at `http://fas.kaicho.net/tenshow/meteor/7p2004/e1.htm` and the observational results of his group at `http://fas.kaicho.net/tenshow/meteor/pw2004/pw2004e.htm`).

Sekanina Z. (1970). "Statistical model of meteor streams. II. Major showers". *Icarus*, **13**, 475–493.

Sekanina Z. (1973). "Statistical model of meteor streams. III. Stream search among 19303 radio meteors". *Icarus*, **18**, 253–284.

Sekanina Z. (1976). "Statistical model of meteor streams. IV - A study of radio streams from the synoptic year". *Icarus*, **27**, 265–321.

Southworth R. B. and Hawkins G. S. (1963). "Statistics of meteor streams". *Smithsonian Contributions to Astrophysics*, **7**, 261–285.

Whipple F. L. (1954). "Photographic meteor orbits and their distribution in space". *Astronomical Journal*, **59**, 201–217.

Wright F. W., Jacchia L. G., and Whipple F. L. (1957). "Photographic ι-Aquarid meteors and evidence for the northern δ-Aquarids". *Astronomical Journal*, **62**, 225–233.

Handling Editor: Jürgen Rendtel

Preliminary results

Results of the IMO Video Meteor Network — April 2016

Sirko Molau[1], *Stefano Crivello*[2], *Rui Goncalves*[3], *Carlos Saraiva*[4], *Enrico Stomeo*[5], *and Javor Kac*[6]

In 2016 April, a total of 78 video cameras of the IMO Video Meteor Network recorded more than 16 000 meteors in almost 7 700 hours of observing time. The flux density profile of the Lyrids 2016 is presented and compared to the average for the years 2011–2015. The flux density increased significantly as twilight set in on the morning of 2016 April 22. A similar increase was also seen in 2012. The population index of the Lyrids is also derived from observations around the shower maximum.

Received 2016 September 10

1 Introduction

39 observers with 78 video systems reported their observations to the IMO Video Network in April. The weather was mediocre with larger gaps in the observing statistics, which is not unusual for this time of year. If we put aside the year 2015 with its exceptional observing conditions, the output of 2016 is comparable with the previous years both with respect to the effective observing time and meteor count. With 48 cameras, almost two out of three cameras managed to observe on twenty or more observing nights (Table 1 and Figure 1). No geographic region was particularly advantaged or disadvantaged.

2 Lyrids

Unfortunately, on the night of the Lyrid maximum the weather conditions were far from perfect, so that we obtained less data than usual. But the Lyrid activity profile is the same every year, is it not?

In Figure 2 (left) we compare the flux density profile of 2016 (red) with the average profile during the years 2011–2015 (green). There is good agreement indeed, except that on the maximum night the rate increase is stronger in 2016 than the average of 2011–2015. In addition, a comparison of the profiles of 2012 and 2016 (Figure 2, right), which cover almost the same solar longitude interval, yields a perfect match.

The average profile of recent years shows that the peak activity of the Lyrids is reached at 32.°17 solar longitude, which translates in 2016 to $02^{h}20^{m}$ UT on April 22. In both 2012 and 2016 there is a remarkable increase of rates at the end of the peak night in the European observing window. Closer inspection of this night in 2016 (Figure 4, left) reveals that the flux density increased almost instantly at $02^{h}50^{m}$ UT by a factor of two to three.

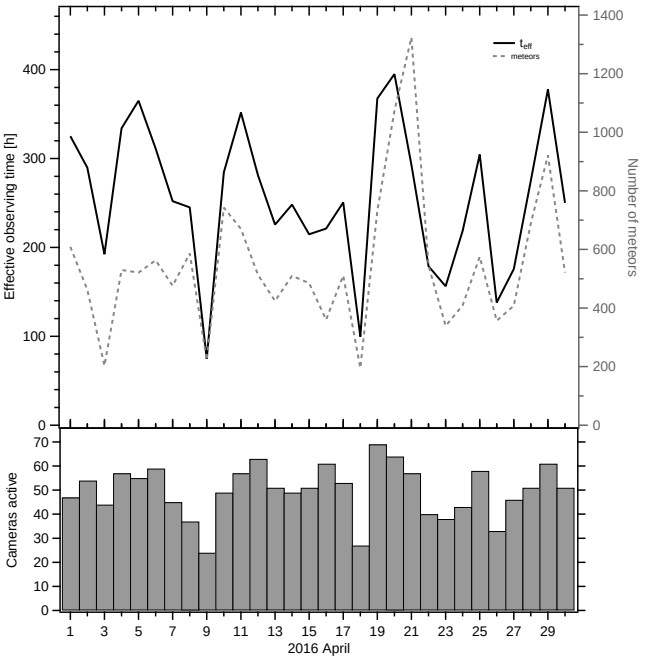

Figure 1 – Monthly summary for the effective observing time (solid black line), number of meteors (dashed gray line) and number of cameras active (bars) in 2016 April.

Unfortunately, twilight in Europe had already progressed to the stage whereby only the more western cameras were still active at this time. Moreover, the weather there was not optimal, and as a result the five Templar cameras of Rui Goncalves were not active, for example. Hence it is debatable as to whether the rate increase is real or just a camera selection effect.

We cannot fall back on visual observations this year, since the full moon could hardly motivate any meteor observer and thus the IMO did not receive a single visual observing report. If we reduce the data set to only those cameras which were still active after $03^{h}00^{m}$ UT (Bmh1, Mincam1, Mincam3, Mincam4, Mincam6, Ro3), the increase starts a bit earlier but is otherwise confirmed. This is evidence that rates have indeed increased significantly in the European dawn of April 22.

[1]Abenstalstr. 13b, 84072 Seysdorf, Germany.
Email: sirko@molau.de
[2]Via Bobbio 9a/18, 16137 Genova, Italy.
Email: stefano.crivello@libero.it
[3]Urbanizacao da Boavista, Lote 46, Linhaceira, 2305-114 Asseiceira, Tomar, Portugal. Email: rui.goncalves@ipt.pt
[4]Rua Aquilino Ribeiro, 23 - 1 Dto. 2790028 Carnaxide, Portugal. Email: carlos.saraiva@netcabo.pt
[5]via Umbria 21/d, 30037 Scorze (VE), Italy.
Email: stom@iol.it
[6]Na Ajdov hrib 24, 2310 Slovenska Bistrica, Slovenia.
Email: javor.kac@orion-drustvo.si

IMO bibcode WGN-445-molau-vidapr
NASA-ADS bibcode 2016JIMO...44..170M

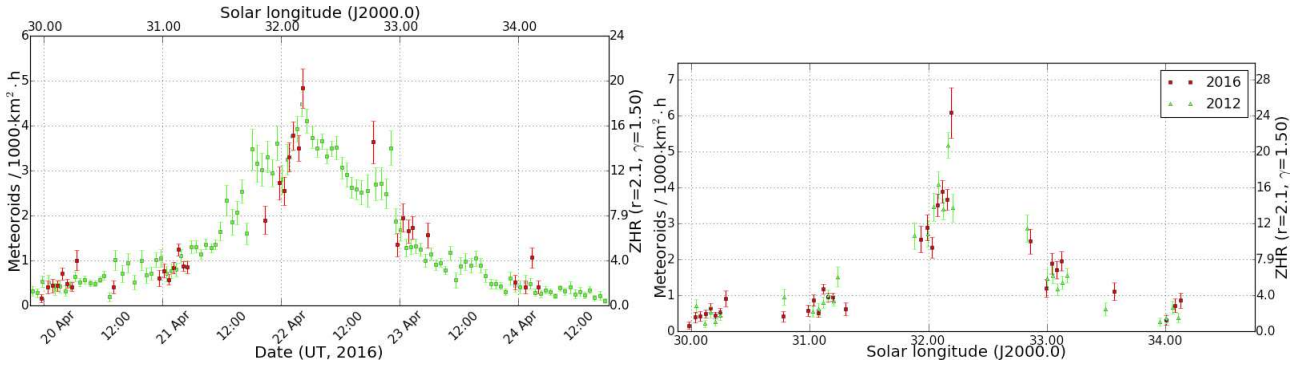

Figure 2 – Comparison of (left) the flux density profile of the Lyrids in 2016 (red, dark squares) with the average of 2011–2015 (green, light squares), and (right) between the profiles of 2012 (green, light squares) and 2016 (red, dark squares) obtained from observations of the IMO Video Network.

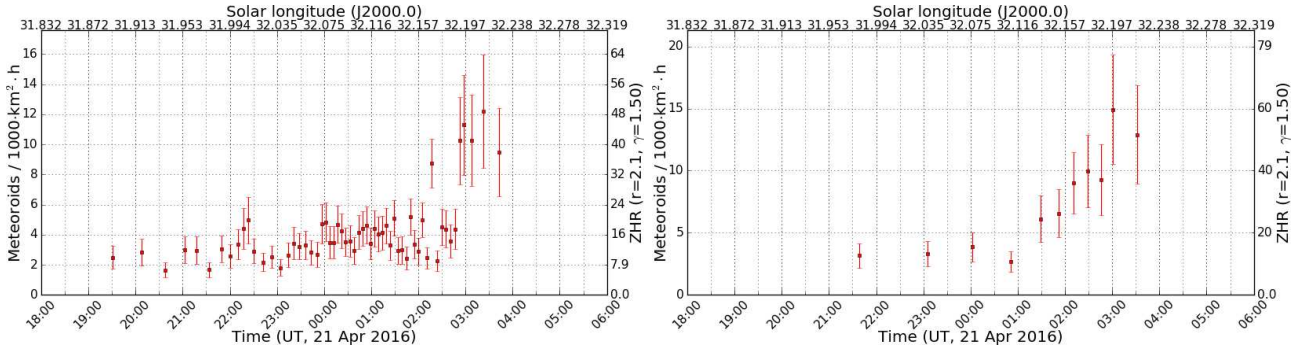

Figure 3 – Detailed flux density profile from the peak of the Lyrids 2016. On the left side the data of all cameras are included, on the right side only from cameras which were still active after $03^{h}00^{m}$ UT.

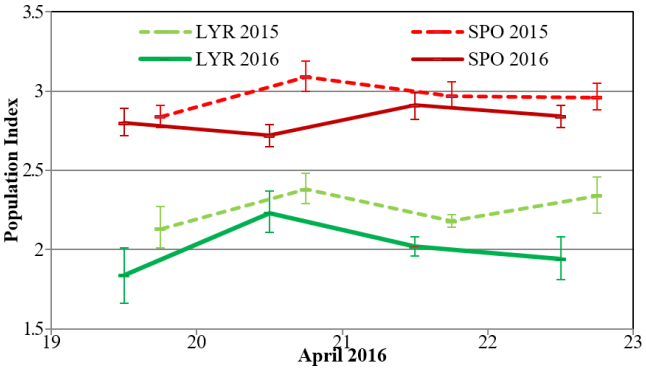

Figure 4 – Population index of the Lyrids and sporadic meteors in 2016 April. For comparison, the values from 2015 are also shown, with the data points being arranged by solar longitude.

The calculation of the r-values did not yield any surprise (Figure 4). With $r = 2.0$, the population index of the Lyrids was lower by about 0.25 than in the year 2015, which can be attributed to the full moon in 2016. At the same time, we determined a sporadic population index of $r = 2.8$, compared to $r = 2.95$ in the year 2015. Thus, the population index of the Lyrids obtained from video data is by about 0.7 to 0.8 lower than the sporadic r-value and matches to the value of $r = 2.1$ given in the IMO Meteor Shower Calendar (Rendtel, 2015).

References

Rendtel J. (2015). "2016 Meteor Shower Calendar". International Meteor Organization. IMO INFO(2-15).

Handling Editor: Javor Kac

Code	Name	Location	Camera	FOV [°²]	Stellar LM [mag]	Eff.CA [km²]	Nights	Time [h]	Meteors
ARLRA	Arlt	Ludwigsfelde/DE	Ludwig2 (0.8/8)	1475	6.2	3779	27	107.2	455
BANPE	Bánfalvi	Zalaegerszeg/HU	Huvcse01 (0.95/5)	2423	3.4	361	15	10.7	73
BERER	Berkó	Ludányhalászi/HU	Hulud1 (0.8/3.8)	5542	4.8	3847	13	58.7	267
BOMMA	Bombardini	Faenza/IT	Mario (1.2/4.0)	5794	3.3	739	22	114.7	232
BREMA	Breukers	Hengelo/NL	Mbb3 (0.75/6)	2399	4.2	699	26	134.5	161
BRIBE	Klemt	Herne/DE	Hermine (0.8/6)	2374	4.2	678	17	84.7	160
		Bergisch Gladbach/DE	Klemoi (0.8/6)	2286	4.6	1080	19	99.4	142
CASFL	Castellani	Monte Baldo/IT	Bmh1 (0.8/6)	2350	5.0	1611	18	94.6	155
			Bmh2 (1.5/4.5)*	4243	3.0	371	18	83.0	120
CRIST	Crivello	Valbrevenna/IT	Bilbo (0.8/3.8)	5458	4.2	1772	24	108.4	170
			C3P8 (0.8/3.8)	5455	4.2	1586	22	76.9	89
			Stg38 (0.8/3.8)	5614	4.4	2007	26	136.5	302
DONJE	Donani	Faenza/IT	Jenni (1.2/4)	5886	3.9	1222	22	128.8	344
ELTMA	Eltri	Venezia/IT	Met38 (0.8/3.8)	5631	4.3	2151	18	76.0	162
FORKE	Förster	Carlsfeld/DE	Akm3 (0.75/6)	2375	5.1	2154	20	104.4	203
GONRU	Goncalves	Tomar/PT	Templar1 (0.8/6)	2179	5.3	1842	23	154.4	334
			Templar2 (0.8/6)	2080	5.0	1508	23	149.2	258
			Templar3 (0.8/8)	1438	4.3	571	21	126.2	86
			Templar4 (0.8/3.8)	4475	3.0	442	21	132.9	208
			Templar5 (0.75/6)	2312	5.0	2259	22	119.3	195
GOVMI	Govedič	Središče ob Dravi/SI	Orion2 (0.8/8)	1447	5.5	1841	20	91.5	160
			Orion3 (0.95/5)	2665	4.9	2069	12	51.9	71
			Orion4 (0.95/5)	2662	4.3	1043	11	51.1	102
HERCA	Hergenrother	Tucson/US	Salsa3 (0.8/3.8)	2336	4.1	544	15	108.3	163
IGAAN	Igaz	Budapest/HU	Hupol (1.2/4)	3790	3.3	475	13	58.8	44
JONKA	Jonas	Budapest/HU	Husor (0.95/4)	2286	3.9	445	21	126.0	132
			Husor2 (0.95/3.5)	2465	3.9	715	21	132.8	119
KACJA	Kac	Ljubljana/SI	Orion1 (0.8/8)	1399	3.8	268	22	129.2	208
		Kamnik/SI	Cvetka (0.8/3.8)*	4914	4.3	1842	17	106.6	271
			Rezika (0.8/6)	2270	4.4	840	17	100.2	303
			Stefka (0.8/3.8)	5471	2.8	379	13	73.4	88
KOSDE	Koschny	Izana Obs./ES	Icc7 (0.85/25)*	714	5.9	1464	1	8.0	32
			Lic1 (2.8/50)*	2255	6.2	5670	2	13.1	93
		La Palma/ES	Icc9 (0.85/25)*	683	6.7	2951	23	148.0	1094
			Lic2 (3.2/50)*	2199	6.5	7512	26	185.4	1384
		Noordwijkerhout/NL	Lic4 (1.4/50)*	2027	6.0	4509	11	50.8	51
LOJTO	Łojek	Grabniak/PL	Pav57 (1.0/5)	1631	3.5	269	13	74.7	128
LOPAL	Lopes	Lisbon/PT	Naso1 (0.75/6)	2377	3.8	506	19	109.7	52

Table 1 – Observers contributing to 2016 April data of the IMO Video Meteor Network. Eff.CA designates the effective collection area; the overall number of nights is the number of nights with at least one camera operating, the overall observing time and number of meteors are sums over all cameras.

Table 1 – Observers contributing to 2016 April data of the IMO Video Meteor Network – continued from previous page.

Code	Name	Location	Camera	FOV [°²]	Stellar LM [mag]	Eff.CA [km²]	Nights	Time [h]	Meteors
MACMA	Maciejewski	Chełm/PL	Pav35 (0.8/3.8)	5495	4.0	1584	20	108.9	265
			Pav36 (0.8/3.8)*	5668	4.0	1573	22	95.8	202
			Pav43 (0.75/4.5)*	3132	3.1	319	16	86.6	122
			Pav60 (0.75/4.5)	2250	3.1	281	20	108.1	252
MARGR	Maravelias	Lofoupoli-Crete/GR	Loomecon (0.8/12)	738	6.3	2698	16	120.7	133
MARRU	Marques	Lisbon/PT	Cab1 (0.8/3.8)	5291	3.1	467	23	164.4	266
			Ran1 (1.4/4.5)	4405	4.0	1241	16	94.8	95
MASMI	Maslov	Novosibirsk/RU	Nowatec (0.8/3.8)	5574	3.6	773	10	26.3	94
MOLSI	Molau	Seysdorf/DE	Avis2 (1.4/50)*	1230	6.9	6152	21	118.0	501
			Escimo2 (0.85/25)	155	8.1	3415	20	114.0	193
			Mincam1 (0.8/8)	1477	4.9	1084	20	101.1	228
		Ketzür/DE	Remo1 (0.8/8)	1467	6.5	5491	26	145.3	535
			Remo2 (0.8/8)	1478	6.4	4778	26	145.5	474
			Remo3 (0.8/8)	1420	5.6	1967	5	35.6	47
			Remo4 (0.8/8)	1478	6.5	5358	26	146.5	479
MORJO	Morvai	Fülöpszállás/HU	Huful (1.4/5)	2522	3.5	532	23	163.0	150
MOSFA	Moschini	Rovereto/IT	Rover (1.4/4.5)	3896	4.2	1292	14	5.0	31
OTTMI	Otte	Pearl City/US	Orie1 (1.4/5.7)	3837	3.8	460	14	60.9	79
PERZS	Perkó	Becsehely/HU	Hubec (0.8/3.8)*	5498	2.9	460	23	66.6	268
ROTEC	Rothenberg	Berlin/DE	Armefa (0.8/6)	2366	4.5	911	21	19.6	111
SARAN	Saraiva	Carnaxide/PT	Ro1 (0.75/6)	2362	3.7	381	20	115.0	125
			Ro2 (0.75/6)	2381	3.8	459	22	128.1	138
			Ro3 (0.8/12)	710	5.2	619	22	141.4	232
			Sofia (0.8/12)	738	5.3	907	19	108.0	99
SCALE	Scarpa	Alberoni/IT	Leo (1.2/4.5)*	4152	4.5	2052	20	57.6	75
SCHHA	Schremmer	Niederkrüchten/DE	Doraemon (0.8/3.8)	4900	3.0	409	20	81.3	140
SLAST	Slavec	Ljubljana/SI	Kayak1 (1.8/28)	563	6.2	1294	17	100.8	132
			Kayak2 (0.8/12)	741	5.5	920	9	42.4	60
STOEN	Stomeo	Scorze/IT	Min38 (0.8/3.8)	5566	4.8	3270	22	86.1	217
			Noa38 (0.8/3.8)	5609	4.2	1911	23	89.4	240
			Sco38 (0.8/3.8)	5598	4.8	3306	25	107.9	326
STRJO	Strunk	Herford/DE	Mincam2 (0.8/6)	2354	5.4	2751	27	122.9	330
			Mincam3 (0.8/6)	2338	5.5	3590	26	122.8	183
			Mincam4 (1.0/2.6)	9791	2.7	552	22	86.9	87
			Mincam5 (0.8/6)	2349	5.0	1896	23	118.7	180
			Mincam6 (0.8/6)	2395	5.1	2178	22	110.9	166
TEPIS	Tepliczky	Agostyán/HU	Huago (0.75/4.5)	2427	4.4	1036	24	169.2	171
			Humob (0.8/6)	2388	4.8	1607	24	161.4	242
TRIMI	Triglav	Velenje/SI	Sraka (0.8/6)*	2222	4.0	546	14	24.5	61
YRJIL	Yrjölä	Kuusankoski/FI	Finexcam (0.8/6)	2337	5.5	3574	17	76.1	137
						Overall	30	7 698.1	16 477

* active field of view smaller than video frame

Results of the IMO Video Meteor Network — May 2016

Sirko Molau[1], *Stefano Crivello*[2], *Rui Goncalves*[3], *Carlos Saraiva*[4], *Enrico Stomeo*[5], *and Javor Kac*[6]

The IMO Video Meteor Network cameras recorded more than 17 000 meteors in 7 000 hours of observing time in 2016 May. The flux density profile of the η-Aquariids is presented, showing a short peak of about 90 meteoroids per 1000 km^2 per hour on May 7. Comparison if made for the η-Aquariids with other major showers with respect to the peak flux density and peak width. The flux density profile is also presented for the minor shower η-Lyrids.

Received 2016 October 19

1 Introduction

May started mediocre but improved towards the end of the month significantly. 44 out of 77 cameras in operation managed to observe in twenty or more observing nights. Salsa3 did not experience any break at all and also observers in Southern Europe (Italy, Portugal) managed to obtain long observing series. Although May 26/27 had the largest number of active cameras (61 cameras and 300 observing hours), twice as many meteors were recorded thanks to the η-Aquariids on May 5/6 and 6/7 than May 26/27.

With almost exactly 7 000 hours of effective observing time (Table 2 and Figure 1), May of 2016 performed a few percent worse than in the two preceding years. With respect to the meteor count it fall in-between the two preceding years.

2 η-Aquariids

When talking about major meteor showers, a European observer will immediately think of the Quadrantids (QUA), Perseids (PER) and Geminids (GEM), but for southern hemisphere observers the η-Aquariids (ETA) of May are much more attractive. Before we analyze if they may also be considered a major shower, we first want to have a look at the overall ETA activity profile for 2016 (Figure 2). Around April 26, at a solar longitude of 37°, the η-Aquariids start to stand out from the sporadic background. By May 2 they already reached a flux density of twenty meteoroids per 1 000 km^2 per hour, and two days later the peak time started, which lasted for about three days. The flux density lasted a full week above twenty meteoroids per 1 000 km^2 per hour and only by the last third of May (solar longitude 60°) did the activity vanish into the sporadic background.

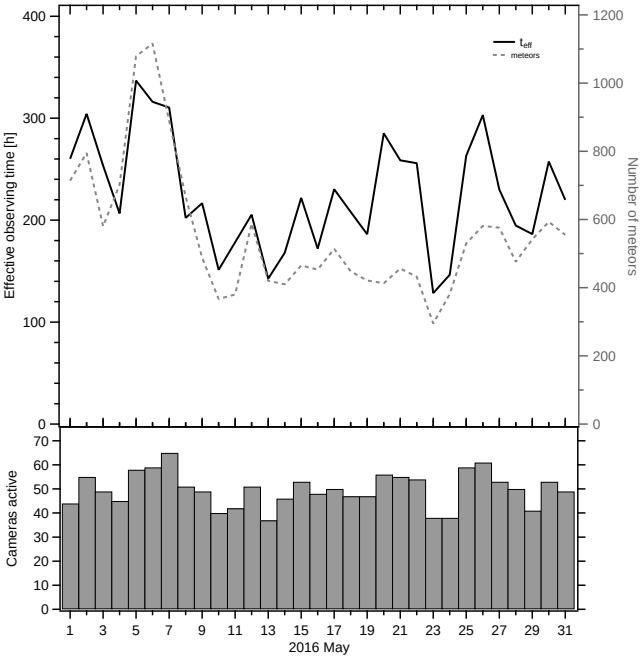

Figure 1 – Monthly summary for the effective observing time (solid black line), number of meteors (dashed gray line) and number of cameras active (bars) in 2016 May.

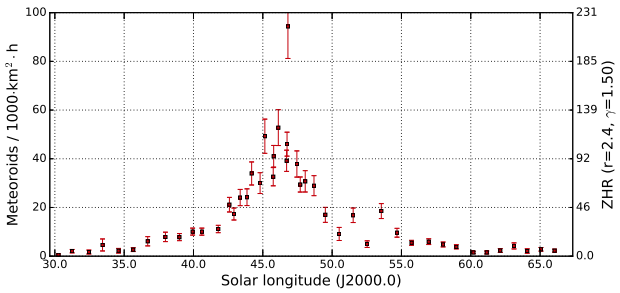

Figure 2 – Flux density profile of the η-Aquariids in 2016, obtained from observations of the IMO Video Meteor Network.

Particularly prominent in 2016 is a short peak of up to 90 meteoroids per 1 000 km^2 per hour in the morning hours of May 7. This value is impressive, but it is not exceptional for the η-Aquariids. Previously in 2012 we obtained a similar flux density at about the same time, and one year later on May 5 the shower clearly passed the mark of 100 meteoroids per 1 000 km^2 per hour. The 2016 peak occurred once more at the end of the European observing window when only a few cameras were still active and larger error bars are possible.

[1]Abenstalstr. 13b, 84072 Seysdorf, Germany.
Email: sirko@molau.de
[2]Via Bobbio 9a/18, 16137 Genova, Italy.
Email: stefano.crivello@libero.it
[3]Urbanizacao da Boavista, Lote 46, Linhaceira, 2305-114 Asseiceira, Tomar, Portugal. Email: rui.goncalves@ipt.pt
[4]Rua Aquilino Ribeiro, 23 - 1 Dto. 2790028 Carnaxide, Portugal. Email: carlos.saraiva@netcabo.pt
[5]via Umbria 21/d, 30037 Scorze (VE), Italy.
Email: stom@iol.it
[6]Na Ajdov hrib 24, 2310 Slovenska Bistrica, Slovenia.
Email: javor.kac@orion-drustvo.si

IMO bibcode WGN-445-molau-vidmay
NASA-ADS bibcode 2016JIMO...44..174M

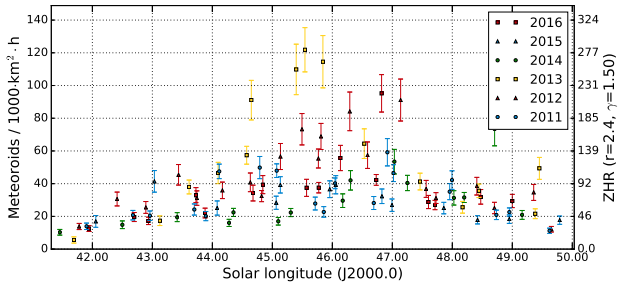

Figure 3 – Comparison of the flux density profile of the η-Aquariids in the first third of May of the years 2011 to 2016, obtained from observations of the IMO Video Meteor Network.

Figure 3 shows the details for the first third of May in the years 2011 to 2016. Since the peak activity changes significantly from one year to the next, there is only little value in creating an average activity profile.

2.1 Comparison of η-Aquariids to other major showers

Now back to the question if the η-Aquariids belong to the major showers or if they play only in the "2nd division". An attractive shower for visual observers needs to provide high rates in the optical range for a long time. So we calculated from the flux density profiles since 2011 the peak time, peak flux density and full width at half maximum of QUA, ETA, PER and GEM. The problem was that we have no continuous activity profiles, but that only the European longitudes are well covered. For this reason, we did not rely on the observed peak flux density, but we fitted an exponential function to the ascending and descending activity branch and defined the intersection point of both as the peak. That works in some case better than in others. In particular for the Quadrantids with their short activity interval we are often missing important parts of the profile and need to extrapolate the existing data significantly. Also additional peaks e.g. by dust trail encounters may distort the result. Such uncertain figures are put in brackets in Table 1.

As a consistency check we calculated for each shower an average profile over all data (even though this includes averaging over years with big differences in activity as remarked before). Those average values are printed in bold in Table 1.

In Figures 4 and 5 we present the results graphically. Figure 4 plots the peak flux density vs. the full width at half maximum, Figure 5 vs. the time of peak (relative to the average peak solar longitude).

What can we learn from the graphs? In Figure 4, each shower forms his own cluster. The Quadrantids have a FWHM of just about 0.°4 solar longitude, and they reach an average peak flux density of 30 meteoroids per 1 000 km^2 per hour. We reported already before on the large scatter in QUA peak activity (Molau et al., 2016).

With a FWHM of 1.°3 solar longitude, the Geminids last three times as long, and with 75 meteoroids per 1 000 km^2 per hour they reach the highest flux density of all considered showers. There is only little scatter in strength and duration of the peak.

The Perseids are slightly longer active with a FWHM of 1.°4 solar longitude, and their peak flux density of about 45 meteoroids per 1 000 km^2 per hour is clearly smaller. The scatter is about as large as in case of the Geminids.

The flux density of the η-Aquariids is a bit higher (over 50 meteoroids per 1 000 km^2 per hour on average) and the mean duration of almost 5° solar longitude is unrivaled. The year 2013 was totally exceptional.

Table 1 – Peak time, peak flux density and full width at half maximum (FWHM) of the Quadrantids, η-Aquariids, Perseids and Geminids since 2011. Figures in brackets have larger uncertainties, figures printed in bold are obtained from an averaged activity profile over all years.

Shower	Year	Peak $\lambda_\odot$ [°]	Flux Density [1 000 km^{-2}h^{-1}]	FWHM [° $\lambda_\odot$]
QUA	(2012)	(283.18)	(25.0)	(0.37)
	(2013)	(282.94)	(27.3)	(0.35)
	(2014)	(283.09)	(54.8)	(0.37)
	2015	283.14	10.0	0.57
	(2016)	(283.22)	(36.7)	(0.39)
	2012–2016	**283.23**	**30.0**	**0.39**
ETA	2011	45.86	48.9	4.79
	2012	46.11	70.9	4.29
	(2013)	(45.60)	(120.0)	(2.47)
	(2014)	(47.23)	(43.7)	(7.07)
	2015	46.33	39.3	6.08
	2016	46.56	54.8	4.08
	2011–2016	**46.18**	**52.5**	**4.89**
PER	(2011)	(140.04)	(43.8)	(1.62)
	(2012)	(140.08)	(37.3)	(2.06)
	2013	140.23	34.1	2.10
	2014	140.15	49.1	1.88
	2015	139.95	51.0	1.33
	(2016)	(139.64)	(48.7)	(1.41)
	2011–2016	**139.92**	**45.4**	**1.41**
GEM	(2011)	(262.12)	(100.1)	(1.04)
	2012	262.24	82.4	0.89
	2013	261.98	78.9	0.98
	(2014)	(262.18)	(79.6)	(1.06)
	(2015)	(262.15)	(74.0)	(1.05)
	2011–2015	**262.19**	**76.3**	**1.26**

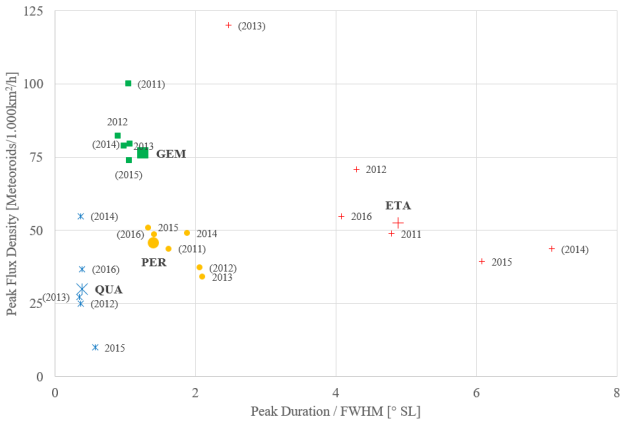

Figure 4 – Comparison between Quadrantids, η-Aquariids, Perseids and Geminids with respect to their peak flux density and FWHM.

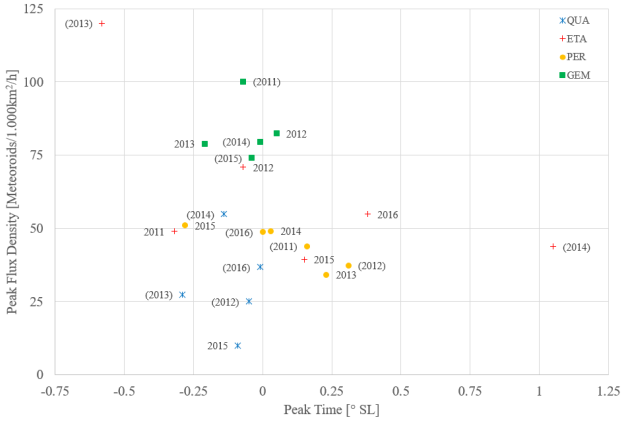

Figure 5 – Comparison between Quadrantids, η-Aquariids, Perseids and Geminids with respect to their peak flux density and time of peak relative to the mean profile.

Thus, the η-Aquariids rank at least second – if there was not the problem of the short observing window. Perseids and Geminids can be observed all night long in the mid-northern latitudes. The Quadrantids reach sufficient radiant altitudes after midnight, but in the mid-northern latitudes the η-Aquariids can only be observed at dawn with low radiant altitudes. If the radiant was located farther away from the Sun at a larger declination, the η-Aquariids would beat all other showers. In the given situation, they still belong to the "premier league" but they remain a southern hemisphere shower.

If you ask yourself why the data points in Figure 4 have a tendency from up left to down right for each cluster, the explanation is simple: The higher the peak activity, the larger is also the FWHM rate and the shorter is the time interval with such a high activity.

Figure 5 shows no clear trend. Early peaks of the η-Aquariids and Perseids seem to be somewhat more intense than later peaks, but that are not really sound dependencies given the small amount of data.

3 η-Lyrids

Complementary, we will have a look at a really small shower. The η-Lyrids are active just a few days after the η-Aquariids. Their activity is not only significantly smaller, but shows also fewer variations. Figure 6 compares the activity profile of 2016 with the average profile from 2011 to 2015. There is overall good agreement – only the peak rates between 49° and 50° solar longitude are somewhat smaller in 2016.

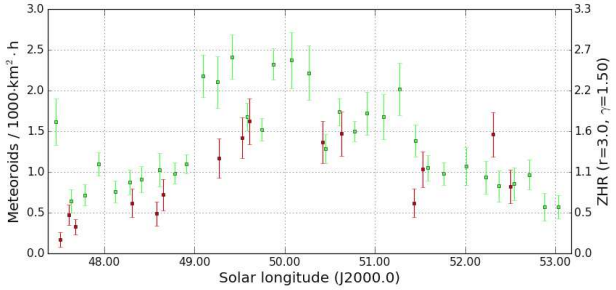

Figure 6 – Comparison of the flux density profile of the η-Lyrids in 2016 (darker, red squares) with the average profile of 2011–2015 (lighter, green squares) obtained from observation of the IMO Video Meteor Network.

4 Four cameras simultaneously with MetRec

With respect to software, there were no activities in the last month, but we experimented with new hardware. Already for some years, MetRec supports to use more than one Matrox framegrabber per computer. Some observers run two instances of MetRec on the same PC, but there have been repeated reports on stability issues.

To analyze the problem, Sirko Molau acquired a used FSC Celsius W370 midi tower with Win 7 / 32 bit, 4 PCI slots, a quad Core CPU with 4×2.4 GHz clock rate and 4 GB RAM. This computer was equipped with the maximum possible number of 4 framegrabbers. Indeed, there were first severe stability issues and the computer froze quickly. After an intensive root cause analysis it was clear that shared interrupt requests (IRQs) are to blame for that. Hence, the external PCI-E graphics card was removed and replaced by internal on-board graphics. Additionally, a number of hardware components that used the same IRQs as the Matrox framegrabbers were deactivated in Windows (USB ports and PCI bridges). AHCI had to be deactivated in the BIOS for the SATA HDD controller as well. In the end, a unique IRQ was exclusively assigned to each framegrabber, and then the system was running stable in a test period of several weeks. Performance issues were not observed either – the CPU load was typically only about 30%, so that previous observations could be simultaneously re-processed with PostProc, for example. This proves, that in the maximum configuration four Matrox framegrabbers and MetRec instances run stable and without bottlenecks on a single PC if all hardware conflicts are solved.

References

Molau S., Crivello S., Goncalves R., Saraiva C., Stomeo E., and Kac J. (2016). "Results of the IMO Video Meteor Network – January 2016". *WGN, Journal of the IMO*, **44:3**, 92–97.

Handling Editor: Javor Kac

Code	Name	Location	Camera	FOV [°²]	Stellar LM [mag]	Eff.CA [km²]	Nights	Time [h]	Meteors
ARLRA	Arlt	Ludwigsfelde/DE	Ludwig2 (0.8/8)	1475	6.2	3779	26	105.7	431
BANPE	Bánfalvi	Zalaegerszeg/HU	Huvcse01 (0.95/5)	2423	3.4	361	8	3.5	23
BERER	Berkó	Ludányhalászi/HU	Hulud1 (0.8/3.8)	5542	4.8	3847	6	35.5	109
BOMMA	Bombardini	Faenza/IT	Mario (1.2/4.0)	5794	3.3	739	24	101.5	282
BREMA	Breukers	Hengelo/NL	Mbb3 (0.75/6)	2399	4.2	699	19	83.4	117
BRIBE	Klemt	Herne/DE	Hermine (0.8/6)	2374	4.2	678	24	102.5	210
		Bergisch Gladbach/DE	Klemoi (0.8/6)	2286	4.6	1080	18	80.3	124
CASFL	Castellani	Monte Baldo/IT	Bmh1 (0.8/6)	2350	5.0	1611	23	128.6	271
			Bmh2 (1.5/4.5)*	4243	3.0	371	20	95.2	134
CRIST	Crivello	Valbrevenna/IT	Bilbo (0.8/3.8)	5458	4.2	1772	17	67.9	186
			C3P8 (0.8/3.8)	5455	4.2	1586	18	78.7	172
			Stg38 (0.8/3.8)	5614	4.4	2007	28	117.5	410
DONJE	Donani	Faenza/IT	Jenni (1.2/4)	5886	3.9	1222	26	115.9	361
ELTMA	Eltri	Venezia/IT	Met38 (0.8/3.8)	5631	4.3	2151	14	67.0	154
FORKE	Förster	Carlsfeld/DE	Akm3 (0.75/6)	2375	5.1	2154	20	90.9	197
GONRU	Goncalves	Tomar/PT	Templar1 (0.8/6)	2179	5.3	1842	25	128.2	290
			Templar2 (0.8/6)	2080	5.0	1508	27	127.6	214
			Templar3 (0.8/8)	1438	4.3	571	17	76.6	85
			Templar4 (0.8/3.8)	4475	3.0	442	25	110.2	193
			Templar5 (0.75/6)	2312	5.0	2259	24	94.4	170
GOVMI	Govedič	Središče ob Dravi/SI	Orion2 (0.8/8)	1447	5.5	1841	24	101.0	158
			Orion3 (0.95/5)	2665	4.9	2069	19	67.1	88
			Orion4 (0.95/5)	2662	4.3	1043	23	73.3	105
HERCA	Hergenrother	Tucson/US	Salsa3 (0.8/3.8)	2336	4.1	544	31	260.8	442
IGAAN	Igaz	Budapest/HU	Hupol (1.2/4)	3790	3.3	475	13	64.7	25
JONKA	Jonas	Budapest/HU	Husor (0.95/4)	2286	3.9	445	18	95.7	87
			Husor2 (0.95/3.5)	2465	3.9	715	21	93.6	90
KACJA	Kac	Ljubljana/SI	Orion1 (0.8/8)	1399	3.8	268	19	86.4	171
		Kamnik/SI	Cvetka (0.8/3.8)*	4914	4.3	1842	16	87.2	233
			Rezika (0.8/6)	2270	4.4	840	16	82.4	313
			Stefka (0.8/3.8)	5471	2.8	379	14	70.4	111
KOSDE	Koschny	Izana Obs./ES	Icc7 (0.85/25)*	714	5.9	1464	1	8.1	54
			Lic1 (2.8/50)*	2255	6.2	5670	7	55.6	496
		La Palma/ES	Icc9 (0.85/25)*	683	6.7	2951	22	135.5	1361
			Lic2 (3.2/50)*	2199	6.5	7512	28	195.5	1566
LOJTO	Łojek	Grabniak/PL	Pav57 (1.0/5)	1631	3.5	269	24	129.1	260
LOPAL	Lopes	Lisbon/PT	Naso1 (0.75/6)	2377	3.8	506	19	100.0	47

Table 2 – Observers contributing to 2016 May data of the IMO Video Meteor Network. Eff.CA designates the effective collection area; the overall number of nights is the number of nights with at least one camera operating, the overall observing time and number of meteors are sums over all cameras.

Table 2 – Observers contributing to 2016 May data of the IMO Video Meteor Network – continued from previous page.

Code	Name	Location	Camera	FOV [°²]	Stellar LM [mag]	Eff.CA [km²]	Nights	Time [h]	Meteors
MACMA	Maciejewski	Chełm/PL	Pav35 (0.8/3.8)	5495	4.0	1584	28	108.2	304
			Pav36 (0.8/3.8)*	5668	4.0	1573	22	101.3	206
			Pav43 (0.75/4.5)*	3132	3.1	319	27	142.9	176
			Pav60 (0.75/4.5)	2250	3.1	281	28	138.3	310
MARGR	Maravelias	Lofoupoli-Crete/GR	Loomecon (0.8/12)	738	6.3	2698	7	44.9	38
MARRU	Marques	Lisbon/PT	Cab1 (0.8/3.8)	5291	3.1	467	27	156.3	265
			Ran1 (1.4/4.5)	4405	4.0	1241	21	104.8	162
MASMI	Maslov	Novosibirsk/RU	Nowatec (0.8/3.8)	5574	3.6	773	18	52.6	131
MOLSI	Molau	Seysdorf/DE	Avis2 (1.4/50)*	1230	6.9	6152	24	93.3	494
			Escimo2 (0.85/25)	155	8.1	3415	20	90.0	172
			Mincam1 (0.8/8)	1477	4.9	1084	19	87.9	250
		Ketzür/DE	Remo1 (0.8/8)	1467	6.5	5491	25	115.8	496
			Remo2 (0.8/8)	1478	6.4	4778	25	116.0	487
			Remo3 (0.8/8)	1420	5.6	1967	4	12.6	32
			Remo4 (0.8/8)	1478	6.5	5358	24	115.4	492
MORJO	Morvai	Fülöpszállás/HU	Huful (1.4/5)	2522	3.5	532	23	105.8	93
MOSFA	Moschini	Rovereto/IT	Rover (1.4/4.5)	3896	4.2	1292	17	8.2	50
OTTMI	Otte	Pearl City/US	Orie1 (1.4/5.7)	3837	3.8	460	18	100.3	99
PERZS	Perkó	Becsehely/HU	Hubec (0.8/3.8)*	5498	2.9	460	22	104.1	231
ROTEC	Rothenberg	Berlin/DE	Armefa (0.8/6)	2366	4.5	911	18	51.1	102
SARAN	Saraiva	Carnaxide/PT	Ro1 (0.75/6)	2362	3.7	381	19	94.3	102
			Ro2 (0.75/6)	2381	3.8	459	19	97.7	149
			Ro3 (0.8/12)	710	5.2	619	20	111.7	208
			Sofia (0.8/12)	738	5.3	907	22	101.9	101
SCALE	Scarpa	Alberoni/IT	Leo (1.2/4.5)*	4152	4.5	2052	19	63.6	58
SCHHA	Schremmer	Niederkrüchten/DE	Doraemon (0.8/3.8)	4900	3.0	409	20	66.7	111
SLAST	Slavec	Ljubljana/SI	Kayak1 (1.8/28)	563	6.2	1294	20	81.3	112
			Kayak2 (0.8/12)	741	5.5	920	11	49.3	43
STOEN	Stomeo	Scorze/IT	Min38 (0.8/3.8)	5566	4.8	3270	26	83.8	323
			Noa38 (0.8/3.8)	5609	4.2	1911	25	94.7	323
			Sco38 (0.8/3.8)	5598	4.8	3306	28	98.5	333
STRJO	Strunk	Herford/DE	Mincam2 (0.8/6)	2354	5.4	2751	20	80.9	265
			Mincam3 (0.8/6)	2338	5.5	3590	21	91.8	170
			Mincam4 (1.0/2.6)	9791	2.7	552	20	96.1	73
			Mincam5 (0.8/6)	2349	5.0	1896	19	90.6	155
			Mincam6 (0.8/6)	2395	5.1	2178	20	80.4	138
TEPIS	Tepliczky	Agostyán/HU	Huago (0.75/4.5)	2427	4.4	1036	19	97.5	80
			Humob (0.8/6)	2388	4.8	1607	24	97.5	148
TRIMI	Triglav	Velenje/SI	Sraka (0.8/6)*	2222	4.0	546	17	24.8	58
YRJIL	Yrjölä	Kuusankoski/FI	Finexcam (0.8/6)	2337	5.5	3574	13	29.9	46
* active field of view smaller than video frame						Overall	31	7 000.3	17 326

The International Meteor Organization

www.imo.net

Follow us on Facebook
InternationalMeteorOrganization

Follow us on Twitter
@IMOMeteors

Council

President: Cis Verbeeck,
Bogaertsheide 5, 2560 Kessel, Belgium.
e-mail: cis.verbeeck@scarlet.be

Vice-President: Jürgen Rendtel,
Eschenweg 16, D-14476 Marquardt, Germany.
tel. +49 33208 50753
e-mail: jrendtel@aip.de

Secretary-General: Robert Lunsford,
1828 Cobblecreek Street, Chula Vista,
CA 91913-3917, USA. tel. +1 619 585 9642
e-mail: lunro.imo.usa@cox.net

Treasurer: Marc Gyssens, Heerbaan 74,
B-2530 Boechout, Belgium.
e-mail: marc.gyssens@uhasselt.be
BIC: GEBABEBB
IBAN: BE30 0014 7327 5911
Bank transfer costs are always at your expense.

Other Council members:

Megan Argo, Jodrell Bank Centre for Astrophysics,
Alan Turing building, University of Manchester,
Oxford Road, Manchester, M13 9PL, UK.
e-mail: megan.argo@gmail.com

Geert Barentsen, NASA Ames Research Center,
M/S 244-30, Moffett Field CA 94035, USA.
e-mail: hello@geert.io

Javor Kac (see details under WGN)

Detlef Koschny, Zeestraat 46,
NL-2211 XH Noordwijkerhout, Netherlands.
e-mail: detlef.koschny@esa.int

Masahiro Koseki, 4-3-5 Annaka, Annaka-shi,
Gunma-ken 379-0116, Japan.
e-mail: geh04301@nifty.ne.jp

Sirko Molau, Abenstalstraße 13b, D-84072 Seysdorf,
Germany. e-mail: sirko@molau.de

Jean-Louis Rault, Société Astronomique de France,
16, rue de la Vallée, 91360 Epinay sur Orge,
France. e-mail: f6agr@orange.fr

Paul Roggemans, Pijnboomstraat 25, 2800 Mechelen,
Belgium, e-mail: paul.roggemans@gmail.com

Galina Ryabova, Res. Inst. of Appl. Math. & Mech.,
Tomsk State University, Lenin pr. 36, build. 27,
634050 Tomsk, Russian Federation.
e-mail: ryabova@niipmm.tsu.ru

Damir Šegon, J. Rakovca 3, 52100 Pula,
Croatia. e-mail: damir.segon@pu.t-com.hr

Juraj Tóth, Fac. Math., Phys. & Inf., Comenius
Univ., Mlynska dolina, 84248 Bratislava, Slovakia.
e-mail: toth@fmph.uniba.sk

Commission Directors

Visual Commission: Rainer Arlt (rarlt@aip.de)
Generic e-mail address: visual@imo.net
Electronic visual report form:
http://www.imo.net/visual/report/electronic

Video Commission: Sirko Molau (video@imo.net)

Photographic Commission: Bill Ward
(William.Ward@glasgow.ac.uk)
Generic e-mail address: photo@imo.net

Radio Commission: Jean-Louis Rault (radio@imo.net)

Fireballs: Online fireball reports:
http://fireballs.imo.net

Outreach Officer

Jure Atanackov, e-mail: jureatanackov@gmail.com

Press Officer

Megan Argo, e-mail: megan.argo@gmail.com

Webmaster

Karl Antier, e-mail: webmaster@imo.net

WGN

Editor-in-chief: Javor Kac
Na Ajdov hrib 24, SI-2310 Slovenska Bistrica,
Slovenia. e-mail: wgn@imo.net;
include METEOR in the e-mail subject line

Editorial board: Ž. Andreić, M. Argo, D.J. Asher,
F. Bettonvil, J. Correira, M. Gyssens,
C. Hergenrother, T. Heywood, J. Rendtel,
J.-L. Rault, C. Verbeeck, D. Vida, S. de Vet.

IMO Sales

Available from the Treasurer or the Electronic Shop on the IMO Website	€	$
IMO membership, including subscription to WGN Vol. 44 (2016)		
Surface mail	26	35
Air Mail (outside Europe only)	49	65
Electronic subscription only	21	25
Proceedings of the International Meteor Conference on paper		
1990, 1991, 1993, 1995, 1996, 1999, 2000, 2002, 2003, per year	9	12
2007, 2010, 2011, per year	15	20
2012, 2013, 2014, 2015 per year	25	34
2016	30	40
Proceedings of the Meteor Orbit Determination Workshop 2006	15	20
Radio Meteor School Proceedings 2005	15	20
Handbook for Meteor Observers	15	20
Meteor Shower Workbook	12	16
Electronic media		
Meteor Beliefs Project ZIP archive	6	8

Now available!

See page 134 for details

ISBN 978-2-87355-030-1

Proceedings of the International Meteor Conference

Egmond, the Netherlands

2–5 June, 2016

Published by the International Meteor Organization

Edited by Adriana Roggemans and Paul Roggemans